Engineering Synthetic Coculture Systems for Enhanced Bioproduction Applications

by

Andrew David Flores

A Dissertation Presented in Partial Fulfillment
of the Requirements for the Degree
Doctor of Philosophy

Approved April 2021 by the
Graduate Supervisory Committee:

David R. Nielsen, Co-Chair
Xuan Wang, Co-Chair
Brent Nannenga
Arul Varman
Ian Wheeldon

ARIZONA STATE UNIVERSITY

May 2021

ABSTRACT

Bioconversion of lignocellulosic sugars is often suboptimal due to global regulatory mechanisms such as carbon catabolite repression and incomplete/inefficient metabolic pathways. While conventional bioprocessing strategies for metabolic engineering have predominantly focused on a single engineered strain, the alternative development of synthetic microbial communities facilitates the execution of complex metabolic tasks by exploiting unique community features (i.e., modularity, division of labor, and facile tunability). In this dissertation, these features are leveraged to develop a suite of generalizable strategies and transformative technologies for engineering *Escherichia coli* coculture systems to more efficiently utilize lignocellulosic sugar mixtures. This was achieved by rationally pairing and systematically engineering catabolically-orthogonal *Escherichia coli* sugar specialists. Coculture systems were systematically engineered, as derived from either wild-type *Escherichia coli* W, ethanologenic LY180, lactogenic TG114 or succinogenic KJ122. Net catabolic activities were then readily balanced by simple tuning of the inoculum ratio between sugar specialists, ultimately enabling improved co-utilization (98% of 100 g L^{-1} total sugars) of glucose-xylose mixtures (2:1 by mass) under simple batch fermentation conditions. We next extended this strategy to a coculture-coproduction system capable of capturing and fixing CO_2 evolved during biofuel production through inter-strain metabolic cooperation. Holistically, this work contributes to an improved understanding of the dynamic behavior of synthetic microbial consortia as enhanced bioproduction platforms and carbon conservation strategy for renewable fuels and chemicals from non-food carbohydrates.

DEDICATION

For my family

to my parents, for their unconditional love and endless support

to my grandparents, for their strength and wisdom

to my aunts and uncles, for being my guardians

to my cousins, for all good times and memories together

and to Delia, my partner in life, for being my source of joy. For with you, I am home

"He no longer dreamed of storms, nor of women, nor of great occurrences, nor of great fish, no fights, nor contests of strength, nor of this wife. He only dreamed of places now and of the lions on the beach"

-Ernest Hemingway, The Old Man and the Sea

ACKNOWLEDGMENTS

The author is grateful to Professors David R. Nielsen and Xuan Wang for their exquisite guidance, wisdom and friendship. Both Professors have made my doctoral training a gratifying and truly unique experience. They have fine-tuned my critical and analytical skills and instilled the desire to continue advancing microbial production and bioprocess development as a career. I'm glad we crossed paths and look forward continuing our friendship.

I appreciate my committee members Professor Arul Varman, Professor Brent Nannenga and Professor Ian Wheeldon for taking the time to provide constructive feedback during the completion of this dissertation. A special thank you to Ian Wheeldon for taking a chance on me many years ago, as an undergraduate at the University of California, Riverside. Ian introduced me into the arena of metabolic engineering and microbial production, which has now become a life-time career and will forever be grateful.

To all the ASU peeps, it was a pleasure working side-by-side with you during all hours of the day, sometimes even burning the midnight oil together, and weekends. It is hotter than a pistol in Arizona, but we managed to always find time to quench our thirst! Thank you.

The author kindly thanks the National Science Foundation (NSF), ASU Graduate and Professional Student Association (GPSA), ASU Light Works, ASU School for Engineering of Matter, Transport and Energy (SEMTE), and ASU School of Life Sciences (SoLs) for providing financial support during the completion of my Ph.D.

TABLE OF CONTENTS

Page

CHAPTER Page

CHAPTER Page

CHAPTER Page

CHAPTER Page

APPENDIX Page

LIST OF TABLES

Table Page

Table Page

LIST OF FIGURES

Figure Page

Figure Page

Figure Page

CHAPTER 1

INTRODUCTION

This chapter contains excerpts and reproductions with permission from:

Flores A.D., Kurgan G.L., Wang X. (2017) Engineering Bacterial Sugar Catabolism and Tolerance Toward Lignocellulose Conversion. In: Gosset G. (eds) Engineering of Microorganisms for the Production of Chemicals and Biofuels from Renewable Resources. Springer, Cham. https://doi.org/10.1007/978-3-319-51729-2_6

1.1 Bioconversion of Lignocellulosic Sugars

While biomass is a promising feedstock for producing renewable fuels and chemicals, the most abundant and sustainable sources come in the form of lignocellulose. Lignocelluloses account for more than 60% of total biomass and are renewable due to carbon-fixing photosynthetic processes of plants, with a net productivity of 155 billion tons per year [1-4]. Regardless of source, most lignocellulosic biomass contains cellulose, hemicellulose, and lignin as three major polymeric components as shown in **Fig. 1.1**.

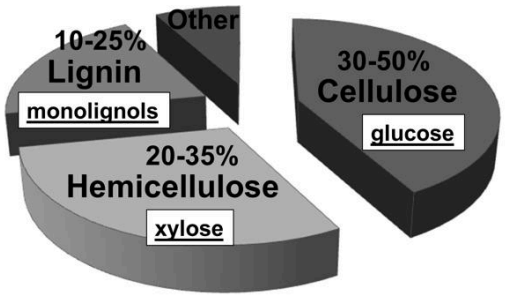

Representative sugar composition (% dry weight) of lignocellulose

Glucose	Xylose	Arabinose + mannose	galactose	total
43.8 ± 1.4	23.4 ± 2.1	5.6 ± 0.7	3.5 ± 0.4	76.3 ± 2.7

Figure 1.1. Composition of lignocellulose.

The approximate lignocellulose composition is given as a percentage of total dry weight. The major carbon monomers of the main polymeric components for typical lignocelluloses are underlined in a white box. The representative sugar composition shown in the table was obtained from a sugarcane bagasse sample [5].

Cellulose (30-50% of lignocellulose dry weight) is composed of D-glucose and hemicellulose (20-35% of lignocellulose dry weight) is composed of a mixture of pentoses and hexoses mostly with D-xylose as the major sugar (**Fig. 1.1**) [2,3,5]. Thus, fermentable sugar content of lignocelluloses occupy 50 to 70% dry weight of biomass, however, direct use of these carbon sources for microbial conversion is difficult for the following reasons.

First, co-utilization of sugar mixtures by microbes is hindered by a global regulatory mechanism called carbon catabolite repression [6-8]. This regulation is common for most microbes, if not all, and is tightly controlled at transcriptional and biochemical levels [8,9]. Glucose is often the preferred substrate, and its presence represses the catabolism of other secondary sugars in lignocellulose such D-xylose and D-arabinose [10,11]. Under anaerobic or micro-aerobic fermentation, complete consumption of sugar mixtures at high rates is difficult; especially for sugar concentrations of 100 g/L total sugars or higher [8]. This results in sugar loss, decreased productivity, and lower product titers for lignocellulose conversion. Another contributing factor to poor sugar mixture utilization is the inability for some common industrial microbes to metabolize the most abundant pentose in hemicelluloses, D-xylose (**Fig. 1.1**) [12-14]. For example, industrial microbes for ethanol production such as *Saccharomyces cerevisiae* and *Zymomonas mobilis* do not natively metabolize xylose, and these catabolic pathways must be integrated into the hosts for xylose utilization [2,13].

In this chapter, we will comprehensively review knowledge and research progress related to bacterial transport and catabolism of lignocellulosic sugars, strategies used to mitigate carbon catabolite repression, and how the unique characteristics of microbial communities can be used to enhance the co-utilization of sugar mixtures.

1.2 Bacterial Transport and Catabolism of Lignocellulosic Sugars

In many bacterial species, the phosphoenolpyruvate: sugar phosphotransferase system (PTS) facilitates the transport and concomitant phosphorylation of exogenous carbohydrates across the cytoplasmic membrane [15]. Using *Escherichia coli* as an example, the PTS is a multiprotein phosphorelay system consisting of two soluble and non sugar-

specific enzymes Enzyme I (EI) and the histidine protein (HPr), encoded by the ptsI and ptsH genes, respectively, and the sugar-specific enzyme Enzyme II (EII) system [11] (**Fig. 1.2**). EII is a multicomponent complex composed of two hydrophilic domains, EIIA and EIIB, and one or two carbohydrate-selective transmembrane domains, EIIC and EIID [16]. These mentioned domains of EII may occur as individual proteins or as a combination of subunits in variable order and number [16] (**Fig. 1.2**).

Multiple parallel EII complexes facilitate cellular uptake of different carbohydrates. The *E. coli* genome encodes for more than 20 different EII complexes, thus allowing for the transport and simultaneous phosphorylation of more than 20 different carbohydrates [17]. In the PTS, relay of the phosphoryl group initiates with the autophosphorylation of EI from phosphoenolpyruvate (PEP) and subsequently transfers the phosphoryl group to a histidine residue on the HPr (His-15) [11,18]. HPr then phosphorylates various sugar-specific EII complexes. The glucose specific EII complex comprises of the soluble enzyme $EIIA^{Glc}$ and the integral membrane permease $EIIBC^{Glc}$, encoded by *crr* and *ptsG*, respectively [18]. The reported kinetic activity of EII^{Glc} with glucose as substrate is reported to have a high affinity with K_m and V_{max} values of 3-10 μM and 126 μmol min^{-1} g^{-1}, respectively [19,20]. Lastly, the phosphoryl group is transferred to EII's corresponding sugar during transport across the cytoplasmic membrane [11] (**Fig. 1.2**). With the monosaccharide phosphorylated it can now be catabolized through the respective pathways. For example, in *E. coli* glucose-6-phospate can be catabolized by the Embden-Meyerhof-Parnas (EMP) pathway or the Pentose Phosphate Pathway (PPP).

Transport of extracellular lignocellulose-derived pentoses such as xylose and arabinose across the plasma membrane in *E. coli* occurs not through the PTS but through

two unique set of transport systems: an ATP-binding cassette (ABC) and a proton symporter. The ABC transporters XylFGH for xylose and AraFGH for arabinose, encoded by xylFGH and araFGH, respectively, actively transport sugars with the cost of one ATP per sugar, whereas the proton symporters XylE for xylose and AraE for arabinose, encoded by *xylE* and *araE*, respectively, uses a proton gradient to transport the monosaccharide across the plasma membrane [21-25].

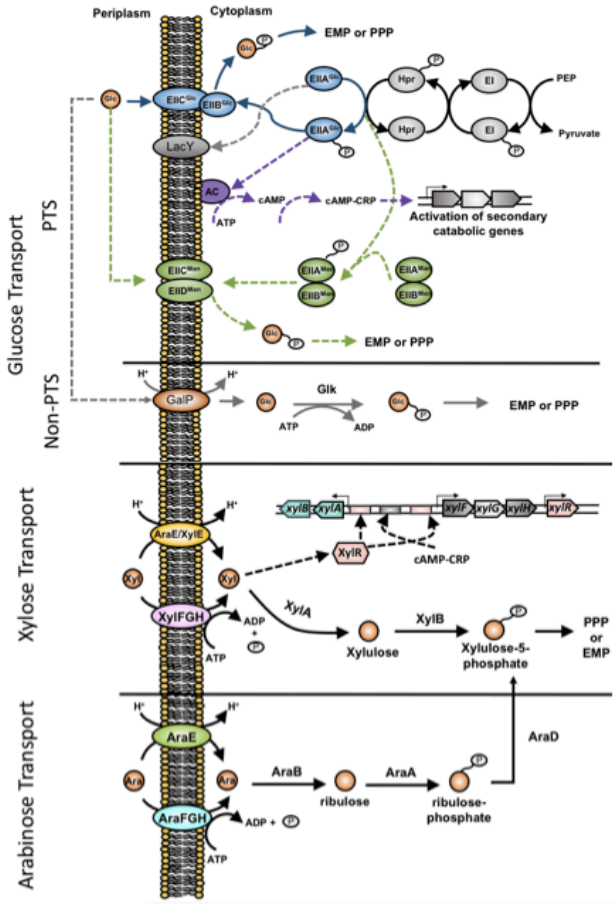

Enzyme Abbreviation	Enzyme Name	Gene Name
AC	Adenylate Cyclase	*cyaA*
AraE	Arabinose Proton Symporter	*araE*
AraFGH	Arabinose ABC Transporter ATPase	*araFGH*
AraB	Ribulokinase	*araB*
AraA	Arabinose isomerase	*araA*
AraD	Ribulose-5-phosphate 4-epimerase	*araD*
CRP	Catabolite Repression Protein	*crp*
EI	Enzyme I	*ptsI*
$EIIA^{Glu}$	Enzyme IIA Glucose Specific	*crr*
$EIIBC^{Glu}$	Enzyme IIBC Glucose Specific	*ptsG*
$EIIAB^{Man}$	Enzyme IIAB Mannose Specific	*manX*
$EIICD^{Man}$	Enzyme IICD Mannose Specific	*manYZ*
GalP	Galactose Proton Symporter	*galP*
Glk	Glucokinase	*glk*
HPr	Histidine Protein	*ptsH*
LacY	Lactose permease transporter	*lacY*
XylE	Xylose Proton Symporter	*xylE*
XylFGH	Xylose ABC Transporter ATPase	*xylFGH*
XylA	Xylose isomerase	*xylA*
XylB	Xylulose kinase	*xylB*
XylR	Transcriptional activator	*xylR*

Figure 1.2. Transport, catabolism and catabolite repression mechanisms of major lignocellulose-derived sugars in *E. coli*.

1.3 Carbon Catabolite Repression (CCR)

Glucose commonly represses the catabolism of other secondary sugars such as xylose, arabinose and galactose, which causes hierarchical control of sugar mixture utilization [26-29]. Catabolite repression is a well-studied and classic topic for bacterial global transcriptional regulation. In *E. coli* and many other enteric bacteria, catabolite repression is controlled by two *non-mutually exclusive* mechanisms: 1) operon-specific regulatory mechanisms, such as inducer exclusion, and 2) global regulatory mechanisms [11].

Inducer exclusion is an operon-specific regulatory mechanism that controls the formation or uptake of an operon's inducer. A classic example is the glucose repression of the lac operon transcription through lactose permease transporter, LacY, in *E. coli* [11,30-32].

The catabolite repression caused by global regulatory mechanisms generally involves global transcriptional regulators to modulate the transcription of catabolic genes for secondary sugars (**Fig. 1.2**). In *E. coli*, the main involved global regulator is CRP (cAMP receptor protein), also called catabolite gene-activator protein (CAP), which is the transcriptional activator for catabolic genes for secondary sugars such as xylose and arabinose when bound by cAMP, an important intracellular signaling molecule employed in many different organisms. The global regulator CRP plays an essential role in not only regulating secondary catabolic genes, but also many other important biological processes such as respiratory genes and multidrug resistance, with over 180 genes under its control [30,33].

1.4 Alleviating Bacterial CCR by Genetic Engineering

The inability of bacteria to efficiently consume two or more carbon sources hinders commercial use of lignocellulosic biomass due to increased residence time, lower product titer and productivity [34]. The strategies to abolish catabolite repression have focused on inactivating and/or engineering PTS components [35-42]. Besides engineering PTS to relieve catabolite repression, the global regulator CRP has been an engineering target to enhance sugar co-utilization for bacteria that use CRP as a catabolite repression mechanism, such as *E. coli* and *Klebsiella oxytoca* [15,43-45]. Theoretically, a cAMP-independent CRP variant should activate the catabolic operons of secondary sugars even in the presence of glucose. However, CRP globally regulates transcriptional expression of more than 180 genes and such CRP mutants often have slow growth phenotypes because the CRP mutants might alter the transcriptional control for other important genes [46], thereby limiting wide application of this approach and only yielding limited success.

1.5 Engineering Synthetic Microbial Communities

Despite extensive research efforts spanning decades developing monocultures for co-utilization of lignocellulose-derived sugars, researchers are now investigating the use of microbial consortia systems for enhanced sugar co-utilization. Design of synthetic microbial communities by engineering microbial 'specialists' - having a specific function and/or capability – has been explored. For example, Dr. Eiteman's group engineered two *E. coli* strains for selective-substrate uptake, one that can only metabolize glucose and the other only xylose, by eliminating metabolic pathways for the non-selective substrate [47]. Coculturing the two 'specialists' together had a synergistic effect by consuming glucose and xylose rapidly under both aerobic and anaerobic conditions and demonstrated by aerobic fed-batch that the coculture system has the intrinsic ability to adapt to feed

fluctuations. With increased carbon uptake, the *E. coli* 'specialists' were further engineered for parallel conversion of glucose and xylose to lactate and succinate production [48,49]. These results show high potential for engineering coculture systems. However, high sugar concentrations need to be further investigated. An advantageous benefit of using microbial consortia systems composed of the same species is the compatibility of cultivation conditions (i.e., temperature, pH, oxygen demand and nutritional requirements)[50]. This approach has also been used to simultaneously metabolize glucose, xylose, arabinose and acetate by increasing the number *E. coli* 'specialists' in microbial processes [51,52]. Although all the above-mentioned strategies have enhanced sugar co-utilization at different levels, the effects of these engineering strategies remain to be validated under more industrially relevant conditions (>100 total sugars g/L, cheap medium, low inoculum, oxygen-limiting conditions, etc.).

Progress was made recently in an *E. coli* coculture system for the production of large and complex molecules from lignocellulose-derived sugars, such as cis,cis-muconic acid, flavonoids, perillyl acetate and 3-amino-benzoic acid [53-56]. In these studies, biosynthetic pathways were segregated into one cell containing an upstream module and the other containing the downstream module. Compartmentalizing pathway segments into two microbial hosts offers a unique approach to (i) reduce metabolic stress in long and complex pathways, (ii) easily manipulate the population of individual modules by adjusting inoculum ratio and/or by the addition of a needed strain in the middle of a cultivation process and (iii) provide an optimal intracellular environment for enzymatic activity that would be difficult or incompatible in traditional metabolic engineering (engineering mono-cultures) [57]. Another successful example of engineering two *E. coli* 'specialists' was

demonstrated by Saini et al. for the production of n-butanol from glucose and renewable cellulose hydrolysate [58-60]. Titers reached 5.5 g/L of n-butanol from glucose, which correlated to 2-fold higher than the reference monoculture, and 0.163 g L^{-1} h^{-1} from cellulose hydrolysate. Expanding synthetic microbial communities to multi-species 'specialists' for lignocellulosic biomass conversion to valuable products has shown promise. Isobutanol production by co-culturing two engineered 'specialists', a cellulolytic fungus *Trichoderma reeese*i and *E. coli*, reached titers up to 1.8 g/L with yields up to 62% of theoretical maximum [61]. Other notable coculture systems comprising of mixed species are *E. coli-P. putida* for parathion degradation, *E. coli-S. cerevisiae* for oxygenated isoprenoids and benzylisoquinolin alkaloids and *G. oxydans-K. vulgare* for 2-keto-L-gulonic acid [62-65].

1.6 Outlook and Conclusion

Developing and engineering microbes to efficiently convert lignocellulosic-derived sugars into target products at high titer, yield and productivity is a nontrivial undertaking that continues to limit commercial developments. With these limitations and factors in mind, this dissertation is focused on exploiting engineered synthetic microbial communities for enhanced conversion of lignocellulose-derived sugars to bioproducts and developing novel bioprocess applications to this end. Moreover, in addition to such applied outcomes, this work further seeks to develop improved fundamental understandings of molecular interactions occurring amongst synthetic microbial communities, the likes of which will provide useful insight for developing more robust bioprocesses.

1.7 References

1 Clark, J. H. *et al.* Green chemistry and the biorefinery: A partnership for a sustainable future. *Green Chemistry* **8**, 853-860 (2006).

2 Saha, B. C. Hemicellulose bioconversion. *J Ind Microbiol Biotechnol* **30**, 279-291 (2003).

3 Girio, F. M. *et al.* Hemicelluloses for fuel ethanol: A review. *Bioresour Technol* **101**, 4775-4800, doi:10.1016/j.biortech.2010.01.088 (2010).

4 Singh, A. & Mishra, P. *Microbial Pentose UtilizatJon*. (Elsevier, 1995).

5 Geddes, C. C. *et al.* Optimizing the saccharification of sugar cane bagasse using dilute phosphoric acid followed by fungal cellulases. *Bioresour Technol* **101**, 1851-1857 (2010).

6 Kim, S. R., Ha, S. J., Wei, N., Oh, E. J. & Jin, Y. S. Simultaneous co-fermentation of mixed sugars: a promising strategy for producing cellulosic ethanol. *Trends in Biotechnology* **30**, 274-282 (2012).

7 Doran-Peterson, J. *et al.* Simultaneous saccharification and fermentation and partial saccharification and co-fermentation of lignocellulosic biomass for ethanol production. *Methods Mol Biol* **581**, 263-280 (2009).

8 Kim, J. H., Block, D. E. & Mills, D. A. Simultaneous consumption of pentose and hexose sugars: an optimal microbial phenotype for efficient fermentation of lignocellulosic biomass. *Appl Microbiol Biot* **88**, 1077-1085 (2010).

9 Kolb, A., Busby, S., Buc, H., Garges, S. & Adhya, S. Transcriptional Regulation by Camp and Its Receptor Protein. *Annual Review of Biochemistry* **62**, 749-795 (1993).

10 Deutscher, J. The mechanisms of carbon catabolite repression in bacteria. *Curr Opin Microbiol* **11**, 87-93 (2008).

11 Gorke, B. & Stulke, J. Carbon catabolite repression in bacteria: many ways to make the most out of nutrients. *Nat Rev Microbiol* **6**, 613-624, doi:10.1038/nrmicro1932 (2008).

12 Toivari, M. H., Salusjarvi, L., Ruohonen, L. & Penttila, M. Endogenous xylose pathway in Saccharomyces cerevisiae. *Appl Environ Microbiol* **70**, 3681-3686, doi:10.1128/AEM.70.6.3681-3686.2004 (2004).

13 Jeffries, T. W. Utilization of xylose by bacteria, yeasts, and fungi. *Adv Biochem Eng Biotechnol* **27**, 1-32 (1983).

14 Jeffries, T. W. & Shi, N. Q. Genetic engineering for improved xylose fermentation by yeasts. *Adv Biochem Eng Biotechnol* **65**, 117-161 (1999).

15 Stulke, J. & Hillen, W. Carbon catabolite repression in bacteria. *Curr Opin Microbiol* **2**, 195-201, doi:10.1016/S1369-5274(99)80034-4 (1999).

16 Kotrba, P., Inui, M. & Yukawa, H. Bacterial phosphotransferase system (PTS) in carbohydrate uptake and control of carbon metabolism. *J Biosci Bioeng* **92**, 502-517 (2001).

17 Tchieu, J. H., Norris, V., Edwards, J. S. & Saier, M. H., Jr. The complete phosphotransferase system in Escherichia coli. *J Mol Microbiol Biotechnol* **3**, 329-346 (2001).

18 Postma, P. W., Lengeler, J. W. & Jacobson, G. R. Phosphoenolpyruvate:carbohydrate phosphotransferase systems of bacteria. *Microbiol Rev* **57**, 543-594 (1993).

19 Stock, J. B., Waygood, E. B., Meadow, N. D., Postma, P. W. & Roseman, S. Sugar transport by the bacterial phosphotransferase system. The glucose receptors of the Salmonella typhimurium phosphotransferase system. *J Biol Chem* **257**, 14543-14552 (1982).

20 Misset, O., Blaauw, M., Postma, P. W. & Robillard, G. T. Bacterial phosphoenolpyruvate-dependent phosphotransferase system. Mechanism of the transmembrane sugar translocation and phosphorylation. *Biochemistry* **22**, 6163-6170 (1983).

21 Horazdovsky, B. F. & Hogg, R. W. High-affinity L-arabinose transport operon. Gene product expression and mRNAs. *J Mol Biol* **197**, 27-35 (1987).

22 Sumiya, M., Davis, E. O., Packman, L. C., McDonald, T. P. & Henderson, P. J. Molecular genetics of a receptor protein for D-xylose, encoded by the gene xylF, in Escherichia coli. *Receptors Channels* **3**, 117-128 (1995).

23 Jojima, T., Omumasaba, C. A., Inui, M. & Yukawa, H. Sugar transporters in efficient utilization of mixed sugar substrates: current knowledge and outlook. *Applied microbiology and biotechnology* **85**, 471-480, doi:10.1007/s00253-009-2292-1 (2010).

24 Davis, E. O. & Henderson, P. J. The cloning and DNA sequence of the gene xylE for xylose-proton symport in Escherichia coli K12. *The Journal of biological chemistry* **262**, 13928-13932 (1987).

25 Maiden, M. C., Jones-Mortimer, M. C. & Henderson, P. J. The cloning, DNA sequence, and overexpression of the gene araE coding for arabinose-proton symport in Escherichia coli K12. *The Journal of biological chemistry* **263**, 8003-8010 (1988).

26 Liu, M. Z. *et al.* Global transcriptional programs reveal a carbon source foraging strategy by Escherichia coli. *Journal of Biological Chemistry* **280**, 15921-15927, doi:10.1074/jbc.M414050200 (2005).

27 Blencke, H. M. *et al.* Transcriptional profiling of gene expression in response to glucose in Bacillus subtilis: regulation of the central metabolic pathways. *Metabolic engineering* **5**, 133-149 (2003).

28 Moreno, M. S., Schneider, B. L., Maile, R. R., Weyler, W. & Saier, M. H., Jr. Catabolite repression mediated by the CcpA protein in Bacillus subtilis: novel modes of regulation revealed by whole-genome analyses. *Molecular microbiology* **39**, 1366-1381 (2001).

29 Yoshida, K. *et al.* Combined transcriptome and proteome analysis as a powerful approach to study genes under glucose repression in Bacillus subtilis. *Nucleic Acids Res* **29**, 683-692 (2001).

30 Escalante, A., Salinas Cervantes, A., Gosset, G. & Bolivar, F. Current knowledge of the Escherichia coli phosphoenolpyruvate-carbohydrate phosphotransferase system: peculiarities of regulation and impact on growth and product formation. *Applied microbiology and biotechnology* **94**, 1483-1494, doi:10.1007/s00253-012-4101-5 (2012).

31 Nelson, S. O., Wright, J. K. & Postma, P. W. The mechanism of inducer exclusion. Direct interaction between purified III of the phosphoenolpyruvate:sugar phosphotransferase system and the lactose carrier of Escherichia coli. *EMBO J* **2**, 715-720 (1983).

32 Osumi, T. & Saier, M. H., Jr. Regulation of lactose permease activity by the phosphoenolpyruvate:sugar phosphotransferase system: evidence for direct binding of the glucose-specific enzyme III to the lactose permease. *Proceedings of the National Academy of Sciences of the United States of America* **79**, 1457-1461 (1982).

33 Geng, H. F. & Jiang, R. R. cAMP receptor protein (CRP)-mediated resistance/tolerance in bacteria: mechanism and utilization in biotechnology. *Appl Microbiol Biot* **99**, 4533-4543 (2015).

34 Gosset, G. Improvement of Escherichia coli production strains by modification of the phosphoenolpyruvate:sugar phosphotransferase system. *Microb Cell Fact* **4**, 14, doi:10.1186/1475-2859-4-14 (2005).

35 Dien, B. S., Nichols, N. N. & Bothast, R. J. Fermentation of sugar mixtures using Escherichia coli catabolite repression mutants engineered for production of L-lactic acid. *J Ind Microbiol Biotechnol* **29**, 221-227, doi:10.1038/sj.jim.7000299 (2002).

36 Dien, B. S., Nichols, N. N. & Bothast, R. J. Recombinant Escherichia coli engineered for production of L-lactic acid from hexose and pentose sugars. *Journal of industrial microbiology & biotechnology* **27**, 259-264, doi:10.1038/sj/jim/7000195 (2001).

37 Nichols, N. N., Dien, B. S. & Bothast, R. J. Use of catabolite repression mutants for fermentation of sugar mixtures to ethanol. *Applied microbiology and biotechnology* **56**, 120-125 (2001).

38 Flores, N., Xiao, J., Berry, A., Bolivar, F. & Valle, F. Pathway engineering for the production of aromatic compounds in Escherichia coli. *Nature biotechnology* **14**, 620-623, doi:10.1038/nbt0596-620 (1996).

39 Hernandez-Montalvo, V., Valle, F., Bolivar, F. & Gosset, G. Characterization of sugar mixtures utilization by an Escherichia coli mutant devoid of the phosphotransferase system. *Applied microbiology and biotechnology* **57**, 186-191 (2001).

40 Hernandez-Montalvo, V. *et al.* Expression of galP and glk in a Escherichia coli PTS mutant restores glucose transport and increases glycolytic flux to fermentation products. *Biotechnology and bioengineering* **83**, 687-694, doi:10.1002/bit.10702 (2003).

41 Balderas-Hernandez, V. E., Hernandez-Montalvo, V., Bolivar, F., Gosset, G. & Martinez, A. Adaptive evolution of Escherichia coli inactivated in the phosphotransferase system operon improves co-utilization of xylose and glucose under anaerobic conditions. *Applied biochemistry and biotechnology* **163**, 485-496, doi:10.1007/s12010-010-9056-3 (2011).

42 Chiang, C. J. *et al.* Systematic Approach To Engineer Escherichia coli Pathways for Co-utilization of a Glucose-Xylose Mixture. *J Agr Food Chem* **61**, 7583-7590 (2013).

43 Kim, J., Adhya, S. & Garges, S. Allosteric changes in the cAMP receptor protein of Escherichia coli: hinge reorientation. *Proc Natl Acad Sci U S A* **89**, 9700-9704 (1992).

44 Cirino, P. C., Chin, J. W. & Ingram, L. O. Engineering Escherichia coli for xylitol production from glucose-xylose mixtures. *Biotechnol Bioeng* **95**, 1167-1176 (2006).

45 Ji, X. J. *et al.* Elimination of carbon catabolite repression in Klebsiella oxytoca for efficient 2,3-butanediol production from glucose-xylose mixtures. *Appl Microbiol Biotechnol* **89**, 1119-1125, doi:10.1007/s00253-010-2940-5 (2011).

46 Khankal, R., Chin, J. W., Ghosh, D. & Cirino, P. C. Transcriptional effects of CRP* expression in Escherichia coli. *J Biol Eng* **3**, 13, doi:10.1186/1754-1611-3-13 (2009).

47 Eiteman, M. A., Lee, S. A. & Altman, E. A co-fermentation strategy to consume sugar mixtures effectively. *J Biol Eng* **2**, 3, doi:10.1186/1754-1611-2-3 (2008).

48 Eiteman, M. A., Lee, S. A., Altman, R. & Altman, E. A substrate-selective co-fermentation strategy with Escherichia coli produces lactate by simultaneously consuming xylose and glucose. *Biotechnol Bioeng* **102**, 822-827, doi:10.1002/bit.22103 (2009).

49 Xia, T., Altman, E. & Eiteman, M. A. Succinate production from xylose-glucose mixtures using a consortium of engineered Escherichia coli. *Eng Life Sci* **15**, 65-72, doi:10.1002/elsc.201400113 (2015).

50 Chen, Y. Development and application of co-culture for ethanol production by co-fermentation of glucose and xylose: a systematic review. *J Ind Microbiol Biotechnol* **38**, 581-597, doi:10.1007/s10295-010-0894-3 (2011).

51 Lakshmanaswamy, A., Rajaraman, E., Eiteman, M. A. & Altman, E. Microbial removal of acetate selectively from sugar mixtures. *Journal of industrial microbiology & biotechnology* **38**, 1477-1484, doi:10.1007/s10295-010-0932-1 (2011).

52 Xia, T., Eiteman, M. A. & Altman, E. Simultaneous utilization of glucose, xylose and arabinose in the presence of acetate by a consortium of Escherichia coli strains. *Microb Cell Fact* **11**, 77, doi:10.1186/1475-2859-11-77 (2012).

53 Zhang, H. & Stephanopoulos, G. Co-culture engineering for microbial biosynthesis of 3-amino-benzoic acid in Escherichia coli. *Biotechnol J* **11**, 981-987, doi:10.1002/biot.201600013 (2016).

54 Zhang, H. R., Pereira, B., Li, Z. J. & Stephanopoulos, G. Engineering Escherichia coli coculture systems for the production of biochemical products. *Proceedings of the National Academy of Sciences of the United States of America* **112**, 8266-8271, doi:10.1073/pnas.1506781112 (2015).

55 Jones, J. A. *et al.* Experimental and computational optimization of an Escherichia coli co-culture for the efficient production of flavonoids. *Metabolic engineering* **35**, 55-63, doi:10.1016/j.ymben.2016.01.006 (2016).

56 Willrodt, C., Hoschek, A., Buhler, B., Schmid, A. & Julsing, M. K. Coupling limonene formation and oxyfunctionalization by mixed-culture resting cell fermentation. *Biotechnology and bioengineering* **112**, 1738-1750, doi:10.1002/bit.25592 (2015).

57 Zhang, H. & Wang, X. Modular co-culture engineering, a new approach for metabolic engineering. *Metabolic engineering* **37**, 114-121, doi:10.1016/j.ymben.2016.05.007 (2016).

58 Saini, M., Li, S. Y., Wang, Z. W., Chiang, C. J. & Chao, Y. P. Systematic engineering of the central metabolism in Escherichia coli for effective production of n-butanol. *Biotechnology for biofuels* **9**, 69, doi:10.1186/s13068-016-0467-4 (2016).

59 Saini, M., Hong Chen, M., Chiang, C. J. & Chao, Y. P. Potential production platform of n-butanol in Escherichia coli. *Metabolic engineering* **27**, 76-82, doi:10.1016/j.ymben.2014.11.001 (2015).

60 Saini, M., Chiang, C. J., Li, S. Y. & Chao, Y. P. Production of biobutanol from cellulose hydrolysate by the Escherichia coli co-culture system. *FEMS microbiology letters* **363**, doi:10.1093/femsle/fnw008 (2016).

61 Minty, J. J. *et al.* Design and characterization of synthetic fungal-bacterial consortia for direct production of isobutanol from cellulosic biomass. *Proceedings of the National Academy of Sciences of the United States of America* **110**, 14592-14597, doi:10.1073/pnas.1218447110 (2013).

62 Gilbert, E. S., Walker, A. W. & Keasling, J. D. A constructed microbial consortium for biodegradation of the organophosphorus insecticide parathion. *Applied microbiology and biotechnology* **61**, 77-81, doi:10.1007/s00253-002-1203-5 (2003).

63 Zhou, K., Qiao, K., Edgar, S. & Stephanopoulos, G. Distributing a metabolic pathway among a microbial consortium enhances production of natural products. *Nature biotechnology* **33**, 377-383, doi:10.1038/nbt.3095 (2015).

64 Minami, H. *et al.* Microbial production of plant benzylisoquinoline alkaloids. *Proceedings of the National Academy of Sciences of the United States of America* **105**, 7393-7398, doi:10.1073/pnas.0802981105 (2008).

65 Wang, E. X., Ding, M. Z., Ma, Q., Dong, X. T. & Yuan, Y. J. Reorganization of a synthetic microbial consortium for one-step vitamin C fermentation. *Microbial cell factories* **15**, 21, doi:10.1186/s12934-016-0418-6 (2016).

CHAPTER 2

ENGINEERING A SYNTHETIC, CATABOLICALLY-ORTHOGONAL COCULTURE SYSTEM FOR ENHANCED CONVERSION OF LIGNOCELLULOSE-DERIVED SUGARS TO ETHANOL

Abstract

Fermentation of lignocellulosic sugar mixtures is often suboptimal due to inefficient xylose catabolism and sequential sugar utilization caused by carbon catabolite repression. Unlike in conventional applications employing a single engineered strain, the alternative development of synthetic microbial communities facilitates the execution of complex metabolic tasks by exploiting the unique community features, including modularity, division of labor and facile tunability. A series of synthetic, catabolically-orthogonal co-culture systems were systematically engineered, as derived from either wild-type *Escherichia coli* W or ethanologenic LY180. Net catabolic activities were effectively balanced by simple tuning of the inoculum ratio between specialist strains, which enabled co-utilization (98% of 100 g L^{-1} total sugars) of glucose-xylose mixtures (2:1 by mass) for both culture systems in simple batch fermentations. The engineered ethanologenic co-cultures achieved ~~e~~thanol titer (46 g L^{-1}), productivity (488 mg L^{-1} h^{-1}) and yield (~90% of theoretical maximum), which were all significantly increased compared to LY180 monocultures.

This chapter contains excerpts and reproductions with permission from:

Flores, A. D., Ayla, E. Z., Nielsen, D. R., & Wang, X. (2019). Engineering a synthetic, catabolically-orthogonal coculture system for enhanced conversion of lignocellulose-derived sugars to ethanol. *ACS Synthetic Biology*, *8*(5), 1089-1099.

2.1 Introduction

As discussed in chapter 1, plant-derived lignocellulose from agricultural residues and energy crops (e.g., corn stover and switchgrass, respectively) are renewable carbon and energy sources that can be converted by microbial biocatalysts to fuels and chemical products.[66] Lignocellulose, the major structural material of plant biomass, is comprised of a complex matrix of mostly polysaccharides and phenolic polymers. Of particular utility for microbial fermentative production are the carbohydrate components, which are composed of both cellulose and hemicellulose fractions and account for approximately 60-70% of total biomass dry weight.[2] The sole monomer of cellulose is glucose while the most abundant monosaccharide in most hemicellulose fractions is xylose, a five-carbon aldose (20-40% total dry weight).[2] Xylose is difficult or, in many cases impossible (e.g., in the case of native *Saccharomyces cerevisiae* and *Zymomonas mobilis*), for many microbes to metabolize.[8,67] Even microorganisms with the ability to natively catabolize xylose often do so poorly in the presence of glucose as a result of carbon catabolite repression (CCR);[11] a complex, global regulatory mechanism that prevents simultaneous utilization of multiple sugars such as glucose-xylose mixtures, resulting in diauxic growth.[8,10] CCR leads to much of the available xylose in fermentation broth unused, especially under oxygen-limiting fermentation conditions.[42,68,69] Previous efforts to improve sugar co-utilization in *E. coli* monocultures have typically involved multiple genetic manipulations along with experimental adaptation.[34,35,42,70] However, as such past efforts have repeatedly demonstrated, optimal balancing of both glucose and xylose catabolic functions in the same strain is particularly challenging, and suboptimal fermentative performance often arises as a result.[34,35,70]

Benefitting from unique features such as division of labor, cooperative interactions and diversified metabolism, synthetic microbial communities represent a promising engineering platform with the potential to address a diversity of important challenges in synthetic biology and metabolic engineering.[71-73] For instance, several engineered microbial communities have to date been developed to facilitate the parallel catabolism of substrate mixtures, such as sugars derived from lignocellulose. Wild-type *Pichia stipitis* (capable of using both glucose and xylose) and *S. cerevisiae* (using glucose only), for example, were combined to ferment glucose-xylose mixtures to ethanol.[50] However, suboptimal sugar co-utilization was ultimately observed because *i)* the two strains both competed for available glucose, and *ii)* xylose metabolism in *P. stipitis* remained inhibited by CCR. In contrast, a coculture composed of complementary biocatalysts with orthogonal catabolic functions (i.e., each specialist strain engineered to use only one designated sugar) offers the potential to achieve co-utilization of sugar mixtures without CCR through labor division.

The Eiteman group first reported on the engineering of catabolically-orthogonal *E. coli* cocultures to enhance co-utilization of sugar mixtures. Sets of *E. coli* specialist strains were engineered and combined to enable the simultaneous catabolism of sugar mixtures.[47,52] In contrast of other past efforts,[50] coculture engineering using the same species (i.e., *E. coli*) ensures compatibility of cultivation conditions (e.g., pH, temperature, nutrient requirements) between the final strains. A similar strategy was also adopted to develop a synthetic coculture composed of three distinct, hexose-specific *E. coli* strains to improve the simultaneous consumption of a mixture of glucose, galactose, and mannose.[74] In addition to improving the catabolic performance of *E. coli* on sugar mixtures, this strategy

of utilizing community engineering has furthermore proven useful for enhancing the production of various fermentation products, including lactate, succinate, and pyruvate,[48,49,75] as well as in other biosynthesis applications.[76-79] However, in these reported *E. coli* coculture systems, orthogonal catabolic functions, especially for xylose, were not further enhanced through rational genetic engineering or adaptation, thus leading to low utilization rates for sugar mixtures and suboptimal production metrics.

In this chapter, we further explore and extend the concept of engineering synthetic, catabolically-orthogonal cocultures, ultimately developing novel *E. coli* cocultures for conversion of glucose-xylose mixtures to ethanol with high production metrics. A series of genetic modifications were explored to confer and enhance either glucose or xylose utilization abilities with minimal cross-catabolic activities. Moreover, a tuning strategy to optimize the inoculum ratio between individual specialist strains significantly increased both the rates and extent of total sugar consumption as well as ethanol production compared to the corresponding monocultures. The strain and consortium engineering strategies presented here provide useful insights into the optimal design of synthetic microbial communities.

2.2 Results and Discussion

2.2.1 Carbon Catabolite Repression Limits Sugar Co-Utilization in Wild-Type and Ethanologenic *E. coli* Fermentation Monocultures

E. coli W (ATCC 9637) was used as the host strain to develop a synthetic coculture due to its faster anaerobic growth and catabolic rates compared to other *E. coli* strains commonly used for bioproduction such as BL21, C, Crooks, DH5α, MG1655, and

W3110.[80] To demonstrate the extent by which CCR limits mixed sugar fermentation in *E. coli* W, cells were fermented in a mineral salts medium containing 66 g L^{-1} glucose and 34 g L^{-1} xylose; a glucose-xylose ratio representing the composition of these sugars in typical lignocellulose.[81] As shown in **Table 2.1** and **Figure 2.1a**, glucose was completely utilized within 48 h with maximum specific rate of 610 ± 50 mg $gDCW^{-1}$ h^{-1} (254 ± 2 mg $gDCW^{-1}$ h^{-1} as the overall specific rate for 96 h). In contrast, only minor xylose utilization (< 6 g L^{-1}) occurred, representing an overall specific rate of just 23 ± 4 mg $gDCW^{-1}$ h^{-1}. Thus, as a consequence of CCR, total sugar utilization was merely 73% of provided sugar mixture, resulting in the production of 2.7 ± 0.1 gDCW L^{-1} biomass (**Figure 2.1b**). An ethanologenic *E. coli*

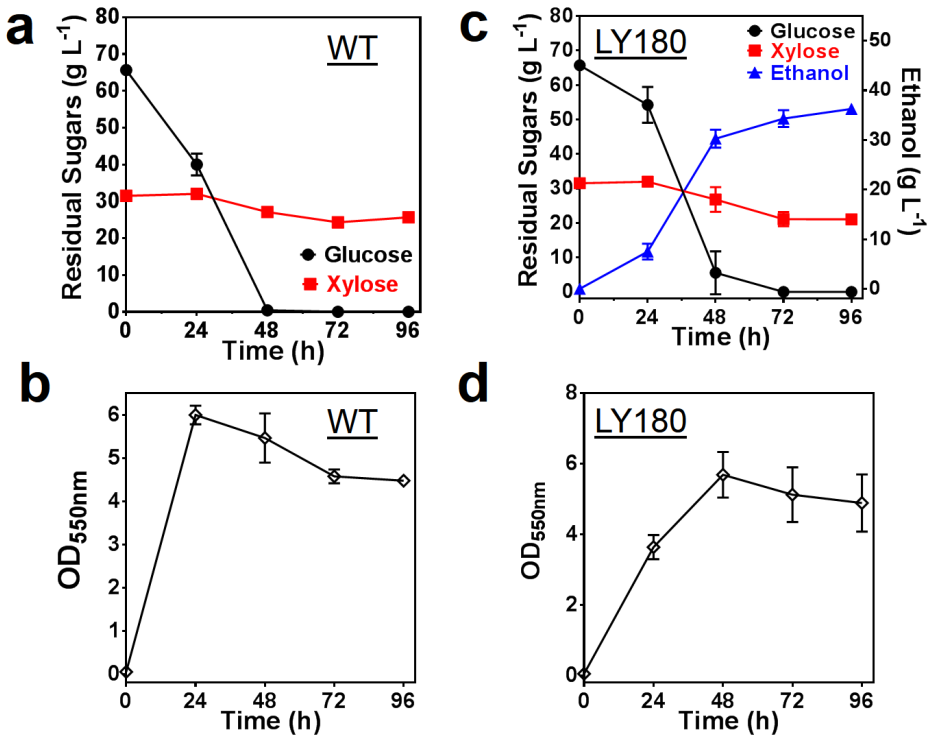

Figure 2.1. Fermentation of wild-type *E. coli* W and ethanologenic *E. coli* LY180 on glucose-xylose mixtures.

a) Sugar utilization and b) fermentative growth of E. coli W were measured at different time intervals in mineral salts medium containing the total 100 g L^{-1} glucose-xylose mixtures (approximately 2:1 by mass). c) Sugar utilization, ethanol production, and d) fermentative growth of LY180 were measured under the same fermentation condition. Symbols: glucose (round); xylose (square); ethanol (triangle); OD$_{550nm}$ (diamond).

strain LY180 (a derivative of KO11 strain based on *E. coli* W) was previously developed to convert xylose into ethanol at a high efficiency (a titer at ~45 g L^{-1} and a yield of 0.48 g g xylose^{-1} when fermenting 100 g L^{-1} xylose).[82,83] However, its ethanologenic fermentation was similarly limited when fermenting glucose-xylose mixtures (**Figure 2.1c** and **2.1d**). Only 78% of total supplied sugars were used during 96 h fermentation, with overall specific rates of glucose and xylose utilization reaching 280 ± 30 and 44 ± 3 mg gDCW^{-1} h^{-1}, respectively (**Table 2.1**). Although glucose was completely consumed by 72 h, only 33%

of supplied xylose was consumed after 96 h of fermentation. Ethanol production only reached a final titer of 36 ± 1 g L^{-1} (75% of the maximum theoretical yield) at a volumetric productivity of 378 ± 9 mg L^{-1} h^{-1}, whereas biomass production similarly reached 2.5 ± 0.3 gDCW L^{-1} (**Table 2.1**). This suboptimal fermentation performance suggests that CCR still remains a significant bottleneck in LY180 limiting ethanol production from sugar mixtures despite extensive efforts to optimize its xylose fermentation through rational engineering and adaptive laboratory evolution.[82,84]

Table 2.1. Performance of wild-type and ethanologenic monoculture and coculture fermentations using 100 g L^{-1} of Glucose-Xylose Mixtures (Ratio 2:1 by mass).

Summary of data showing the strain(s), percentage of sugar utilized, biomass, specific substrate rate, volumetric productivity, ethanol yield and ethanol titer. [a] *Sugar utilized per sugar supplied.* [b] *Dry cell weight (DCW) values are calculated from maximum* OD_{550nm} *(0.44 gDCW* L^{-1} *with an optical density of 1.0 at 550 nm).* [c] *q (specific substrate rate) and Q (volumetric productivity) values are calculated using maximum biomass and 96 h.* [d] *gram ethanol per gram total sugar consumed.* [e] *Maximum specific rates are calculated when the slope is most linear during a 24 h period and using maximum biomass occurring within the same time period. They are not distinguished from overall specific rates if sugar utilization rates remain similar for the entire 96 h fermentation. Abbreviation: Glucose (Glc); Xylose (Xyl); No Consumption (N.C.) < 1% sugar utilized; No Rate (N.R.) < 1 mg* $gDCW^{-1}$ h^{-1}.

Strains(s) Fermented	Sugar Utilized (%)[a]			Biomass[b] gDCW L^{-1}	q (mg $gDCW^{-1}$ h^{-1})[c]				$Q_{Ethanol}$[c] mg L^{-1} h^{-1}	Yield[d] g g^{-1}	Titer g L^{-1}
	Glc	Xyl	Total		Glc Overall	Glc Max[e]	Xyl Overall	Xyl Max[e]			
E. coli W	100 ± 0	18 ± 3	73 ± 1	2.7 ± 0.1	254 ± 2	610 ± 50	23 ± 4	23 ± 4		-	-
WTglc	100 ± 0	13 ± 2	71 ± 1	2.6 ± 0.2	270 ± 30	565 ± 9	17 ± 4	17 ± 4	-	-	-
WTxyl4	12 ± 1	89 ± 1	37 ± 1	1.6 ± 0.1	50 ± 2	50 ± 2	178 ± 7	460 ± 10	-	-	-
WTglc:WTxyl4 Ratio 1:1	100 ± 0	65 ± 1	89 ± 1	3.3 ± 0.2	210 ± 10	460 ± 90	64 ± 3	130 ± 20	-	-	-
WTglc:WTxyl4 Ratio 1:5	99 ± 1	96 ± 1	98 ± 1	2.3 ± 0.3	300 ± 50	700 ± 200	140 ± 20	270 ± 70	-	-	-
LY180	100 ± 0	33 ± 5	78 ± 1	2.5 ± 0.3	280 ± 30	810 ± 30	44 ± 3	44 ± 3	378 ± 9	0.47 ± 0.01	36 ± 1
LYglc1	100 ± 0	7.8 ± 4	70 ± 1	2.6 ± 0.2	270 ± 20	700 ± 100	10 ± 5	10 ± 5	329 ± 9	0.46 ± 0.02	32 ± 1
LYxyl3	N.C.	84 ± 1	25 ± 4	1.7 ± 0.2	N.R.	N.R.	160 ± 20	440 ± 30	132 ± 4	0.52 ± 0.09	12 ± 1
LYglc1:LYxyl3 Ratio 1:1	100 ± 0	26 ± 6	75 ± 2	2.4 ± 0.1	288 ± 6	800 ±100	38 ± 9	38 ± 9	353 ± 4	0.44 ± 0.01	33 ± 1
LYglc1:LYxyl3 Ratio 1:500	100 ± 0	95 ± 1	98 ± 1	2.2 ± 0.1	329 ± 9	620 ± 60	152 ± 2	300 ± 60	488 ± 6	0.45 ± 0.01	46 ± 1

2.2.2 Development of Catabolically-Orthogonal Specialist Strains from *E. coli* W

A pair of complementary, catabolically-orthogonal specialist strains were first developed by targeting genes associated with glucose transport and/or xylose catabolic

regulation in *E. coli* W. More specifically, a glucose specialist strain was engineered by deleting *xylR* (encoding xylose-specific transcriptional activator XylR) to disable xylose catabolism, whereas a xylose specialist strain was engineered by deleting several components of glucose transport systems (i.e., *ptsI, ptsG* and *galP*) while also increasing xylose utilization by introducing specific mutations to *xylR*.[68] Details regarding the construction of each strain are thoroughly explained below.

In past studies, engineering of glucose specialist strains has typically been achieved by deleting *xylA* (encoding xylose isomerase) to prevent xylose utilization.[47-49,52,75] In contrast, deletion of *xylR* does not only prevent transcriptional activation of catabolic genes (*xylA* and *xylB*), but also prevents xylose uptake by further disrupting transcriptional activation of the genes responsible for xylose transport (*xylFGH)*. *E. coli* W with deletion of *xylR*, WTglc, completely fermented glucose within 48 h at the maximum specific glucose utilization rate of 565 ± 9 mg $gDCW^{-1}$ h^{-1} in batch fermentations of a glucose-xylose mixture while only 4.2 ± 0.6 g L^{-1} xylose was utilized over 96 h (**Figure 2.2a** and **2.2b**). The catabolic performance of WTglc was similar to that of its parent strain, *E. coli* W, as was the maximum cell density (**Table 2.1**; **Figure 2.1a**, **2.1b** and **2.4a**). No significant changes in the product profile (including lactate, succinate, acetate, pyruvate and ethanol) were detected between these strains (results not shown).

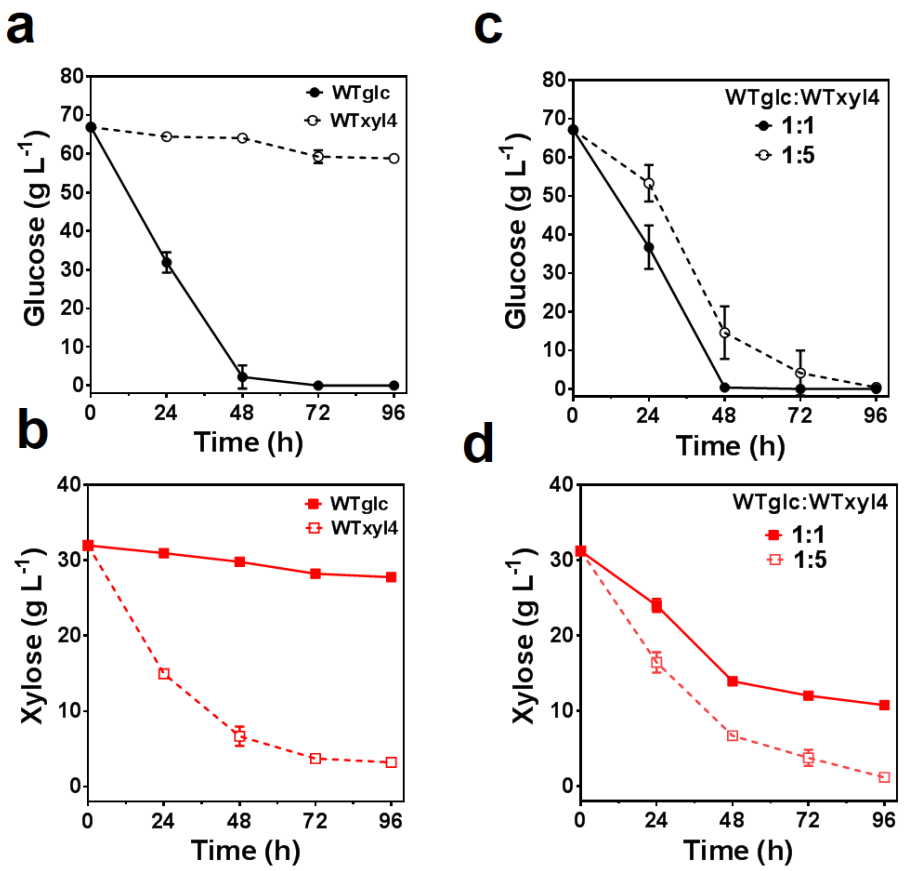

Figure 2.2. Fermentation of monocultures and cocultures of sugar specialist strains engineered from *E. coli* W using glucose-xylose mixtures (total 100 g L^{-1} with 2:1 by mass).

The concentrations of a) glucose and b) xylose in fermentation broths were measured in batch monoculture fermentations of glucose specialist strain WTglc (solid symbols) and xylose specialist strain WTxyl4 (open symbols). The concentrations of c) glucose and d) xylose were measured for coculture fermentations of WTglc:WTxyl4 with a 1:1 inoculum ratio (solid symbols) and a 1:5 inoculum ratio (open symbols).

To engineer a xylose specialist strain, wild-type *xylR* was replaced with a mutant copy (P363S and R121C; denoted as *xylR**) that was recently discovered and characterized by our lab[68] to enhance xylose fermentation and release the control of CCR. The XylR* variant has a higher DNA binding affinity than wild-type XylR which leads to stronger activation of xylose catabolic and transport genes (i.e., *xylA, xylB,* and *xylFGH*) and independency

from the control of CCR.[68] The ability of the resulting strain (LN06) to utilize glucose was next eliminated by deleting key components of the phosphotransferase system (PTS), the primary mechanism in *E. coli* to transport and subsequently phosphorylate glucose. Enzyme I (encoded by *ptsI*) in the PTS initiates the transfer of phosphate from phosphoenolpyruvate (PEP) through a cascade of enzymes to the final glucose-specific transport components, Enzyme $IIBC^{Glc}$ (encoded by *ptsG*). Accordingly, *ptsI* alone or both *ptsI* and *ptsG* were deleted in LN06, yielding the strains WTxyl1 and WTxyl2, respectively. In past studies, PTS has typically been inactivated by deleting *ptsG* in xylose specialists (or other non-glucose specialist strains described in **Table 2.2**).[47-49,52,74,75] Deletion of *manZ* which encodes Enzyme $IICD^{Man}$, another glucose non-specific PTS membrane transporter, has also been employed to engineer a xylose specialist strain. [16,47-49,75] Individual batch fermentations of WTxyl1 and WTxyl2 in a glucose-xylose mixture revealed that both strains displayed only minimal ability to consume glucose (<3% utilized after 96 h; **Figure 2.3**). Interestingly, the combined deletion of both *ptsI* and *ptsG* in strain WTxyl2 appeared to synergistically increase both the specific rate and extent

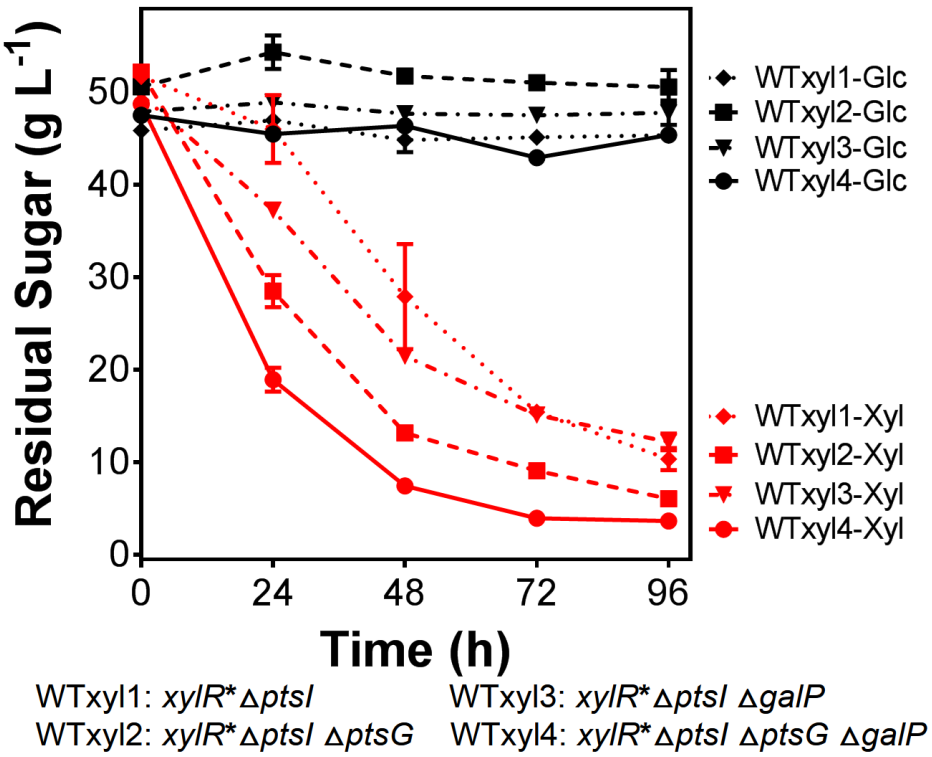

Figure 2.3. Fermentation of xylose specialist strains engineered from *E. coli* W

Fermentation of E. coli strains with genetic modifications to inactivate glucose transport and enhance xylose fermentation. Fermentations of E. coli strains WTxyl1, WTxyl2, WTxyl3, and WTxyl4 were performed in mineral salts medium containing glucose-xylose mixtures, each 50 g L^{-1}. Sugars in fermentation broths were measured at approximately 24 h time intervals. Glucose and xylose concentrations are indicated in black and red, respectively.

of xylose utilization relative to WTxyl1 (**Figure 2.3**). While the specific xylose utilization rate for 96 h batch fermentation exhibited by WTxyl1 was 195 ± 8 mg gDCW^{-1} h^{-1} with 80% total consumption of supplied xylose, WTxyl2 reached 260 ± 1 mg gDCW^{-1} h^{-1} and 88%, respectively.

The galactose permease (GalP) encoded by *galP* has been shown to have the activity of transporting glucose into the cell.[34,85] To further reduce glucose consumption by WTxyl1 and WTxyl2, *galP* was deleted in WTxyl1 and WTxyl2, resulting in strains WTxyl3 and

WTxyl4, respectively. Under analogous fermentation conditions, while glucose utilization by WTxyl3 and WTxyl4 remained minimal (< 2.5 g L^{-1} utilized after 96 h), overall rates of xylose utilization were increased by *galP* deletion (**Figure 2.3**). Relative to WTxyl1, the overall specific rate of xylose utilization by WTxyl3 was slightly increased (250 ± 10 vs. 195 ± 8 mg $gDCW^{-1}$ h^{-1}) during 96 h of fermentation. WTxyl4 (*E. coli* W *xylR*::*xylR** Δ*ptsI* Δ*ptsG* Δ*galP*) showed the highest volumetric xylose utilization rate and used most xylose during the 96 h fermentation among these four xylose specialist strains (**Figure 2.3**), and was accordingly selected for further study. In mineral salt media containing a mixture of 66 g L^{-1} glucose and 34 g L^{-1} xylose, WTxyl4 fermented xylose (~90% after 72 h; **Figure 2.2b**) at a maximum and overall specific rate of 460 ± 10 and 178 ± 7 mg $gDCW^{-1}$ h^{-1}, respectively (**Table 2.1**), while producing 1.6 ± 0.1 gDCW L^{-1} biomass much lower than that produced by WTglc fermentation (**Figure 2.4a**). The mechanism responsible for the improved xylose utilization caused by inactivation of both PTS and GalP is unclear although it is possible that PTS components and GalP function directly as negative regulators for xylose catabolism. Alternatively, deletion of PTS components and *galP* may influence the function of CRP or other global transcriptional regulators, thus indirectly affecting xylose catabolism. These possible mechanisms warrant future investigation.

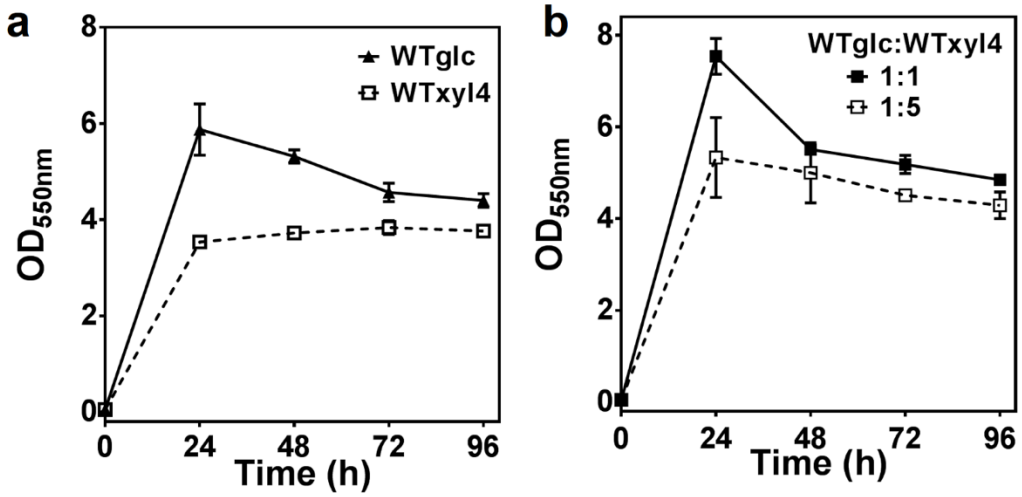

Figure 2.4. Fermentative growth of monocultures and cocultures of orthogonal sugar specialist strains engineered from E. coli W on glucose-xylose mixtures.

Shows optical densities at 550 nm of a) batch monoculture fermentations of sugar specialist strains WTglc (solid line with closed symbols) and WTxyl4 (dotted line with open symbols) and b) coculture fermentations of WTglc:WTxyl4 in a 1:1 inoculum ratio (solid line with closed symbols) and 1:5 inoculum ratio (dotted line with open symbols) were measured at approximately 24 h time intervals.

2.2.3 Engineering and Optimizing a Synthetic Coculture of Wild-Type Derived, Catabolically-Orthogonal Specialist Strains for Glucose-Xylose Co-Utilization

A synthetic coculture composed of WTglc and WTxyl4 was next developed to enable co-utilization of a glucose-xylose mixture. In all coculture fermentations, the same total initial cell concentration used in monocultures (OD_{550nm} = 0.05) was likewise employed. As shown in **Figure 2.2c** and **2.2d**, when the two strains were first inoculated at an initial population ratio of 1:1, glucose was completely consumed within 48 h (similar to WTglc monocultures; **Figure 2.2a**) while, even after 96 h, 34% of xylose remained unused (compared to just 11% in WTxyl4 monocultures; **Figure 2.2b**); collectively representing a total sugar consumption of 89% (**Table 2.1**). To compensate for the reduced volumetric rate of xylose utilization, the starting inoculum population ratio between WTglc and

WTxyl4 was thus tuned to 1:5. Reduced abundance of WTglc in the inoculum population led to an expected decrease in glucose consumption, as was most pronounced in the first 24 h (**Figure 2.2c**). However, the overall specific rate of total sugar utilization (i.e., glucose and xylose combined) for 96 h was 60% greater than that of monocultures of *E. coli* W (440 ± 70 vs. 276 ± 3 mg $gDCW^{-1}$ h^{-1}). 98% of total glucose-xylose mixtures were co-utilized within 96 h without the observed CCR (**Figure 2.2c** and **2.2d**). For comparison, a coculture of wild-type MG1655 derived *E. coli* specialist strains developed by Eiteman et al. achieved co-utilization of 14 g L^{-1} glucose-xylose mixture under a two-stage aerobic-anaerobic process (**Table 2.2**).[47] Fast maximum specific rates (1300 and 400 mg $gDCW^{-1}$ h^{-1} for glucose and xylose, respectively) of sugar utilization achieved in this coculture system are likely due to the high amount of biomass accumulated at the first aerobic growth phase and low sugar loading. Among reported metrics of *E. coli* cocultures with enhanced catabolism for sugar mixtures (summarized in **Table 2.2**), the wild-type derived coculture reported in this study, WTglc:WTxyl4 with 1:5 inoculum ratio, has the highest values for the quantity of total sugars used by a simple batch fermentation. As is consistent with prior works and proposed composition tunability of synthetic communities,[86-88] optimization of the inoculum ratio represents a simple, but effective community-level tuning strategy for synthetic cocultures that enables successful titration of individual sugar catabolic rates, leading to co-utilization of glucose-xylose mixtures (98% of 100 g L^{-1} total sugars through batch fermentations).

2.2.4 Development of Catabolically-Orthogonal Specialist Strains from Ethanologenic *E. coli*

To test if the synthetic coculture engineering strategy developed from wild-type *E. coli* can be effectively used in an extensively engineered bioproduction host, ethanologenic *E. coli* LY180 was selected since CCR remains a bottleneck limiting co-utilization of glucose-xylose mixtures in this strain (**Figure 2.1c**). The same sets of genetic manipulations employed to generate WTglc and WTxyl4 were implemented in LY180. First, to prevent xylose utilization, the *xylR* gene was deleted, yielding LYglc. Similar to WTglc, batch fermentation of LYglc revealed no xylose utilization (**Figure 2.2b** and **Figure 2.5b**). However, in this case after 48 h fermentation only 24 ± 5 g L^{-1} glucose was used by LYglc whereas 65 ± 3 g L^{-1} for WTglc (**Figure 2.5a** and **Figure 2.2a**). In addition, the maximum biomass of LYglc only reached to 1.0 ± 0.2 gDCW L^{-1}; a 1.5-fold decrease relative to LY180 when grown using the same sugar mixtures (**Table 2.1**). This unexpected outcome likely resulted from the fact that LY180 was previously extensively adapted solely using xylose as carbon source.[83,84] Thus, adaptive laboratory evolution was next applied to improve glucose utilization and fermentative growth of LYglc in the glucose-xylose media. Following replacement of *lacZ* with a *cat-sacB* cassette (to facilitate later population studies in coculture fermentations), the resulting strain (LYglcCm; chloramphenicol resistant) was evolved in minimal media containing 66 g L^{-1} glucose and 34 g L^{-1} xylose. After just three transfers, evolved cultures showed improved rates of both cell growth (**Figure 2.5e**) and glucose utilization (**Figure 2.5f**). Three independent clones were isolated from the evolved population at the seventh transfer and batch fermentations revealed essentially identical performance by all three mutants. One representative clone, LYglc1,

was chosen for further study. LYglc1 reached the maximum ethanol titer at 48 h (**Figure 2.5c**) and grew much faster than its precursor LYglc (**Figure 2.5d**), displaying a maximum specific glucose utilization rate of 700 ± 100 mg gDCW^{-1} h^{-1} (**Table 2.1**) and 100% consumption of supplied glucose within 48 h (**Figure 2.5a**). Meanwhile, only minimal xylose consumption (<2.5 g L^{-1}) was observed over the course of 96 h and maximum biomass production levels were restored to that of LY180 (a 1.3-fold increase compared to LYglc) (**Table 2.1**).

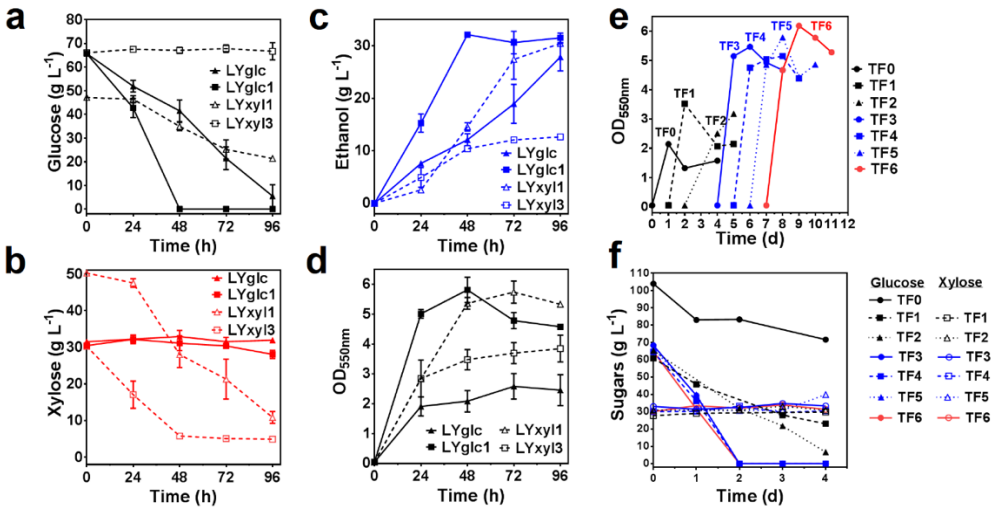

Figure 2.5. Construction of the glucose and xylose specialist strains in LY180 background.

The concentrations of a) glucose, b) xylose, c) ethanol in fermentation broth as well as d) optical densities at 550 nm were measured for batch fermentations of glucose and xylose specialist strains: LYglc (solid triangle), LYglc1 (solid square), LYxyl1 (open triangle) and LYxyl3 (open square). Batch fermentations were performed in mineral salts medium containing the total 100 g L^{-1} glucose-xylose mixtures with the initial mass ratio at 2:1 except for LYxyl1 (1:1). The strain LYglcCm was sub-cultured once using 100 g L^{-1} glucose (Initial culture; TF0) and subsequently sub-cultured 6 times (TF1 to TF6) using sugar mixtures of 66 g L^{-1} glucose and 33 g L^{-1} xylose. e) Optical densities of the cultures (OD_{550nm}) and f) sugars (open and filled symbols for xylose and glucose, respectively) in the fermentation broths were determined for this adaptive laboratory evolution process. The final strain LYglc1 was isolated from the final culture (TF6).

Using the same engineering strategy implemented for WTxyl4, glucose transport systems were disrupted (deleting *ptsI*, *ptsG* and *galP*) to prevent glucose consumption by LY180, yielding LYxyl1, an ethanologenic xylose specialist strain. Unexpectedly, glucose utilization was not halted in this case (**Figure 2.5a**). Instead, despite the lack of a functional PTS and GalP, 53% of the initially supplied glucose was still consumed after 96 h at an overall specific utilization rate of 117 ± 6 mg $gDCW^{-1}$ h^{-1}. This difference suggests that one or more alternative sugar transporters with activity towards glucose are present and/or upregulated in LY180 but not in the wild-type background. Since this putative transport mechanism is currently unknown, to fully eliminate glucose catabolism, glucokinase was inactivated (the coding gene *glk* replaced by a kanamycin resistance gene; note: *glk* inactivation has previously been used to disrupt glucose utilization in other coculture systems as summarized in **Table 2.2**). Inactivation of Glk disrupts phosphorylation of glucose to glucose-6-phospate, which is a required step for glycolysis in the absence of PTS. While the resulting strain, LYxyl2, could no longer use glucose, it only used 17 ± 2 g L^{-1} xylose (50% of provided xylose) throughout a 96 h fermentation. To improve xylose catabolism in this strain, *xylR* was replaced with the mutant copy *xylR**. Subsequent fermentation of the resulting strain LYxyl3 showed that 25 ± 1 g L^{-1} xylose was consumed (or 84% of provided xylose) after 48 h fermentation with a maximum specific xylose utilization rate reaching 440 ± 30 mg $gDCW^{-1}$ h^{-1} (**Figure 2.5b** and **Table 2.1**). LYxyl3 is the best-performing ethanologenic xylose specialist strain developed in this work and thus used for further coculture study. Similar to other xylose specialist strains such as WTxyl4 developed in this study, biomass accumulation by LYxyl3 was reduced following disruption of glucose catabolism (**Figure 2.5d**, **2.5a** and **Table 2.1**). This phenotypic

difference of xylose 'specialists' is likely due to the lower energy yield of xylose fermentation compared to that of glucose fermentation (more energy is required to transport and phosphorylate xylose than glucose).[89-91]

2.2.5 Engineering and Optimizing a Synthetic Ethanologenic *E. coli* coculture

The engineered ethanologenic specialist strains LYglc1 and LYxyl3 were next used to develop a synthetic coculture to convert glucose-xylose mixtures into ethanol. An inoculum ratio of 1:1 was first employed. However, this initial coculture did not exhibit increased sugar utilization (**Figure 2.6a** and **2..6b**) and ethanol production (**Figure 2.6c**) compared to monocultures of the parent strain LY180 (quantitative comparison in **Table 2.1**). More specifically, while all the glucose was consumed within 48 h (similarly to LYglc1 monocultures; **Figure 2.5a**), only 26% of initially supplied xylose was utilized (versus 84% for LYxyl3 monocultures; **Figure 2.5b**). As proven effective in wild-type derived cocultures, community-level tuning was next used to improve overall catabolic functions and ethanol production by titrating the relative rates and extent of glucose and xylose utilization in this coculture. The initial population ratio in the starting inoculum was first adjusted to 1:5 (LYglc1:LYxyl3). However, unlike wild-type derived cocultures of WTglc:WTxyl4 with 1:5 inoculum ratio, only a minor increase in xylose utilization was realized (38% of initially supplied xylose) along with just 79% consumption of total sugars after 96 h (**Figure 2.6a** and **2.6b**).

The further increased relative initial abundance of LYxyl3 at an inoculum ratio of 1:10 resulted in a slightly improved xylose utilization close to 50% of supplied xylose while still also supporting complete glucose consumption within 48 h (**Figure 2.6a** and **2.6b**). With

an additional increase in xylose utilization, this resulted in the ability to consume 83% of total sugars (versus 78%, 75%, and 79% for LY180 monocultures, 1:1 co- culture, and 1:5 coculture, respectively). To further enhance xylose catabolic rates in cocultures, cocultures were next investigated using initial inoculum ratios of 1:100, 1:500, and 1:1000 between LYglc1:LYxyl3. At 1:100, total sugar utilization was further increased to 86% without loss in glucose utilization performance (**Figure 2.6a** and **2.6b**), leading to an overall specific utilization rate of total sugars greater than LY180 (430 ± 10 vs. 320 ± 30 mg $gDCW^{-1}$ h^{-1}). A 1:500 initial inoculum ratio supported a two-fold increase in xylose utilization, leading to co-utilization of both glucose and xylose (94% total sugars by 72 h and ≥ 98% by 96 h; **Figure 2.6a** and **2.6b**). At this output, the overall utilization rate of total sugars was 50% greater than that LY180 monocultures (480 ± 10 vs. 320 ± 30 mg $gDCW^{-1}$ h^{-1}). Meanwhile, the final ethanol titer reached 46 ± 1 g L^{-1} whereas just 36 ± 1 g L^{-1} was achieved in LY180 monocultures representing 90% vs. 73% of the maximum theoretical yield, respectively (**Figure 2.6c** and **2.1c**). Finally, extending the initial inoculum ratio of 1:1000 offered the similar performance in terms of sugar co-utilization and ethanol production compared to the coculture with an inoculum ratio of 1:500 (**Figure 2.6a**, **2.6b** and **2.6c**). Similar to wild-type cocultures (**Figure 2.4b**), with the increased xylose specialist LYxyl3 ratio in the initial inoculum, the total cell growth rates reduced in the initial 24 h for the cocultures of LYglc1:LYxyl3 with the inoculum ratio of 1:500 and 1:1000 (**Figure 2.6d**), consistent with the observation that xylose specialist strains have slower growth rates than glucose specialist strains (**Figure 2.5d** and **2.4a**). Despite an improved overall rate of total sugar co-utilization, one caveat of increasing the abundance of xylose specialist cells during inoculation, however, is that consumption rates of glucose were expectedly reduced and

complete glucose consumption for the inoculum ratios 1:500 and 1:1000 (LYglc1:LYxyl3) required at least 72 h versus just 48 h for initial inoculum ratios of 1:1 through 1:100 (**Figure 2.6a**). Still, even in spite of this trade-off, these findings support that community-level tuning is an effective strategy to optimize composite catabolic functions and thus overall fermentation performance.

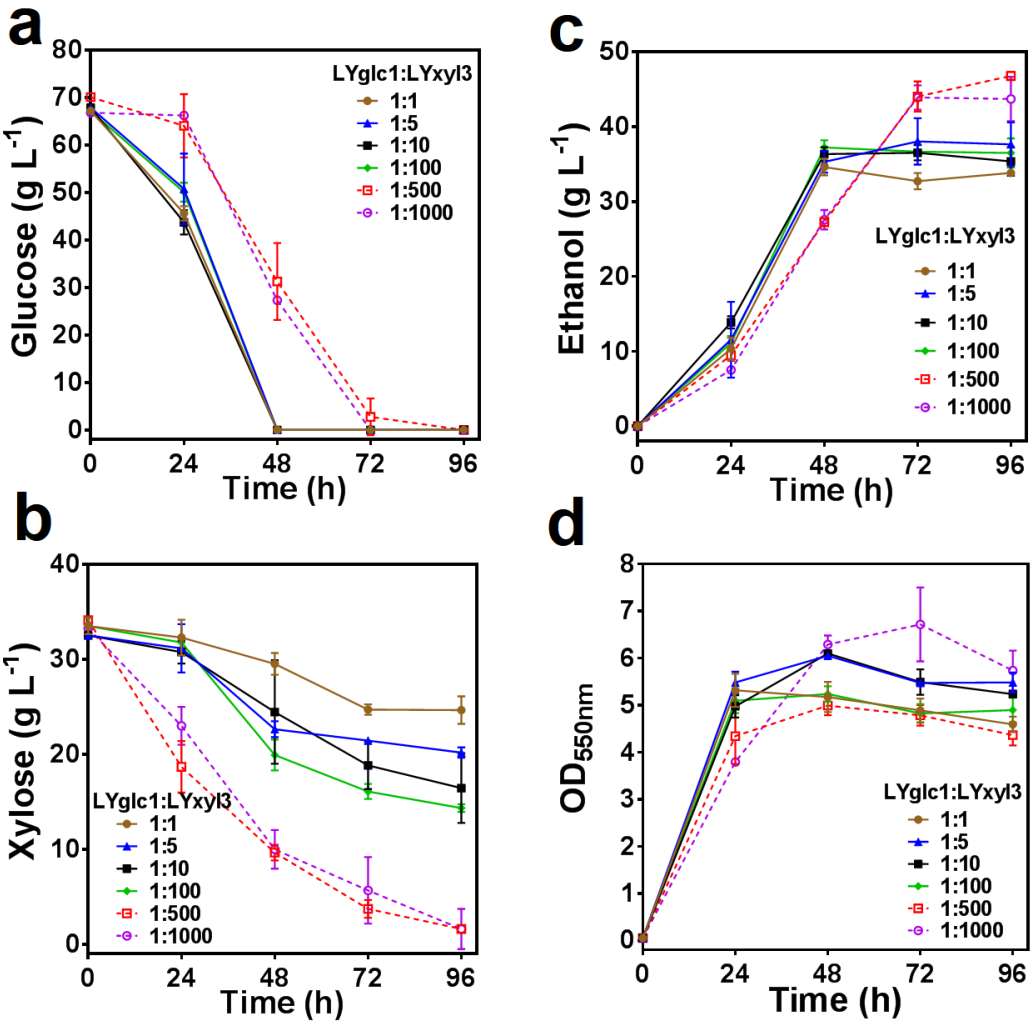

Figure 2.6. Fermentation of cocultures of ethanologenic sugar specialist strains using glucose-xylose mixtures.

The concentrations of a) glucose, b) xylose, c) ethanol in fermentation broth as well as d) optical densities at 550 nm were measured for coculture batch fermentations of LYglc1:LYxyl3 with the inoculum ratios of 1:1 (solid circle), 1:5 (solid triangle), 1:10 (solid square), 1:100 (solid diamond), 1:500 (open square), and 1:1000 (open circle). All

fermentations were performed in mineral salts medium containing the total 100 g L^{-1} glucose-xylose mixtures (approximately 2:1 by mass).

Although fermentative products such as lactate (titer 37 g L^{-1}), succinate (titer 40 g L^{-1}) and pyruvate (titer 39 g L^{-1}) have been produced in *E. coli* cocultures,[48,49,75] to our knowledge this is the first report of an *E. coli* coculture system that successfully converts a glucose-xylose mixture to ethanol with high production metrics (titer 46 g L^{-1}; 90% of theoretical maximum yield; **Table 2.1** and **2**). Additionally, unlike many previous reports for ethanol production by microbial cocultures,[50,91] this study operates fermentation in mineral salts media under simple batch and high substrate loading conditions (100 g L^{-1} total sugar; 50 g L^{-1} or more total sugar compared to previous systems; **Table 2.2**). While multiple previous studies take a bioprocess engineering approach (e.g., two-stage processes or sequential co-culturing) to balance differences in strain fitness and catabolic functions of individual specialist,[52,91] this study demonstrates that simple titration of the initial inoculum ratio can lead to optimal performance metrics. Although additional strain engineering efforts are needed to engineer sugar specialist strains in LY180 background compared to wild-type background (**Figure 2**), this community-level tuning strategy is effective for both wild-type and LY180-derived cocultures to achieve successful labor division and co-utilization of glucose-xylose mixtures (98% of 100 g L^{-1} total sugars). Lastly, in this study xylose specialist strains WTxyl4 and LYxyl3 were engineered with enhanced xylose catabolism, which improves the overall performance compared to previously reported *E. coli* cocultures (**Table 2.2**).

Table 2.2. *E. coli* consortia for the co-utilization of lignocellulose-derived sugar mixtures.

Summary of selected E. coli coculture systems. Shows number of members, media and fermentation condition(s), base strain and key mutations, products, and performance metrics. [a] Gene deletion, disruption or modification. [b] q_{Glc} specific glucose rate; q_{Xyl} specific xylose rate; q_{Gal} specific galactose rate; q_{Man} specific mannose rate; q_{Ara} specific arabinose rate; Dry cell weight (DCW) calculated from maximum OD_{550nm} (0.44 gDCW L^{-1} with an optical density of 1.0 at 550 nm). [c] Fermentation consisted of two process phases: initial aerobic growth followed by an anaerobic phase. [d] OD reported to be 9.0 and 13 for glucose and xylose specialists, respectively, at onset of anaerobic growth.

***E. coli* Cocultures**	**Media and Fermentation Condition(s)**	**Base Strain & Key Mutations[a]**	**Product(s)**	**Performance Metric(s)[b]**	**References**
Two	Modified AM1 mineral salts medium 6.6% Glucose 3.4% Xylose Batch Microaerobic	Glucose: E. *coli* W Δ*xylR* Xylose: *E. coli* W Δ*pts1* Δ*ptsG* Δ*galP* *xylR*::*xylR**	Lactate, succinate, ethanol, acetate, pyruvate, & formate	$q_{Glc\text{-}Overall} \approx 300$ mg DCW^{-1} h^{-1} $q_{Glc\text{-}Max} \approx 700$ mg DCW^{-1} h^{-1} $q_{Xyl\text{-}Overall} \approx 140$ mg DCW-1 h^{-1} $q_{Xyl\text{-}Max} \approx 270$ mg DCW-1 h^{-1} Total Sugar Utilized ≈ 98 g L^{-1}	This Study
Two	Basal 0.9% Glucose 0.5% Xylose Fed-batch aerobic-anaerobic[c]	Glucose: *E. coli* MG1655 *xylA*::Tet Xylose: *E. coli* ZSC113 *lacZ827*(UGA) *ptsG22 manZ12 glk-7 relA1* *rpsL223*(strR) *rha-4*	Lactate, succinate, ethanol, acetate, & formate	$q_{Glc\text{-}Max} \approx 1300$ mg DCW^{-1} h^{-1} [d] $q_{Xyl\text{-}Max} \approx 475$ mg DCW^{-1} h^{-1} [d] $q_{Xyl\text{-}Overall} \approx 160$ mg DCW^{-1} h^{-1} [d] Total Sugar Utilized ≈ 14 g L^{-1}	17
Four	Basal 1.5% Glucose 1.1% Xylose 0.7% Arabinose 0.3% Acetate Batch Aerobic	Glucose: *E. coli* C *xylA*::FRT *araA*::Kan^R Xylose: *E. coli* C *ptsG763*::FRT *glk-726*::FRT *manZ743*::FRT *crr-746*::FRT *araA*::FRT Arabinose: *E. coli* C *ptsG763*::FRT *glk-726*::FRT *manZ743*::FRT *crr-746*::FRT *xylA748*::FRT Acetate: *E. coli* C *ptsG763*::FRT *glk-726*::FRT *manZ743*::FRT *crr-746*::FRT *xylA748*::Kan^R *araA*::FRT	Not reported	$q_{Glc} \approx 140$ mg DCW^{-1} h^{-1} $q_{Xyl} \approx 100$ mg DCW^{-1} h^{-1} $q_{Ara} \approx 70$ mg DCW^{-1} h^{-1} Total Sugar Utilized ≈ 33 g L^{-1}	18

Three	2X M9 0.28% Glucose 0.1% Galactose 0.37% Mannose Batch Aerobic (Shake flask)	Glucose: *E. coli* MG1655 Δ*manZ* Δ*galP* Δ*mglC attBΦ80::tetA* Δ*galK* Galactose: *E. coli* MG1655 Δ*ptsG* Δ*crr* Δ*glk* Δ*manZ galR*::Kan^R adapted in M9 galactose Mannose: *E. coli* MG1655 Δ*ptsG* Δ*crr* Δ*glk* Δ*galP* Δ*mglC* Δ*pgi manXYZpro*::Δ*rep zwf*::*cat* adapted in dextrose-mannose and dextrose-galactose-mannose	Not reported	$q_{Glc} \approx 117$ mg DCW^{-1} h^{-1} $q_{Gal} \approx 4.2$ mg DCW^{-1} h^{-1} $q_{Man} \approx 150$ mg DCW^{-1} h^{-1} Total Sugar Utilized ≈ 7 g L^{-1}	19
Two	Modified AM1 6.6% Glucose 3.4% Xylose Batch Microaerobic	Glucose: LY180 (an *E. coli* W derivative engineered for ethanol production) Δ*xylR* adapted in glucose-xylose Xylose: LY180 Δ*ptsI* Δ*ptsG* Δ*galP glk::* Kan^R *xylR*::*xylR**	Ethanol	$q_{Glc\text{-}Overall} \approx 329$ mg DCW^{-1} h^{-1} $q_{Glc\text{-}Max} \approx 620$ mg DCW^{-1} h^{-1} $q_{Xyl\text{-}Overall} \approx 152$ mg DCW-1 h^{-1} $q_{Xyl\text{-}Max} \approx 300$ mg DCW-1 h^{-1} Total Sugar Utilized ≈ 98 g L^{-1} Titer ≈ 46 g L^{-1} Productivity ≈ 488 mg L^{-1} h^{-1} % of Theoretical Maximum Yield ≈ 90%	This Study
Two	Terrific Broth 1% (w/v) Birch Wood Xylan Batch Aerobic (Shake flask)	Hemicellulase Secretor *E. coli* E609 Δ*llp* containing plasmid pCRAXEXYL Ethanol Producer KO11 containing pBBKXYN	Ethanol	Titer ≈ 3.7 g L^{-1} % of Theoretical Maximum Yield ≈ 71%	26
Two	Distillers' grains with solubles 0.6% Glucose 1% Xylose 0.7% Arabinose	Amino Acid utilizer: E. *coli* BW25113 Δ*glnA*, Δ*gdhA*, Δ*lsrA* Carbohydrate Utilizer: *E. coli* B *Δldh*::cam$^+$ Both strains contain plasmids encoding keto acid pathway for fusel alcohol production	Fusel alcohols	Titer ≈ 10 g L^{-1} Total Sugar Utilized ≈ 21 g L^{-1} Total Protein Utilized ≈ 31%	36

2.2.6 Population Dynamics of Ethanologenic Coculture Systems During the Fermentation of Glucose-Xylose Mixtures

To understand how community-level tuning led to the significant enhancement of catabolic performance and production in synthetic ethanologenic cocultures, we further investigated the growth phenotypes of individual ethanologenic specialist strains in both

monoculture and coculture fermentations. In the latter case, inoculum ratios of 1:1 and 1:500 were chosen as representative conditions for both suboptimal and optimal sugar co-utilization, respectively. When cultured alone, the tested strains LYglc1 (chloramphenicol resistant) and LYxyl3 (kanamycin resistant) showed essentially the same CFUs on LB plates with and without appropriate antibiotics, thus excluding the potential influence of antibiotics on cell viability count (**Figure 2.7a**). In a monoculture fermentation, LYglc1 reached a maximum population density of $1.2 \pm 0.2 \times 10^9$ CFU mL^{-1} by 24 h before then rapidly decreasing to $1.2 \pm 0.2 \times 10^4$ CFU mL^{-1} by the end of the 96 h fermentation (**Figure 2.7a**). Monocultures of LYxyl3 also peaked by 24 h, in this case reaching $2.2 \pm 0.4 \times 10^8$ CFU mL^{-1} (**Figure 2.7a**). However, unlike LYglc1, the viable population density of LYxyl3 was sustained at ~10^8 CFU mL^{-1} for the next 72 h before decreasing, although only by about one order of magnitude (to $1.2 \pm 0.4 \times 10^7$ CFU mL^{-1}) over the final 24 h.

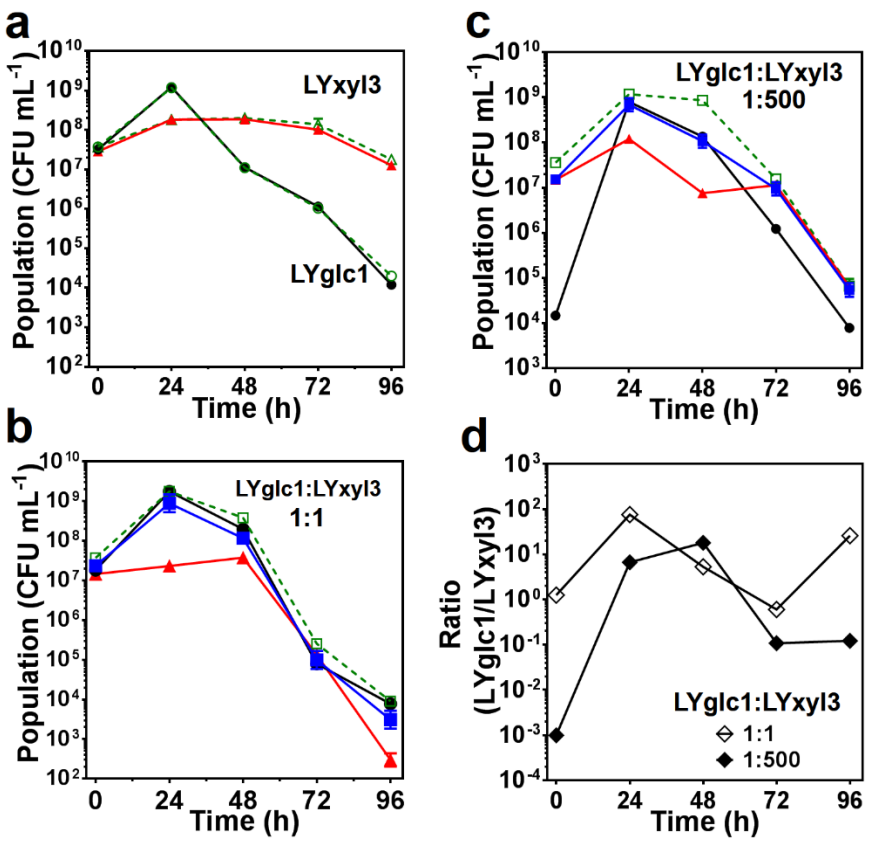

Figure 2.7. Population dynamics of the viable ethanologenic specialist strains during coculture fermentations using glucose-xylose mixtures.

Shows a) colony forming units (CFUs) of LYglc1 (Cm^R; circles) and LYxyl3 (Kan^R; triangles) were measured using LB plates (dotted lines) and LB plates containing appropriate antibiotics (solid lines). Coculture batch fermentations of LYglc1:LYxyl3 with the inoculum ratios of b) 1:1 and c) 1:500 were performed in mineral salts medium containing the total 100 g L^{-1} glucose-xylose mixtures (approximately 2:1 by mass). CFUs mL^{-1} were measured at different time intervals using agar plates containing LB only (dotted lines with open squares), LB with chloramphenicol (black solid lines with solid circles), LB with kanamycin (red solid lines with triangles), and the added numbers (blue solid lines with solid square) obtained from the latter two agar plates. d)The ratio of LYglc1 over LYxyl3 was plotted for coculture fermentations of LYglc1:LYxyl3 with the inoculum ratios of 1:1 (open diamond) and 1:500 (solid diamond).

Population dynamics were next investigated in cocultures with an inoculum ratio of 1:1 between LYglc1 and LYxyl3 (**Figure 2.7b**). In this case, LYglc1 was found to dominate the population throughout the majority of the fermentation. For example, by 24 h, LYglc1

reached a viable cell density on the order of 10^9 CFU mL^{-1} (approximately a 100-fold increase from inoculation and similar to the maximum level achieved during its monoculture fermentation; **Figure 2.7a**), whereas that of LYxyl3 still remained on the order of just about 10^7 CFU mL^{-1} (at least a 10-fold decrease relative to the level achieved during its monoculture fermentation over the same time; **Figure 2.7a** and **2.7b**). By 48 h, viable populations of both strains had severely declined, continuing for the remainder of the fermentation. The observation that, relative to growth in monocultures, LYxyl3 struggled to grow in the presence of LYglc1 suggests that inter-strain interactions might exist within the coculture system. Major fermentation pathways to produce organic acids such as succinate, lactate, and acetate were inactivated in LY180.[30] Therefore, it is unlikely that the decreased fitness of LYxyl3 was caused by these fermentation acidic byproducts due to their limited amount. These undefined metabolic interactions warrant future investigation. Population dynamics were next investigated using an initial inoculum ratio of 1:500 (LYglc1:LYxyl3). Despite of the difference in their initial relative abundance ($1.4 \pm 0.1 \times 10^4$ vs. $1.4 \pm 0.2 \times 10^7$ CFU mL^{-1} for LYglc1 and to LYxyl3, respectively), however, by 24 h the relative population of LYglc1 actually surpassed that of LYxyl3 (reaching about 10^9 vs. 10^8 CFU mL^{-1}, respectively; **Figure 2.7c**). Following this peak, both populations declined over the next 72 h, with the biggest decrease again occurring in the case of LYglc1. Notably, compared with the 1:1 initial inoculum ratio, reduction in population of LYxyl3 was less rapid and less severe when using an initial inoculum ratio of 1:500 (**Figure 2.7c**). Thus, by significantly increasing the relative abundance of LYxyl3 in the starting inoculum, more xylose specialists were capable of persisting throughout the duration of the fermentation, leading to improved overall xylose utilization (**Figure 2.7d**).

Therefore, in addition to balancing relative catabolic activities, this community-level tuning strategy furthermore enables compensation for fitness differences between community members, which likewise aids in improving overall performance of cocultures.

2.3 Conclusions

To conclude, we successfully engineered a series of catabolically-orthogonal coculture systems derived from wild-type and ethanologenic *E. coli* strains for co-utilization of glucose-xylose mixtures (≥98% of 100 g L^{-1} total sugar utilized for both cases). A community-level tuning strategy proved effective for balancing relative catabolic rates and differences in strain fitness. Optimal tuning of the ethanologenic coculture system led to an overall specific rate of total sugar utilization 50% faster (480 mg $gDCW^{-1}$ h^{-1}) than LY180 monoculture fermentations (320 mg $gDCW^{-1}$ h^{-1}). Final ethanol titers achieved 46 ± 1 g L^{-1} (90% of maximum theoretical yield), a 28% improvement over LY180 monocultures. With continued development, this engineering strategy of synthetic cocultures could be further expanded to include more specialist strains with unique and complementary metabolic activities, which will enable optimal co-utilization of complex lignocellulose-derived substrates to produce diverse chemicals.

2.4 Methods

2.4.1 Strain Construction

All strains and plasmids used in chapter 2 are listed in **Table 2.3**. The primers used in this study are listed in **Table 2.4.** All chromosomal modifications were conducted using a λ-red recombinase-mediated method as previously described.[68,92,93] Positive clones with the primary integration of the *cat-sacB* cassette into the target chromosomal region were

selected for conferred chloramphenicol resistance and subsequently verified by colony PCR and Sanger sequencing. The positive clones with the secondary integration to eliminate the *cat-sacB* cassette were identified by screening for insensitivity to sucrose (10% w/v), and loss of the *cat-sacB* cassette by colony PCR and Sanger sequencing.

Table 2.3 List of strains and plasmids used to construct wild-type and ethanologenic derived sugar specialist in Chapter 2.

Strains and Plasmids	Relevant Characteristics	Source
Strains		
E. coli W	wild-type	ATCC
LN06	*E. coli* W *xylR*::*xylR**	71
WTglc	*E. coli* W Δ*xylR*	This Study
WTxyl1	LN06 Δ*ptsI*	This Study
WTxyl2	WTxyl1 Δ*ptsG*	This Study
WTxyl3	WTxyl1 Δ*galP*	This Study
WTxyl4	WTxyl2 Δ*galP*	This Study
LY180	*frdBC*::(*Zm frg celY*$_{Ec}$ *)* Δ*ldhA*::*(Zm frg casAB*$_{Ko}$) *adhE*::(*Zm frg estZ*$_{Pp}$ *FRT)* Δ*ackA*::FRT *rrlE*::(*pdc adhA adhB* FRT) Δ*mgsA::*FRT	86
LYglc	LY180 Δ*xylR*	This Study
LYglcCm	LYglc *lacZ*::*cat-sacB* (Cm^R)	This Study
LYglc1	LYglcCm adapted in glucose-xylose mixtures (Cm^R)	This Study
LYxyl1	LY180 Δ*ptsI* Δ*ptsG* Δ*galP*	This Study
LYxyl2	LYxyl1 *glk*::*kan*^{R} (Kan^R)	This Study
LYxyl3	LYxyl2 *xylR*::*xylR** (Kan^R)	This Study
Plasmids		
XW001	*The cat-sacB* cassette with the *sacB* native terminator cloned into a modified vector pLOI4162	71
pKD46	Red recombinase, temperature-conditional, *bla*	92

Table 2.4 List of primers used to construct wild-type and ethanologenic derived sugar specialist in Chapter 2**.**

F denotes, forward primer; R denotes, reverse primer; H1 corresponds to 500 bp upstream of the gene of interests; H2 corresponds to 500 bp downstream of the gene of interests.

***ptsI* deletion**	
cat-sacB F	GAGTAATTTCCCGGGTTCTTTTAAAAATCAGTCACAAGTAAGGTAGGGTTTCGAGTGTGACGGAAGATC A
cat-sacB R	ACAAACCCATGATCTTCTCCTAAGCAGTAAATTGGGCCGCATCTCGTGGATTAGCCATTTGCCTGCTTTT
*ptsI H1*F	AATCAGTCACAAGTAAGGTAGGGTTTCCACGAGATGCGGCCCAAT T
ptsI H1 R	CCGGAGTCAGGGTAGACTTG
ptsI H2 F	AATTGGGCCGCATCTCGTGGAAACCCTACCTTACTTGTGACTGAT
ptsI H2 R	ACTGTATTGCGCTCTTCGTG
***ptsG* deletion**	
cat-sacB F	CACGCGTGAGAACGTAAAAAAAGCACCCATACTCAGGAGCACTCTCAATTTCGAGTGTGACGGAAGATC A
cat-sacB R	GTAAAAAAGGCAGCCATCTGGCTGCCTTAGTCTCCCCAACGTCTTACGGATTAGCCATTTGCCTGCTTTT
*ptsG H1*F	CGGTTACTGGTGGAAACTGACTCAC
ptsG H1 R	CTTAGTCTCCCCAACGTCTTACGGAAATTGAGAGTGCTCCTGAGTATGGGT
ptsG H2 F	ACCCATACTCAGGAGCACTCTCAATTTCCGTAAGACGTTGGGGAGACTAAG
ptsG H2 R	GACAGTCAGTAAAGGGGTGGAATTTGAAC
***galP* deletion**	
cat-sacB F	TACTCACCTATCTTAATTCACAATAAAAAATAACCATATTGGAGGGCATCTCGAGTGTGACGGAAGATC A
cat-sacB R	GATGACTGCAAGAGGTGGCTTCCTCCGCGATGGGAGGAAGCTTGGGGAGATTAGCCATTTGCCTGCTTTT
*galP H1*F	GGTCGTGAACATTTCCCGTGG
galP H1 R	TGGGAGGAAGCTTGGGGAGAGATGCCCTCCAATATGGTTATTTTTTATTGTGAAT
galP H2 F	ATTCACAATAAAAAATAACCATATTGGAGGGCATCTCTCCCCAAGCTTCCTCCCA
galP H2 R	CGGTAAGCTGATGCTCCTGG
***xylR* deletion**	
cat-sacB F	TCTCAAAGCCGGTTACGTATTACCGGTTTTGAGTTTTTGCATGATTCAGCTCGAGTGTGACGGAAGATCA
cat-sacB R	GATAAGGCTTTTGCTCGCATCAGGTGGCTGTGCTGAGTTCCCTGATGTGACCTTAGCCATTTGCCTGCT
*xylR H1*F	CTGTTACTCGGCGGAATGTT
xylR H1 R	GACGCCGACAATTCTCATCATCGGGTTCCTTTTCCTGCTGAATCATGC
xylR H2 F	GCATGATTCAGCAGGAAAAGAACCCGATGATGAGAATTGTCGGCGTC
xylR H2 R	CTTGCTTGAACGCGTAGACA
lacZ replacement	

cat-sacB F	TCACACAGGAAACAGCTATGACCATGATTACGGATTCACTGGCCGTCGTTTCGAGTGTGACGGAAGATCA
cat-sacB R	CATTCGCCATTCAGGCTGCGCAACTGTTGGGAAGGGCGATCGGTGCGGGCCCTTAGCCATTTGCCTGCT
glk replacement	
kan F	ATTTACAGTGTGAGAAAGAATTATTTTGACTTTAGCGGAGCAGTTGAAGAGTGTAGGCTGGAGCTGCTTC
kan R	TGATTTAAAAGATTATCGGGAGAGTTACCTCCCGATATAACAGGAAGGATCATATGAATATCCTCCTTAGT

2.4.2 Fermentation Condition and Media

All strains were fermented in a modified version of AM1 minimal salt medium[94] prepared as follows: 38.8 mM $(NH_4)_2H_2PO_4$, 15.1 mM $(NH_4)H_2PO_4$, 4.00 mM KCl, 3.00 mM $MgSO_4 \cdot 7H_2O$, 2.00 mM Betaine, 17.8 µM $FeCl_3 \cdot 6H_2O$, 2.52 µM $CoCl_2 \cdot 6H_2O$, 1.76 µM $CuCl_2 \cdot 2H_2O$, 4.40 µM $ZnCl_2$, 2.48 µM $Na_2MO_4 \cdot 2H_2O$, 2.42 µM H_3BO_3, and 5.00 µM $MnCl_2 \cdot 4H_2O$. The coculture batch fermentations were typically performed three times independently similarly as previously described for monoculture fermentation.[68,82] A glucose-xylose mixture with a total sugar concentration of 100 g L^{-1} was used for all fermentations. During strain construction, a glucose:xylose mass ratio of 1:1 was employed. However, this ratio was later switched to 2:1 to better represent the relative abundance of each sugar in a typical biomass sample.[2,81] All monoculture and coculture batch fermentations were inoculated using a total initial OD_{550nm} of 0.05 (approximately 0.022 g dry cell weight (DCW) L^{-1}) and cells were grown at 37 °C in a fermentation vessel with pH maintained at 7.0 by automatic addition of base (2.0 M and 6.0 M KOH for LY180 and W derived strains, respectively).

2.4.3 Analytical Methods and Data Analysis

Cell growth was monitored by measuring OD_{550nm} using a UV/Vis spectrophotometer (Beckman Coulter DU-730; Indianapolis, IN). Substrate and product levels were analyzed

using HPLC (Thermo Fisher Scientific UltiMate 3000, Waltham, MA) as previously described.[68,84] Experimental data represent an average of three or more measurements with standard deviations.

2.4.4 Adaptive Laboratory Evolution to Improve Glucose Catabolism

The strain LYglcCm was repeatedly sub-cultured in media containing glucose to enhance glucose catabolism; once in 100 g L^{-1} glucose, then six additional times in glucose-xylose mixtures (66 g L^{-1} glucose and 34 g L^{-1} xylose). Sub-cultures were transferred to fresh media at approximately 24 h intervals with an initial OD_{550nm} of 0.05. After seven transfers, one evolved clone, designated as LYglc1, was chosen for further study.

2.4.5 Quantification of Viable Cells of Individual Specialist Strains in Cocultures

Each ethanologenic specialist strain was engineered with resistance to either kanamycin or chloramphenicol. Samples were removed from fermentation cultures and colony forming units (CFUs) were manually counted after cells with serial dilutions were plated on LB only plates and LB plates containing appropriate antibiotics.

2.4 References

2 Saha, B. C. Hemicellulose bioconversion. *J Ind Microbiol Biotechnol* **30**, 279-291 (2003).

8 Kim, J. H., Block, D. E. & Mills, D. A. Simultaneous consumption of pentose and hexose sugars: an optimal microbial phenotype for efficient fermentation of lignocellulosic biomass. *Appl Microbiol Biot* **88**, 1077-1085 (2010).

10 Deutscher, J. The mechanisms of carbon catabolite repression in bacteria. *Curr Opin Microbiol* **11**, 87-93 (2008).

11 Gorke, B. & Stulke, J. Carbon catabolite repression in bacteria: many ways to make the most out of nutrients. *Nat Rev Microbiol* **6**, 613-624, doi:10.1038/nrmicro1932 (2008).

16 Kotrba, P., Inui, M. & Yukawa, H. Bacterial phosphotransferase system (PTS) in carbohydrate uptake and control of carbon metabolism. *J Biosci Bioeng* **92**, 502-517 (2001).

34 Gosset, G. Improvement of Escherichia coli production strains by modification of the phosphoenolpyruvate:sugar phosphotransferase system. *Microb Cell Fact* **4**, 14, doi:10.1186/1475-2859-4-14 (2005).

35 Dien, B. S., Nichols, N. N. & Bothast, R. J. Fermentation of sugar mixtures using Escherichia coli catabolite repression mutants engineered for production of L-lactic acid. *J Ind Microbiol Biotechnol* **29**, 221-227, doi:10.1038/sj.jim.7000299 (2002).

42 Chiang, C. J. *et al.* Systematic Approach To Engineer Escherichia coli Pathways for Co-utilization of a Glucose-Xylose Mixture. *J Agr Food Chem* **61**, 7583-7590 (2013).

47 Eiteman, M. A., Lee, S. A. & Altman, E. A co-fermentation strategy to consume sugar mixtures effectively. *J Biol Eng* **2**, 3, doi:10.1186/1754-1611-2-3 (2008).

48 Eiteman, M. A., Lee, S. A., Altman, R. & Altman, E. A substrate-selective co-fermentation strategy with Escherichia coli produces lactate by simultaneously

consuming xylose and glucose. *Biotechnol Bioeng* **102**, 822-827, doi:10.1002/bit.22103 (2009).

49 Xia, T., Altman, E. & Eiteman, M. A. Succinate production from xylose-glucose mixtures using a consortium of engineered Escherichia coli. *Eng Life Sci* **15**, 65-72, doi:10.1002/elsc.201400113 (2015).

50 Chen, Y. Development and application of co-culture for ethanol production by co-fermentation of glucose and xylose: a systematic review. *J Ind Microbiol Biotechnol* **38**, 581-597, doi:10.1007/s10295-010-0894-3 (2011).

52 Xia, T., Eiteman, M. A. & Altman, E. Simultaneous utilization of glucose, xylose and arabinose in the presence of acetate by a consortium of Escherichia coli strains. *Microb Cell Fact* **11**, 77, doi:10.1186/1475-2859-11-77 (2012).

66 Kumar, R., Singh, S. & Singh, O. V. Bioconversion of lignocellulosic biomass: biochemical and molecular perspectives. *J Ind Microbiol Biotechnol* **35**, 377-391, doi:10.1007/s10295-008-0327-8 (2008).

67 Jeffries, T. W. Engineering yeasts for xylose metabolism. *Curr Opin Biotechnol* **17**, 320-326, doi:10.1016/j.copbio.2006.05.008 (2006).

68 Sievert, C. *et al.* Experimental evolution reveals an effective avenue to release catabolite repression via mutations in XylR. *Proc Natl Acad Sci U S A* **114**, 7349-7354, doi:10.1073/pnas.1700345114 (2017).

69 Geddes, C. C. *et al.* Simplified process for ethanol production from sugarcane bagasse using hydrolysate-resistant Escherichia coli strain MM160. *Bioresour Technol* **102**, 2702-2711, doi:10.1016/j.biortech.2010.10.143 (2011).

70 Sawisit, A. *et al.* Mutation in galP improved fermentation of mixed sugars to succinate using engineered Escherichia coli AS1600a and AM1 mineral salts medium. *Bioresource Technol* **193**, 433-441 (2015).

71 Song, H., Ding, M. Z., Jia, X. Q., Ma, Q. & Yuan, Y. J. Synthetic microbial consortia: from systematic analysis to construction and applications. *Chem Soc Rev* **43**, 6954-6981, doi:10.1039/c4cs00114a (2014).

72 Lu, H., Villada, J. C. & Lee, P. K. H. Modular Metabolic Engineering for Biobased Chemical Production. *Trends Biotechnol*, doi:10.1016/j.tibtech.2018.07.003 (2018).

73 Hays, S. G., Patrick, W. G., Ziesack, M., Oxman, N. & Silver, P. A. Better together: engineering and application of microbial symbioses. *Curr Opin Biotechnol* **36**, 40-49, doi:10.1016/j.copbio.2015.08.008 (2015).

74 Chappell, T. C. & Nair, N. U. Co-utilization of hexoses by a microconsortium of sugar-specific E. coli strains. *Biotechnol Bioeng* **114**, 2309-2318, doi:10.1002/bit.26351 (2017).

75 Maleki, N., Safari, M. & Eiteman, M. A. Conversion of glucose-xylose mixtures to pyruvate using a consortium of metabolically engineered Escherichia coli. *Eng Life Sci* **18**, 40-47, doi:10.1002/elsc.201700109 (2018).

76 Zhang, H., Pereira, B., Li, Z. & Stephanopoulos, G. Engineering Escherichia coli coculture systems for the production of biochemical products. *Proc Natl Acad Sci U S A* **112**, 8266-8271, doi:10.1073/pnas.1506781112 (2015).

77 Zhang, H., Li, Z., Pereira, B. & Stephanopoulos, G. Engineering E. coli-E. coli cocultures for production of muconic acid from glycerol. *Microb Cell Fact* **14**, 134, doi:10.1186/s12934-015-0319-0 (2015).

78 Zhang, H. R. & Wang, X. N. Modular co-culture engineering, a new approach for metabolic engineering. *Metab Eng* **37**, 114-121 (2016).

79 Shin, H. D., McClendon, S., Vo, T. & Chen, R. R. Escherichia coli binary culture engineered for direct fermentation of hemicellulose to a biofuel. *Appl Environ Microbiol* **76**, 8150-8159, doi:10.1128/AEM.00908-10 (2010).

80 Monk, J. M. *et al.* Multi-omics Quantification of Species Variation of Escherichia coli Links Molecular Features with Strain Phenotypes. *Cell Syst* **3**, 238-251 e212, doi:10.1016/j.cels.2016.08.013 (2016).

81 Saha, B. C., Iten, L. B., Cotta, M. A. & Wu, Y. V. Dilute acid pretreatment, enzymatic saccharification, and fermentation of rice hulls to ethanol. *Biotechnol Prog* **21**, 816-822, doi:10.1021/bp049564n (2005).

82 Yomano, L. P., York, S. W., Shanmugam, K. T. & Ingram, L. O. Deletion of methylglyoxal synthase gene (mgsA) increased sugar co-metabolism in ethanol-producing Escherichia coli. *Biotechnol Lett* **31**, 1389-1398, doi:10.1007/s10529-009-0011-8 (2009).

83 Miller, E. N. *et al.* Silencing of NADPH-dependent oxidoreductase genes (yqhD and dkgA) in furfural-resistant ethanologenic Escherichia coli. *Appl Environ Microbiol* **75**, 4315-4323, doi:10.1128/AEM.00567-09 (2009).

84 Yomano, L. P., York, S. W., Zhou, S., Shanmugam, K. T. & Ingram, L. O. Re-engineering Escherichia coli for ethanol production. *Biotechnol Lett* **30**, 2097-2103 (2008).

85 McDonald, T. P., Walmsley, A. R. & Henderson, P. J. Asparagine 394 in putative helix 11 of the galactose-H+ symport protein (GalP) from Escherichia coli is associated with the internal binding site for cytochalasin B and sugar. *J Biol Chem* **272**, 15189-15199 (1997).

86 Brenner, K., You, L. & Arnold, F. H. Engineering microbial consortia: a new frontier in synthetic biology. *Trends Biotechnol* **26**, 483-489, doi:10.1016/j.tibtech.2008.05.004 (2008).

87 Shong, J., Jimenez Diaz, M. R. & Collins, C. H. Towards synthetic microbial consortia for bioprocessing. *Curr Opin Biotechnol* **23**, 798-802, doi:10.1016/j.copbio.2012.02.001 (2012).

88 Liu, F. *et al.* Bioconversion of distillers' grains hydrolysates to advanced biofuels by an Escherichia coli co-culture. *Microb Cell Fact* **16**, 192, doi:10.1186/s12934-017-0804-8 (2017).

89 Khankal, R., Chin, J. W. & Cirino, P. C. Role of xylose transporters in xylitol production from engineered Escherichia coli. *J Biotechnol* **134**, 246-252 (2008).

90 Hasona, A., Kim, Y., Healy, F. G., Ingram, L. O. & Shanmugam, K. T. Pyruvate formate lyase and acetate kinase are essential for anaerobic growth of Escherichia coli on xylose. *J Bacteriol* **186**, 7593-7600 (2004).

91 Wang, L., York, S. W., Ingram, L. O. & Shanmugam, K. T. Simultaneous fermentation of biomass-derived sugars to ethanol by a co-culture of an

engineered Escherichia coli and Saccharomyces cerevisiae. *Bioresour Technol* **273**, 269-276, doi:10.1016/j.biortech.2018.11.016 (2018).

92 Datsenko, K. A. & Wanner, B. L. One-step inactivation of chromosomal genes in Escherichia coli K-12 using PCR products. *Proc Natl Acad Sci U S A* **97**, 6640-6645, doi:10.1073/pnas.120163297 (2000).

93 Jantama, K. *et al.* Eliminating side products and increasing succinate yields in engineered strains of Escherichia coli C. *Biotechnol Bioeng* **101**, 881-893, doi:10.1002/bit.22005 (2008).

94 Martinez, A. *et al.* Low salt medium for lactate and ethanol production by recombinant Escherichia coli B. *Biotechnol Lett* **29**, 397-404 (2007).

CHAPTER 3

CATABOLIC DIVISION OF LABOR ENHANCES PRODUCTION OF D-LACTATE AND SUCCINATE FROM GLUCOSE-XYLOSE MIXTURES IN ENGINEERED *ESCHERICHIA COLI* COCULTURE SYSTEMS

Abstract

Although biological upgrading of lignocellulosic sugars represents a promising and sustainable route to bioplastics, diverse and variable feedstock compositions (e.g. glucose from the cellulose fraction and xylose from the hemicellulose fraction) present several complex challenges. Specifically, sugar mixtures are often incompletely metabolized due to carbon catabolite repression while composition variability further complicates the optimization of co-utilization rates. Benefiting from several unique features including division labor, increased metabolic diversity, and modularity, synthetic microbial communities represent a promising platform with the potential to address persistent bioconversion challenges. In this work, two unique and catabolically-orthogonal *E. coli* cocultures systems were developed and used to enhance the production of D-lactate and succinate (two bioplastic monomers) from glucose-xylose mixtures (100 g L^{-1} total sugars, 2:1 by mass). In both cases, glucose specialist strains were engineered by deleting *xylR* (encoding the xylose-specific transcriptional activator, XylR) to disable xylose catabolism, whereas xylose specialist strains were engineered by deleting several key components involved with glucose transport and phosphorylation systems (i.e., *ptsI*, *ptsG*, *galP*, *glk*) while also increasing xylose utilization by introducing specific *xylR* mutations. Optimization of initial population ratios between complementary sugar specialists proved a key design variable for each pair of strains. In both cases, ~91% utilization of total sugars was achieved in mineral salt media by simple batch fermentation. High product titer (88 g L^{-1} D-lactate, 84 g L^{-1} succinate), maximum productivity (2.5 g L^{-1} h^{-1} D-lactate, 1.3 g L^{-1} h^{-1} succinate) and product yield (0.97 g g-total $sugar^{-1}$ for D-lactate, 0.95 g g-total $sugar^{-1}$ for succinate) were also achieved.

This chapter contains excerpts and reproductions from:

Flores, A. D., Choi, H. G., Martinez, R., Onyeabor, M., Ayla, E. Z., Godar, A., Nielsen, D. R., & Wang, X. (2020). Catabolic Division of Labor Enhances Production of D-Lactate and Succinate From Glucose-Xylose Mixtures in Engineered Escherichia coli Coculture Systems. *Frontiers in Bioengineering and Biotechnology*, *8*, 329.

3.1 Introduction

As demonstrated in Chapter 2, division of labor can overcome paramount hurdles related to the biological upgrading of lignocellulosic sugars, and even, outperform monocultures. In this chapter we extend this strategy by applying analogous principles to engineer two unique coculture systems composed of catabolically-orthogonal *E. coli* strains for the production of LA and SA from glucose-xylose mixtures

Production of D-lactate (LA) and succinate (SA) from renewable carbohydrate feedstocks provides a sustainable and greener alternative to their petroleum-based production.[95-97] LA and SA serve as two important monomers in the production of biodegradable plastics, including poly(butylene succinate) (PBS) and poly(lactic acid) (PLA), respectively. SA is largely produced via petroleum-derived maleic anhydride and only a handful of plants producing bio-based SA currently exist.[98] Meanwhile, ~95% of global LA production occurs via fermentation, being derived almost entirely from costly raw materials such as grain starch or sucrose from sugar cane; feedstocks that compete with the food chain.[99,100] Alternatively, lignocellulose-derived sugars from non-food carbohydrates such as agricultural resides, forest products or energy crops represent an attractive feedstock for producing bio-based plastics due to their increased abundance and sustainability, as well as lower cost. [101] The two most abundant sugars in most lignocellulosics are glucose (a hexose, accounting for ~30-50% dry wt.) from the cellulose fraction and xylose (a pentose, constituting ~20-35% dry wt.) from the hemicellulose fraction.[102] Minute quantities of other fermentable sugars (i.e., arabinose, galactose, mannose) are additionally found in lignocellulosic biomass.[102]

For many native and engineered bacteria, the inability to efficiently co-utilize sugar mixtures in mineral salts medium at high catabolic rates (e.g., > 2 g L^{-1} h^{-1} for each sugar) is due to a complex, global regulatory phenomenon known as carbon catabolite repression (CCR), which often results in incomplete and/or sequential sugar utilization. For instance, in *Escherichia coli*, this sequential sugar preference is controlled via the coordinated action of the global transcriptional regulator cyclic AMP (cAMP) receptor protein (CRP) along with a second regulator specific to the secondary sugars of interest, such as xylose. For example, activation of the requisite xylose catabolism operons (i.e., *xylFGH* and *xylAB*) requires both activated CRP (active when bound by cAMP) and XylR (regulator specific for xylose catabolism, active when bound by xylose)[103] (**Figure 3.1**). When wild-type *E. coli* ferments glucose-xylose mixtures, for example, cAMP levels are low because abundant extracellular glucose leads to the active mode of the phosphotransferase system (PTS), increasing the abundance of unphosphorylated PTS components (IIA protein) and inhibiting the activity of adenylyl cyclase (AC; catalyzing cAMP synthesis). Xylose catabolism thus does not occur due to the lack of activated CRP and, as a result, initiates only after glucose is mostly utilized and phosphorylated IIA protein activates AC, leading to high cAMP levels (**Figure 3.1**).

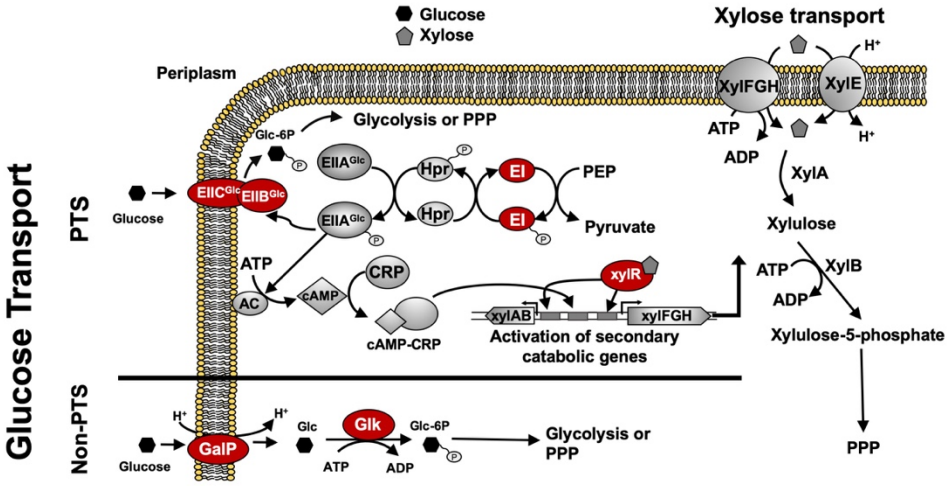

Figure 3.1 Regulatory and catabolic pathways for glucose and xylose metabolism in *E. coli*.

The primary mechanism for glucose transport in E. coli is through the phosphoenolpyruvate: sugar phosphotransferase system (PTS), including components EIIBC^{Glc}, EIIA^{Glc}, Hpr, and EI (encoded by ptsG, crr, ptsH and ptsI, respectively). Under high glucose concentrations, glucose is transported via EIICB^{glc} leading to more abundant unphosphorylated EIICA^{glc} that inhibits adenylate cyclase (AC) and lowers cAMP levels. Glucose-induced catabolite repression is mainly caused by low levels of cAMP which leads to nonfunctional CRP. Without CRP activation, the transcriptional activation of xylose catabolism pathways cannot be achieved. Under low glucose concentrations, AC is active due to the decreased amount of unphosphorylated EIICA^{glc}, thus leading to increased cAMP levels and activated CRP. Both activated CRP and XylR (activated when bound by xylose) are required to activate the xylose catabolic operons, xylAB and xylFGH. Phosphorylated sugar intermediates enter glycolysis or PPP pathways for full degradation. GalP functions as an alternative non-PTS glucose transporter and glk encodes cytoplasmic glucokinase to phosphorylate glucose for further glycolysis. Glucose uptake systems including both PTS components and GalP as well as Glk and XylR indicated in red ovals are genetic engineering targets to construct sugar specialists. Abbreviation: AC, adenylate cyclase; CRP, cAMP receptor protein; PPP, the pentose phosphate pathway; Glc, glucose; Glc-6P, Glucose 6-phosphate; Xyl; xylose.

To date, several engineered microorganisms producing LA (e.g., lactic-acid bacteria (LAB), *Saccharomyces cerevisiae, E. coli*) and SA (e.g., *Mannheimia succiniciproducens, Corynebacterium glutamicum, Bacillus* strains) have been reported using various

substrates.[104-108] While different strains have their own unique advantages/disadvantages (e.g., ease of genetic manipulation, product tolerance, and other physiological benefits), from a bioprocessing perspective it is desirable that it should also be capable of rapidly and simultaneously utilizing the substrate at high initial loadings (e.g., ≥ 100 g L^{-1} total sugar). Under such conditions, *E. coli* has proven to be a particularly promising biocatalyst for the production of both LA and SA. In particular, via a combination of engineering strategies, *E. coli* strains have been developed to produce both LA and SA at high yields (>90%), titers (>90 g L^{-1}) and maximum productivities (>1.0 g L^{-1} h^{-1}). [68,109,110] Despite these achievements, however, challenges still remain with respect to the efficient conversion of glucose-xylose mixtures.

Owing to unique features such as strain-specific specialization and metabolic modularity, the engineering and use of synthetic microbial communities represents a promising bioprocessing strategy[76,111-113], with the potential to surmount many limitations faced by traditional monocultures. [114,115] Through catabolic division of labor, for example, engineered cocultures have specifically emerged as an effective strategy for achieving efficient co-utilization of different mixtures of lignocellulose-derived sugars.[47,74,76,116] Eiteman and co-workers first demonstrated the utility of this approach, engineering a coculture composed of *E. coli* sugar specialist strains to co-utilize glucose-xylose mixtures (~14 g L^{-1} total sugars).[47] This general strategy was later expanded upon by others to develop a three-member community of *E. coli* specialists to co-utilize a mixture of glucose, galactose, and mannose (~7.5 g L^{-1} total sugars).[74] Most recently, meanwhile, our group engineered two different, catabolically-orthogonal coculture systems (derived from wild-type *E. coli* W or ethanologenic *E. coli* LY180), each capable of co-utilizing 100 g L^{-1} of

a glucose-xylose mixture (2:1 by wt.) in mineral salt media by simple batch fermentation.[117] In this work, we further explore the utility of this strategy by applying analogous principles to engineer two unique coculture systems composed of catabolically-orthogonal *E. coli* strains for the production of LA and SA from glucose-xylose mixtures. In both cases, optimization of initial population ratios between each strain pair proved a key design variable towards achieving efficient conversion of the feedstock mixture along with high production metrics. This strategy of 'population-level' tuning helps to alleviate biosynthetic burden while circumventing technical difficulties that would otherwise accompany the more traditional optimization of multiple catabolic pathways in a single strain.

3.2 Results and Discussion

3.2.1 Construction of Catabolically-Orthogonal Sugar Specialist for D-Lactate Production

TG114 (a derivative of *E. coli* KO11 and based on *E. coli* W) has previously been shown to produce LA at maximum volumetric productivity (2.88 g L^{-1} h^{-1}), titer (118 g L^{-1}), yield (98%) and chiral purity (>99.9%) in mineral salts medium containing 120 g L^{-1} glucose.[106] In spite of this, however, poor performance is apparent in sugar-mixtures as a result of CCR (**Figure 3.2 A-D**). Specifically, when cultured using a 100 g L^{-1} glucose-xylose mixture (2:1 by mass), TG114 utilized 88% of the provided glucose within the first 24 h and 100% by 48 h, but only 38% of the supplied xylose by 96 h; corresponding to only ~80% total sugar utilization. LA was produced, meanwhile, at overall and maximum volumetric productivities (Q_{LA}) of 0.80 ± 0.01 and 2.6 ± 0.4 g L^{-1} h^{-1}, a final titer of 77 ± 1 g L^{-1}, and yield ($Y_{p/s}$) of 0.96 ± 0.02 g g-total sugars^{-1}. To overcome the sugar co-utilization

bottleneck experienced by TG114, a division of labor approach was used to construct a pair of complementary, catabolically-orthogonal specialist strains, each capable of catabolizing either glucose or xylose but not both sugars (**Figure 3.3**). Specifically, a glucose specialist strain, TGglc, was constructed by deleting the xylose-specific transcriptional activator XylR (encoded by *xylR*) to inactivate xylose catabolism. A xylose specialist strain, TGxyl, was constructed by deleting the major components of glucose transport and its initial catabolism (i.e. *ptsI*, *ptsG*, *galP, glk*) (**Figure 3.1** and **Table 3.5**). To further enhance xylose utilization of this specialist strain, wild-type XylR was also replaced with a mutant copy (P363S and R121C; denoted as XylR* and reported to enable a stronger activation of the D-xylose catabolic genes.[68]

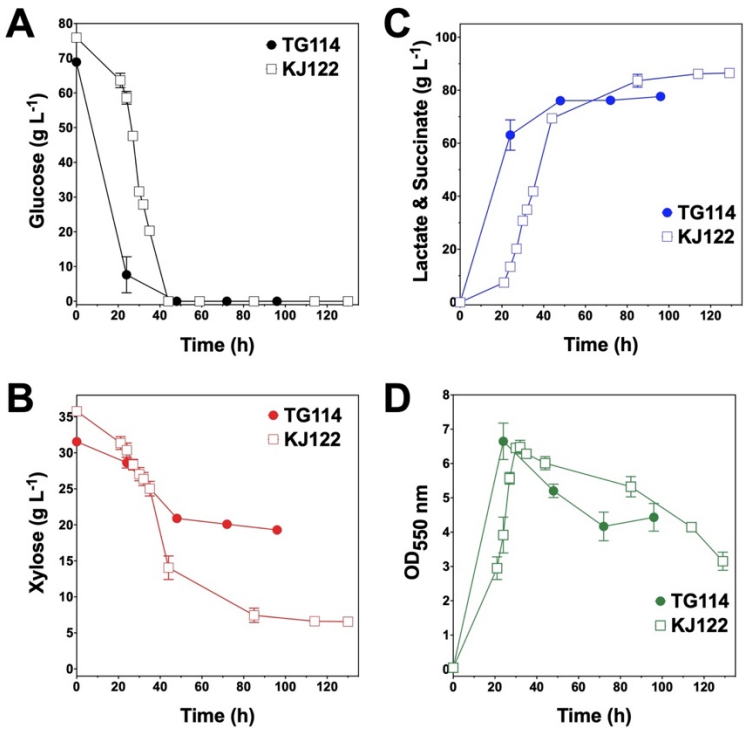

Figure 3.2 Fermentation of glucose-xylose mixtures by lactic acid-producing *E*. coli TG144 and succinogenic *E*. *coli* KJ122.

Concentrations of (A) glucose, (B) xylose, (C) succinate and (D) OD_{550nm} measured in the fermentation broth for TG114 (close circles), KJ122 (open squares). All fermentations were performed in batch mode and in mineral salts media. Data points represent the arithmetic mean of three replicates and error bars represent one standard deviation

Consistent with their respective genotypes, TGglc and TGxyl each preferentially utilized only one sugar when fermented in mineral salt media supplemented with 66 g L^{-1} glucose and 33 g L^{-1} xylose (**Figure 3.4A, 4B** and **Table 3.1**). TGglc utilized 100% of the supplied glucose within 48 h (77% within the first 24 h, similar to TG114) and virtually no xylose. This resulted in a maximum Q_{LA} of 2.0 ± 0.1 g L^{-1} h^{-1} (overall Q_{LA} was 0.68 ± .01 g L^{-1} h^{-1}), final LA titer of 66 ± 1 g L^{-1}, and $Y_{p/s}$ of 0.96 g g-total sugars $^{-1}$ (**Figure 3.4C,**

3.4D and **Table 3.1**). In contrast, under the same conditions, TGxyl consumed just ~80% of supplied xylose by 96 h and no glucose (**Figure 3.4A, 4B**). Growth of TGxyl, meanwhile, was significantly less than that of TGglc and TG114 (1.1 ± 0.1 g-dry cell weight (DCW) L^{-1}, compared to 2.7 ± 0.1 and 2.9 ± 0.2 gDCW L^{-1}, respectively). While this difference is at least in part due to the lower energy yield of xylose relative to glucose, it is also possible that, since TG114 was originally engineered for and adapted in mineral salt media containing only glucose as carbon source,[106] it may have only gained mutations specifically tailored for glucose catabolism. Despite its slower growth rate and reduced biomass accumulation, TGxyl still produced LA at a final titer of 25 ± 1 g L^{-1}, $Y_{p/s}$ of ~0.99 g g-total sugars $^{-1}$ and maximum Q_{LA} of 0.50 ± 0.08 g L^{-1} h^{-1} (**Figure 3.4C, 4D** and **Table 3.1**).

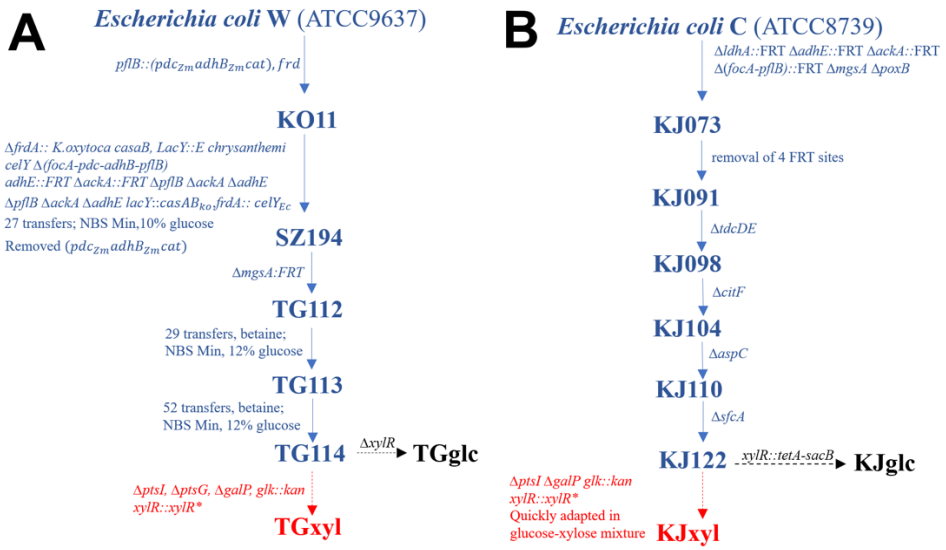

Figure 3.3 Strain lineage for the lactate-producing and succinate-producing sugar specialists.

(A) Strain lineage for lactic acid sugar specialists. (B) Strain lineage for succinic acid sugar specialists. Previously engineered strains are indicated by blue font. And solid arrows Glucose specialists are indicated by black font and dashed arrows. Xylose specialists are indicated by red font and dashed arrows.

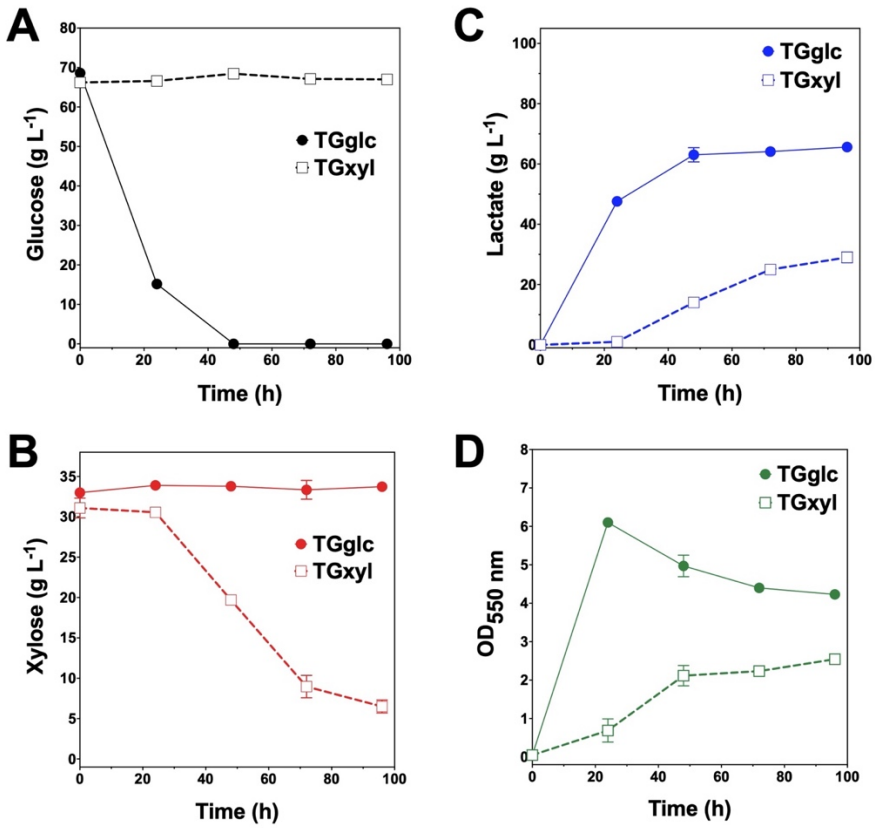

Figure 3.4 Fermentation of glucose-xylose mixtures (2:1 by mass) by lactate-producing sugar specialist strains.

Concentrations of (A) glucose, (B) xylose, (C) D-lactate and (D) OD_{550nm} measured in the fermentation broth for TGglc (closed circles) and TGxyl (open squares). All fermentations were performed in batch mode and in mineral salts media. Data points represent the arithmetic mean of three replicates and the error bars represent one standard deviation.

3.2.2 Engineering and Optimizing a Synthetic Coculture for Efficient Conversion of Glucose-Xylose Mixtures to D-Lactate

Given their promising performance metrics with respect to LA production and minimal cross-catabolic activities, TGglc and TGxyl were next used as complementary specialist strains with which to engineer a synthetic coculture. To balance catabolic rates, simple

titration of the initial inoculum ratio between TGglc and TGxyl (e.g. 1:1, 1:50, 1:100) while maintaining a constant total initial OD_{550nm} of 0.05 (the same initial OD_{550nm} as in monoculture fermentations) was performed. As shown in **Figure 3.5A** and **Table 3.1**, glucose was completely utilized within 48 h for all ratios (similar to TG144 and TGglc monocultures). However, as a result of tuning the initial population, initial volumetric rates of glucose utilization (Q_{Glc}) were subsequently reduced over the first 24 h in a manner proportional to the relative abundance of TGglc (2.4 ± 0.1, 0.82 ± 0.40, and 0.13 ± 0.02 g L^{-1} h^{-1} for ratios 1:1, 1:50, and 1:100, respectively), along with initial rates of biomass accumulation (**Figure 3.5D and Table 3.1**). The corresponding profiles of xylose fermentation (**Figure 3.5B**), meanwhile, revealed the opposite and expected effect with respect to xylose catabolism; increasing abundance of TGxyl in the initial inoculum improves xylose utilization. More specifically, at equal abundance (i.e., 1:1), total xylose utilization reached merely 22% by 96 h. This corresponded to 5% less total sugar utilization than by TG114 monocultures (75% vs. 80% total sugar utilization, respectively; **Table 3.1**). However, by tuning the initial inoculum ratio to 1:50, 2.6- and 1.5-fold increases in xylose utilization (58% total xylose used) were realized relative to cocultures with a 1:1 initial inoculum ratio and TG114 monocultures, respectively (**Table 3.1**). Owing to this significant increase in xylose co-utilization, final LA titers achieved by 1:50 cocultures reached 84 ± 2 g L^{-1} (~11% higher than the 1:1 coculture; **Figure 3.5C**), while still maintaining high overall performance metrics ($Y_{p/s}$ of 0.96 g g^{-1}, maximum Q_{LA} of 3.7 ± 1.1 g L^{-1} h^{-1}; **Table 3.1**). Further increasing the relative initial abundance of TGxyl, 1:100 cocultures then enabled further increased utilization of supplied xylose, in this case reaching ~71% (**Figure 3.5B**). Moreover, total sugar utilized reached 91% by the end of

the 96 h fermentation, achieving a final LA titer of 88 ± 1 g L^{-1}, $Y_{p/s}$ of ~0.97 g g-total $sugars^{-1}$, and maximum Q_{LA} of 2.5 ± 0.2 g L^{-1} h^{-1} (**Table 3.1**). Based on the promising trends observed with 1:50 and 1:100 cocultures, additional tuning of the inoculum ratio to further increase the initial abundance of TGxyl was subsequently performed, in this case at both 1:500 and 1:1000 (data not shown). However, no further performance enhancements were realized in terms of either total sugar utilization or LA production in such cocultures, suggesting that the optimal initial inoculum ratio for TGglc:TGxyl exists at least close to 1:100. Thus, further improvement of this coculture should next focus on enhancing the inherent properties of each individual strain; for example, increasing rates of xylose catabolism in sugar mixtures by TGxyl through adaptation and/or genetic engineering.

Table 3.1 Comparing the performance of individual *E. coli* sugar specialists and cocultures during LA and SA fermentation.

All cultures were initially supplied with ~100 g L^{-1} of glucose-xylose mixtures (ratio 2:1 by mass). Abbreviation: No Consumption (N.C.) < 1% sugar utilized; No Rate (N.R.) < 0.1 g L^{-1} h^{-1}. [A] *Total sugar utilized per sugar supplied.* [B] *Dry cell weight (DCW) values are calculated from maximum $OD_{550\ nm}$ (0.44 gDCW L^{-1} with an optical density of 1.0 at 550 nm).* [C] *Maximum volumetric rates (Q) are calculated when the slope of substrate utilization or product formation is most linear.* [D] *$Y_{p/s}$ denotes the product yield coefficient and is calculated as gram product per gram total sugar utilized*

Strains(s) Fermented	Sugar Utilized (%)			Biomass [B]	Q (g L^{-1} h^{-1})[C]			$Y_{p/s}$ g g^{-1} [D]	Titer g L^{-1}
	Glucose	Xylose	Total[A]	gDCW L^{-1}	Glucose	Xylose	Product		
Lactate									
TGglc	100 ± 0	N.C.	68 ± 1	2.7 ± 0.1	2.2 ± 0.1	N.R.	2.0 ± 0.1	0.96 ± 0.01	65 ± 1
TGxyl	N.C.	80 ± 2	25 ± 1	1.1 ± 0.1	N.R.	0.44 ± 0.01	0.50 ±0.08	0.99 ± 0.1	25 ± 1
TGglc:TGxyl Ratio 1:1	100 ± 0	22 ± 1	75 ± 1	2.8 ± 0.1	5.5 ± 0.4	0.35 ± 0.04	5.8 ± 0.5	0.99 ± 0.04	73 ± 2
TGglc:TGxyl Ratio 1:50	100 ± 0	58 ± 2	86 ± 1	2.7 ± 0.1	3.2 ± 0.6	0.44 ± 0.04	3.7 ± 1.1	0.95 ± 0.02	84 ± 2
TGglc:TGxyl Ratio 1:100	100 ± 0	71 ± 3	91 ± 1	2.7 ± 0.3	2.4 ± 0.2	0.52 ± 0.05	2.5 ± 0.2	0.97 ± 0.01	88 ± 1
Succinate									
KJglc	100 ± 0	N.C.	71 ± 1	2.9 ± 0.1	2.1 ± 0.1	N.R.	1.9 ± 0.1	0.88 ± 0.01	65 ± 1
KJxyl	N.C.	87 ± 2	28 ± 2	2.7 ± 0.2	N.R.	0.60 ± 0.06	0.69±0.20	1.21 ± 0.05	33 ± 1
KJglc:KJxyl Ratio 1:1	93 ± 5	89 ± 2	91 ± 4	3.1 ± 0.2	0.84 ±0.1	0.72 ± 0.04	1.3± 0.1	0.95 ± 0.01	84 ± 1
KJglc:KJxyl Ratio 1:50	19 ± 14	86 ± 2	39 ± 9	2.8 ± 0.2	0.49± 0.2	0.73 ± 0.1	0.82 ± 0.1	0.97 ± 0.1	37 ± 4
KJglc:KJxyl Ratio 1:100	6 ± 4	88 ± 1	31 ± 3	2.9 ± 0.1	0.2 ± 0.1	0.66 ± 0.06	0.69 ± 0.02	0.94 ± 0.1	29 ± 1
KJglc:KJxyl Ratio 2:1	100 ± 0	46 ± 4	83 ± 1	3.4 ± 0.1	1.4 ± 0.1	0.30 ± 0.09	2.1 ± 0.1	0.84 ± 0.08	76 ± 6

LA production performance demonstrated by the 1:100 coculture compares well to that of other cocultures previously-engineered for the same purpose, as well as those developed to produce other related fermentation products (**Table 3.2**). In particular, Eiteman et al.

developed an *E. coli* coculture composed of glucose and xylose specialists capable of co-utilizing and converting a sugar mixture (~47 g L^{-1} total sugar, ratio of glucose to xylose is 1.5:1 by mass) to LA (final titer of 32 g L^{-1}, $Y_{p/s}$ of 0.68 g g-total sugars $^{-1}$) in a two-stage, aerobic-anaerobic process (**Table 3.2**).[48] In this case, rather than tuning the initial population ratio, a sequential inoculation strategy was instead employed to balance the contribution of each specialist to the net catabolic activity, allowing more time initially for the xylose specialist strain to accumulate under aerobic conditions. Upon reaching the anaerobic phase, the population ratio in their coculture was estimated as 2:3 glucose:xylose specialists, which similarly illustrates a need for increased abundance of the xylose specialist in this fermentation. In comparison to LA producing monocultures, Sievert et al. demonstrated that substituting wild-type *xylR* with *xylR** (R121C and P363S; the same mutations used to develop TGxyl in this study) in TG114 enabled co-utilization of 50 g L^{-1} glucose and 43 g L^{-1} xylose (from 100 g L^{-1} glucose-xylose mixture, initially 1:1 by mass) to 86 g L^{-1} LA in mineral salt medium.[68] While minor improvement in terms of sugar utilization was achieved using the present coculture system, a unique advantage of this approach is the facile tunability that it provides. In this case, catabolic rates can be titrated to achieve optimal fermentation performance by altering initial inoculum ratios between the two specialists. This ability will likely be beneficial when utilizing feedstocks of varying compositions, and can be extended beyond simply binary sugar mixtures.

Table 3.2 Comparing the performance of different *E. coli* cocultures engineered to convert glucose and xylose to fermentative products.

A summary of selected E. coli coculture systems comparing media and fermentation condition(s), base strain and key mutations, product(s) and performance metric(s). [A] Gene deletion, disruption or modification. [B] q_{Glc} specific rate of glucose utilization ; Q_{Glc} volumetric rate of glucose utilization; q_{Xyl} specific rate of xylose utilization; Q_{Xyl} volumetric rate of xylose utilization (each calculated when the rate of utilization was approximately constant); Dry cell weight (DCW) calculated from maximum OD_{550nm} (0.44 gDCW L^{-1} with an optical density of 1.0 at 550 nm). [C] Fermentation consisted of two stages: initial aerobic growth followed by an anaerobic phase. [D] Minor amounts of succinate, acetate and ethanol were also detected.

Media and Fermentation Condition(s)	**Base Strain & Key Mutations[A]**	**Product(s)**	**Performance Metric(s)[B]**	**References**
Modified AM1 6.6% Glucose 3.4% Xylose Batch Microaerobic	Glucose: TG114 (an *E. coli* W derivative engineered for lactate production) Δ*xylR* Xylose: TG114 Δ*ptsI* Δ*ptsG* Δ*galP* Δ*glk xylR*::*xylR**	D-Lactate	$Q_{Glc} \approx 2.4$ g L^{-1} h^{-1} $q_{Glc} \approx 886$ mg $gDCW^{-1}$ h^{-1} $Q_{Xyl} \approx 0.5$ g L^{-1} h^{-1} $q_{Xyl} \approx 223$ mg $gDCW^{-1}$ h^{-1} Total Sugar Utilized ≈ 91g L^{-1} Titer ≈ 88g L^{-1} Productivity ≈ 2.5 g L^{-1} h^{-1} $Y_{p/s} \approx 0.97$	This Study
Basal 3.1% Glucose 2.0% Xylose Batch Aerobic-anaerobic[C]	Glucose: E. *coli* MG1655 *xylA748*::FRT *pflB*::Cam Xylose: *E. coli* MG1655 *pflB*::Cam *ptsG763*::FRT *manZ743*::FRT *glk-726*::FRT	D-Lactate	$q_{Glc} \approx 540$ mg $gDCW^{-1}$ h^{-1} $q_{Xyl} \approx 325$ mg $gDCW^{-1}$ h^{-1} Total Sugar Utilized ≈ 47 g L^{-1} Titer ≈ 32 g L^{-1} $Y_{p/s} \approx 0.68$	(Eiteman, Lee et al. 2009)
Modified AM1 6.6% Glucose 3.4% Xylose Batch Microaerobic	Glucose: KJ122 (an *E. coli* C derivative engineered for succinate production) *xylR*::*tetA-sacB* Xylose: KJ122 Δ*galP* Δ*ptsI* *glk*::*Kan*^{R} *xylR*::*xylR**	Succinate	$Q_{Glc} \approx 0.84$ g L^{-1} h^{-1} $q_{Glc} \approx 188$ mg $gDCW^{-1}$ h^{-1} $Q_{Xyl} \approx 0.72$ g L^{-1} h^{-1} $q_{Xyl} \approx 276$ mg $gDCW^{-1}$ h^{-1} Total Sugar Utilized ≈ 91 g L^{-1} Titer ≈ 84 g L^{-1} Productivity ≈ 1.3 g L^{-1} h^{-1} $Y_{p/s} \approx 0.95$ g g^{-1}	This Study
Basal Initial Sugar 3% Glucose 1% Xylose Fed 1.5% Glucose 0.5% Xylose Fed-Batch Aerobic-Anaerobic[D]	Glucose: E. *coli* ATCC8739 *ptsG*::FRT *xylA*::FRT *pflB*::FRT *ldhA*::Kan^R Xylose: *E. coli* ATCC8739 *ptsG*::FRT *glk*::FRT *manZ*::FRT *crr*::FRT *ldhA*::FRT *pflB*::FRT *ppc*::Kan^R	Succinate	Titer ≈ 45 g L^{-1} Productivity ≈ 1.7 g L^{-1} h^{-1} $Y_{p/s} \approx 0.97$ g g^{-1}	(Xia, Altman et al. 2015)

Basal 1.5% Glucose 1.5% Xylose 0.2% Acetate Batch & Fed-Batch Aerobic	<u>Glucose:</u> E. *coli* C *xylA748*::FRT *ace732*::FRT *ldhA744*::FRT *poxB772*::FRT *pps-776*::Kan^R <u>Xylose:</u> *E. coli* C *ptsG763*::FRT *glk-726*::FRT *manZ743*::FRT *aceE732*::FRT *ldhA744*::FRT *poxB772*::FRT *pps-776*::Kan^R	Pyruvate	<u>Batch:</u> Titer ≈ 19 g L^{-1} Yield ≈ 61% Productivity ≈ 1.44 g L^{-1} h^{-1} <u>Fed-Batch:</u> Titer ≈ 39 g L^{-1} Productivity ≈ 1.65 g L^{-1} h^{-1}	(Maleki, Safari et al. 2018)
Modified AM1 6.6% Glucose 3.4% Xylose Batch microaerobic	<u>Glucose:</u> LY180 (an *E. coli* W derivative engineered for ethanol production) Δ*xylR* adapted in glucose-xylose <u>Xylose:</u> LY180 Δ*ptsI* Δ*ptsG* Δ*galP glk*::Kan^R *xylR*::*xylR**	Ethanol	$q_{Glc\text{-}Max}$ ≈ 620 mg DCW^{-1} h^{-1} $q_{Xyl\text{-}Max}$ ≈ 300 mg DCW-1 h^{-1} Total Sugar Utilized ≈ 98 g L^{-1} Titer ≈ 46 g L^{-1} Productivity ≈ 488 mg L^{-1} h^{-1} $Y_{p/s}$ ≈ 0.45 g g^{-1}	(Flores, Ayla et al. 2019)

Finally, one intriguing observation associated with the developed LA coculture system was that the volumetric rate of xylose utilization (Q_{Xyl}) was found to consistently and abruptly decrease in all cocultures upon exhaustion of available glucose. For instance, as seen in **Figures 3.5A** and **3.5B**, prior to glucose exhaustion, maximum Q_{Xyl} were approximately 0.35 ± 0.04, 0.44 ± 0.04 and 0.52 ± 0.05 g L^{-1} h^{-1} for 1:1, 1:50 and 1:100 cocultures, respectively. However, following glucose exhaustion, Q_{Xyl} in the same cocultures then dropped to just 0.034 ± 0.009, 0.062 ± 0.004 and 0.12 ± 0.02 g L^{-1} h^{-1}. It is unlikely that LA or byproduct toxicity is responsible for this behavior since the parent strain (TG114) has been shown to achieve LA titers up to 120 g L^{-1} and almost no other side products are detected during its fermentation.[106] This observation possibly suggests that, although the two strains were engineered to be catabolically-orthogonality, inter-strain interactions certainly do occur throughout these synthetic cocultures. While the exact

nature and extent of this behavior remains unknown, however, and warrants further investigation.

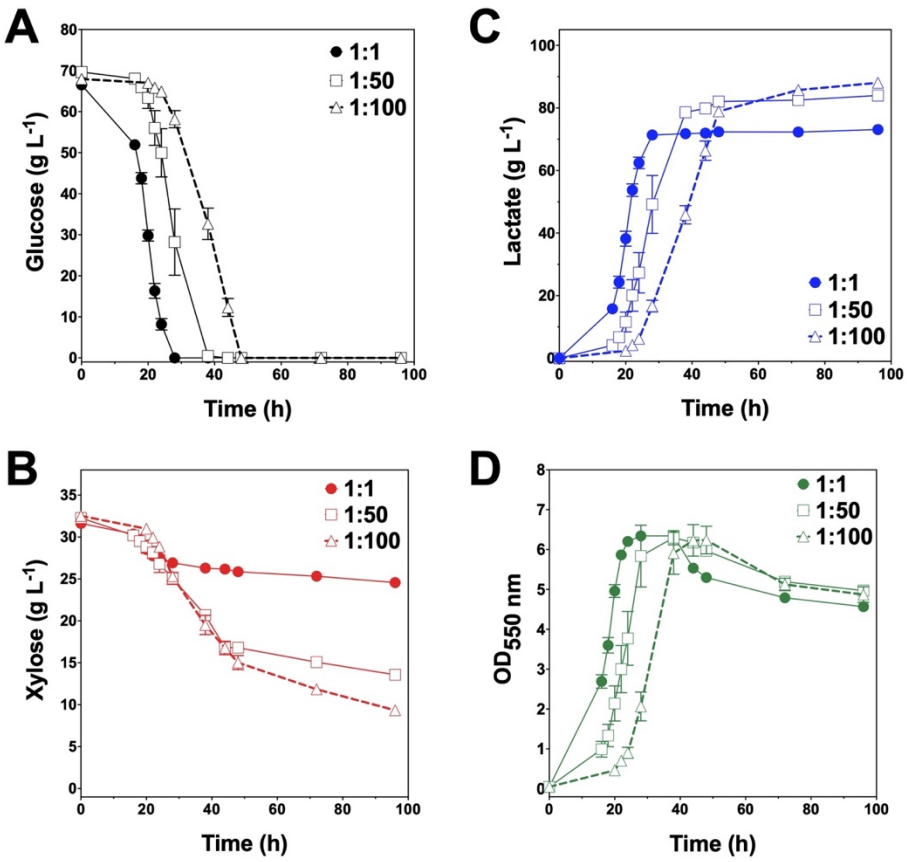

Figure 3.5 Fermentation of glucose-xylose mixtures (2:1 by mass) cocultures composed of catabolically-orthogonal lactate-producing specialist strains.

Concentrations of (A) glucose, (B) xylose, (C) D-lactate and (D) OD_{550nm} measured in the fermentation broth for TGglc:TGxyl cocultures using an initial inoculum ratio of 1:1 (close circles), 1:50 (open squares,) and 1:100 (open triangles). All fermentations were performed in batch mode and in mineral salts media. Data points represent the arithmetic mean of three replicates and the error bars represent one standard deviation.

3.2.3 Construction of Catabolically-Orthogonal Sugar Specialist for Succinic Acid Production

To further investigate the generalizable nature of this coculture strategy along with sets of specific genetic modifications used to create each sugar specialist, the same methodologies were next analogously applied to SA production from glucose-xylose mixtures. In this case, the succinogenic strain KJ122 (a derivative of *E. coli* ATCC 8739) was used as the common parent for constructing the two sugar specialist strains: KJglc and KJxyl (**Figure 3.3** and **Table 3.5**). KJ122 was previously engineered and shown to ferment 100 g L^{-1} glucose to SA (final titer of 82 g L^{-1}, overall Q_{LA} of 0.88 g L^{-1} h^{-1}, $Y_{p/s}$ of 0.90 g g-total $sugars^{-1}$) in mineral salts media.[93] Similar to TGglc, batch fermentation of KJglc also revealed virtually no xylose utilization (**Figure 3.6B**). In this case, glucose was completely utilized within 42 h at a maximum Q_{Glc} of 2.1 ± 0.1 g L^{-1} h^{-1} while SA was produced at a maximum Q_{SA} of 1.9 ± 0.1 g L^{-1} h^{-1}. At this output, the performance of KJglc was similar to that of its parent strain, KJ122 (**Figure 3.6A**; **Table 3.1**; **Figure 3.2A-D**). Likewise, and as expected, KJxyl was unable to utilize glucose throughout the 120 h fermentation (**Figure 3.6A**), but utilized 87% of supplied xylose, leaving just 5 g L^{-1} unused (**Figure 3.6B** and **Table 3.1**). With a maximum Q_{Xyl} and Q_{SA} of 0.60 ± 0.06 and 0.69 ± 0.20 g L^{-1} h^{-1}, respectively, overall performance of KJxyl was also similar to that of KJ122 (**Figure 3.2A)**.

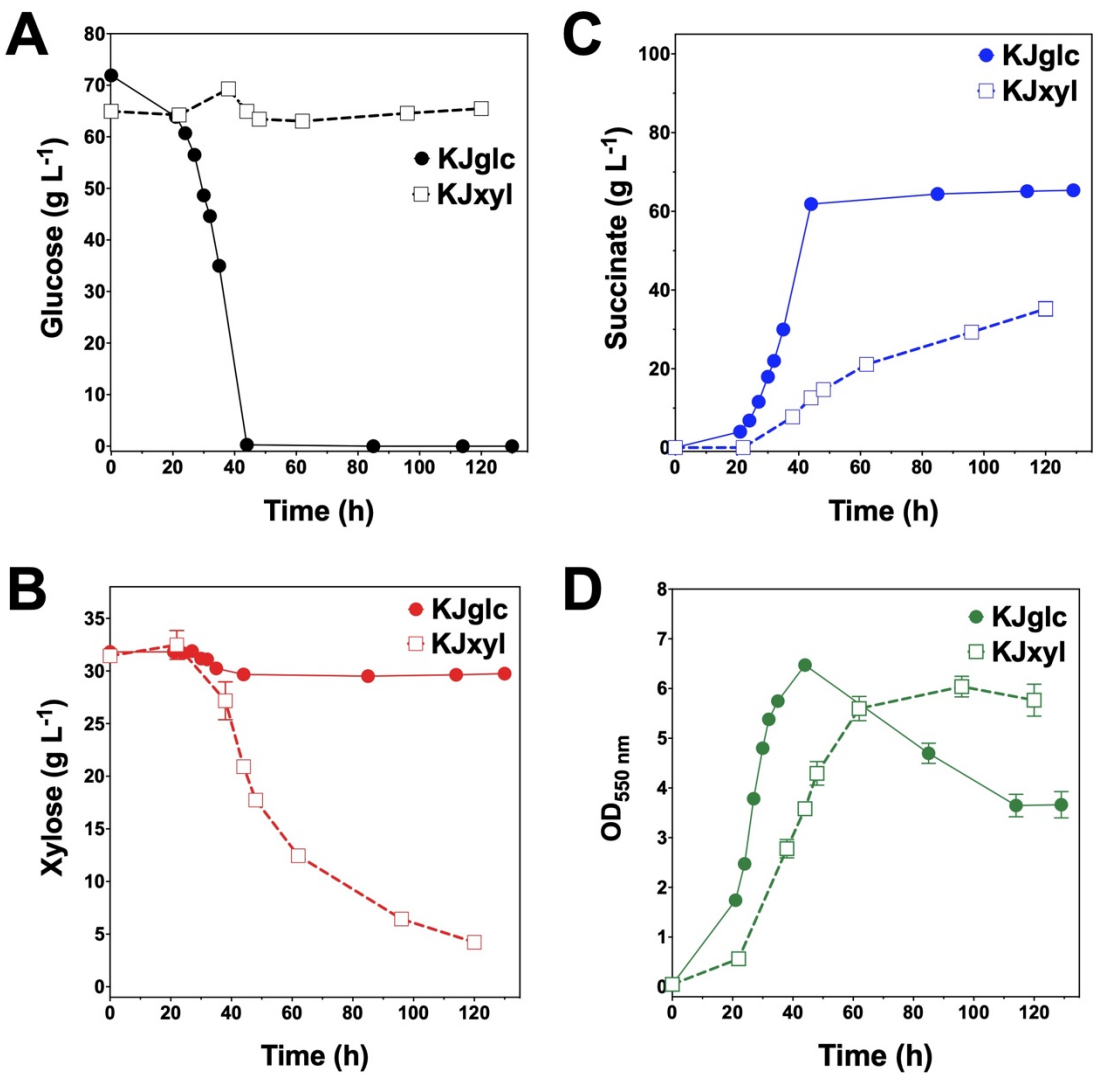

Figure 3.6 Fermentation of glucose-xylose mixtures (2:1 by mass) by succinogenic sugar specialist strains.

Concentrations of (A) glucose, (B) xylose, (C) succinate and (D) OD_{550nm} measured in the fermentation broth for KJglc (closed circles) and KJxyl (open squares). All fermentations were performed in batch mode and in mineral salts media. Data points represent the arithmetic mean of three replicates and the error bars represent one standard deviation.

3.2.4 Engineering and Optimizing a Synthetic Coculture for Efficient Conversion of Glucose-Xylose Mixtures to Succinic Acid

KJglc and KJxyl were next combined to develop a synthetic coculture for producing SA from glucose-xylose mixtures, again employing the same population-level tuning strategy in order to optimize sugar co-utilization. Based on the outcomes revealed for LA production, initial inoculation ratios of 1:1, 1:50 and 1:100 KJglc:KJxyl were first explored. As shown in **Figure 3.7B** and **Table 3.1**, total xylose utilization and Q_{Xyl} were similar for each of the 1:1, 1:50 and 1:100 cocultures (each ~87% and ~0.67 g L^{-1} h^{-1}, respectively) and close to that of the KJxyl monoculture. Meanwhile, however, total glucose utilization unexpectedly declined across this initial series of cocultures (**Figure 3.7A**). For instance, compared to 1:1 cocultures, total glucose utilization dropped by 80% and 94% in the 1:50 and 1:100, respectively; while all three cocultures displayed reduced maximum Q_{Glc} relative to KJglc monoculture (**Figure 3.7B** and **Table 3.1**). Overall, total sugar utilization was 91%, 39% and 31% for the 1:1, 1:50 and 1:100 cocultures, respectively (compared to 71% for KJglc monocultures; **Table 3.1**), with the highest final SA titers reaching 84 g L^{-1} ± 1 at the 1:1 ratio (at least 2-fold greater than by 1:50 or 1:100) along with a maximum Q_{SA} of 1.3 ± 0.1 g L^{-1} h^{-1} (**Figure 3.7C** and **Table 3.1**). Interestingly, in contrast to the above LA cocultures as well as our previous work,[117] increased initial relative abundance of the xylose specialist did not result in enhanced xylose utilization or, in this case, improved production of SA (**Figure 3.7B** and **3.7C**). This is likely because, in contrast to TGxyl, KJxyl displays much greater fitness, as demonstrated, for example, by its ability to accumulate twice as much biomass during monoculture fermentations (2.7 ± 0.2 gDCW L^{-1} vs. 1.1 ± 0.1 gDCW L^{-1} for TGxyl and 1.7 ± 0.1 gDCW L^{-1} for LYglc1, a previously engineered ethanologenic xylose specialist[117]). To test if it was in fact the relative activity of the glucose specialist that instead limited the overall performance of this

SA-producing coculture, an initial inoculum ratio of 2:1 KJglc:KJxyl was at last explored. While the 2:1 coculture utilized glucose at a faster rate and consumed 100% of provided glucose by 96 h (compared to 44 h for KJglc monoculture and KJ122), total xylose utilization, on the other hand, dropped to just 46% overall (about half of that consumed by the 1:1 coculture; **Figure 3.7B** and **Table 3.1**). Based on this outcome, it was determined that the optimal initial inoculum ratio for this specific coculture was close to 1:1. Meanwhile, the finding that a unique optimum initial population ratio was required for the developed LA and SA producing cocultures is not altogether surprising, and likely reflects the fact that the relative fitness levels differ between the two strains that make up each pair.

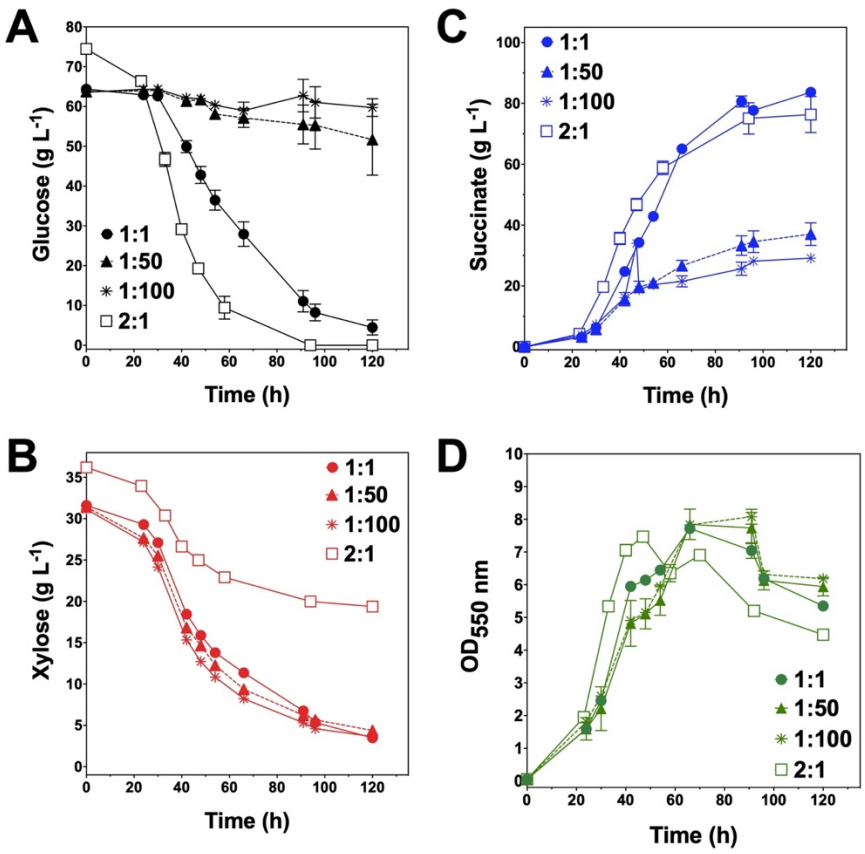

Figure 3.7 Fermentation of glucose-xylose mixtures (2:1 by mass) cocultures composed of catabolically-orthogonal succinogenic specialist strains.

Concentrations of (A) glucose, (B) xylose, (C) succinate and (D) OD_{550nm} measured in the fermentation broth for KJglc:KJxyl cocultures using an initial inoculum ratio of 1:1 (close circles), 1:50 (closed dashed triangle), 1:100 (asterisk) and 2:1 (open squares). All fermentations were performed in batch mode and in mineral salts media. Data points represent the arithmetic mean of three replicates and the error bars represent one standard deviation.

For comparison, Xia et al. previously developed an *E. coli* coculture to convert glucose and xylose to SA via a two stage, aerobic-anaerobic fed-batch process.[49] Specifically, a mixture composed of ~30 g L^{-1} glucose and ~10 g L^{-1} xylose were first utilized aerobically for growth (producing no succinate), before then switching to anaerobic conditions to produce SA (~15 g L^{-1} glucose and ~5 g L^{-1} xylose were provided initially and then

periodically added over 80 h; **Table 3.2**). Total sugar addition to this process over its 115 h duration was ~100 g L^{-1} (3:1 glucose:xylose by mass) and final SA titers reached ~45 g L^{-1}. From a bioprocessing perspective, while this two-stage approach has proven to be effective, use of a process that can operate simple batch mode, such as the coculture systems presented here, simplifies operation and control of the process. Similar to LA production, researchers have also engineered generalist strains to produce SA efficiently from sugar mixtures. For example, KJ122 further engineered to enhance conversion of a series of glucose-xylose mixtures (each 100 g L^{-1} total with 1:1, 2:1 or 3:1 glucose:xylose by mass) to up to ~84 g L^{-1} SA using a combination of genetic engineering and adaptive laboratory evolution.[118] As discussed above, however, the current coculture strategy is appealing due to its ability to facilitate effective catabolism of sugar mixtures through population tuning.

3.3 Conclusion

Overall, we have demonstrated the broad utility of engineering cocultures composed of catabolically-orthogonal *E. coli* strains for efficiently converting sugar mixtures into LA and SA, two important bioplastic monomers. Initial inoculum ratio was revealed to be an important design parameter for maximizing coculture performance, the optimum value of which is unique to each specialist pair and can vary by even several orders of magnitude depending on relative phenotypic differences between member strains (**Figure 3.8**). Ultimately, by applying a population-level tuning strategy to balance rates of glucose and xylose co-utilization, both coculture systems developed here were capable of fermenting a 100 g L^{-1} glucose-xylose mixture at ~91% conversion to either LA or SA at high rates and yields. This population-level-tuning strategy was simple to implement experimentally and

should similarly prove useful in other coculture applications. Holistically, this work contributes to an improved understanding of the behaviors of synthetic microbial consortia as enhanced bioproduction platforms for renewable fuels and chemicals from non-food carbohydrates. Ultimately, however, the ability to elucidate and understand the nature and potential importance of inter-strain interactions and/or metabolite exchanges[119-121] will likely be important to further optimizing these and other coculture systems.

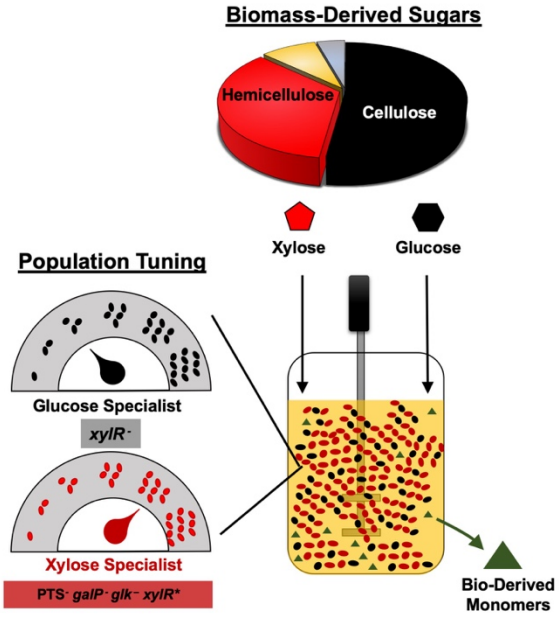

Figure 3.8 Tuning the initial inoculum ratio enables bioplastic monomer production from glucose-xylose mixtures by cocultures of catabolically-orthogonal specialist strains.
This catabolic division of labor and tuning strategy was used to produce D-lactate or succinate.

3.4 Methods

3.4.1 Strain Construction

All *E. coli* strains and plasmids used in chapter 3 are presented in **Table 3.4**. A list of primers used in chapter 3 in **Table 3.5.** The xylose specialist strain (Δ*galP* Δ*ptsI glk::kan*^{R} *xylR*::*xylR**) derived from KJ122 was initially found to grow poorly in media containing glucose-xylose and was accordingly adapted for improved growth under the conditions of interest. Growth was found to be significantly improved after performing just a single transfer, after which one clone, designated as KJxyl, was isolated. All chromosomal modifications were conducted using one- or two-step integration processes.[68,92] Plasmid pXW001, containing a *cat-sacB* cassette, or strain T-SACK, containing a *tetA-sacB* cassette, were used as the PCR template to generate DNA fragments for primary integration into chromosomal sites of interest.[68,122] Primary integration fragments contained the *cat-sacB* or *tetA-sacB* cassette flanked by 50 bp homology sequences from both upstream and downstream regions of the gene of interest. To eliminate the integrated *cat-sacB* or *tetA-sacB* cassette, providing markerless gene deletions, secondary integration fragments were generated containing 500 bp homology sequences from both upstream and downstream regions of the gene of interest, as generated via fusion PCR. Plasmid pKD46, expressing λ-red recombinase, was used to facilitate all chromosomal integrations via double-crossover recombination, as previously described [92]. During both primary and secondary chromosomal integrations, cultures were inoculated in a 250 mL flask containing 25 mL Luria Broth (LB), 50 g L^{-1} arabinose and 50 mg L^{-1} ampicillin, and incubated at 30 °C with shaking at 150 rpm until the optical density at 550 nm (OD_{550}) of the cultures reached approximately 0.5. To prepare competent cells, cultures were subsequently centrifuged (5 min, 6750 x g, 4 °C), the supernatant was discarded, and the remaining cell pellet was resuspended in 20 mL of 4 °C water. The described spin-wash cycle was repeated 3 times.

On the last wash, all the supernatant was discarded except approximately 150-200 µL of remaining supernatant which was used to resuspend pelleted cells. For electroporation, 40 µL of competent cells were combined with 100-200 ng of DNA. Following electroporation, cells were transferred to a sterile test tube containing 1 mL LB and incubated at 30 °C for 4 h. Cells were then plated on LB plates containing the appropriate antibiotic. Colony PCR and Sanger sequencing was used to verify positive clones after selecting for appropriate antibiotic resistance during primary integration and sucrose insensitivity (10% w/v) and loss of antibiotic resistance during secondary integration.

Table 3.4 List of strains and plasmids used to construct lactate and succinate sugar specialist in Chapter 3.

[A]pck denotes a mutated form of pck (G to A at position -64 relative to the ATG start codon).[B]ptsI* denotes a mutated form of ptsI (single base deletion at position 1,673 causing a frameshift mutation in the carboxyl-terminal region.*

Strains and Plasmids	Relevant Characteristics	Source
Strains		
TG114	ATCC 9637 Δ*pflB frdBC*::FRT *adhE*::FRT *ackA*::FRT *mgsA*::FRT evolved for converting glucose to D-lactate	106
TGglc	TG114 Δ*xylR*	This Study
TGxyl	TG114 Δ*ptsI* Δ*ptsG* Δ*galP glk*::*kan*^{R} (Kan^R) *xylR::xylR**	This Study
KJ122	ATCC 8739 *pck**^{A} *ptsI**^{B} Δ*ldhA* Δ*adhE* Δ*ackA*, Δ(*focA-pflB*) Δ*mgsA* Δ*poxB* Δ*tdcDE* Δ*citF* Δ*aspC* Δ*sfcA*	118
KJglc	KJ122 *xylR*::*tetA-sacB* (Tet^R)	This Study
KJxyl	KJ122 Δ*galP* Δ*ptsI glk*::*kan*^{R} (Kan^R) *xylR::xylR** quickly adapted in glucose-xylose mixture	This Study
T-SACK	W3110 *ara*D<>*tetA-sacB-amp flic*<>*cat argG::Tn*5	177
Plasmids		
pXW001	The *cat-sacB* cassette with the *sacB* native terminator cloned into a modified vector pLOI4162	71
pKD46	Red recombinase, temperature-conditional, *bla*	175

Table 3.5. List of primers used to construct lactate and succinate sugar specialist in Chapter 3**.**

F denotes, forward primer; R, reverse primer; H1 corresponds to 500 bp upstream of the gene of interests; H2 corresponds to 500 bp downstream of the gene of interests.

Primer Name	**Primer Sequence**
***ptsI* deletion**	
cat-sacB F	GAGTAATTTCCCGGGTTCTTTTAAAAATCAGTCACAAGTAAGGTAGGGTTT CGAGTGTGACGGAAGATCA
cat-sacB R	ACAAACCCATGATCTTCTCCTAAGCAGTAAATTGGGCCGCATCTCGTGGAT TAGCCATTTGCCTGCTTTT
*ptsI H1*F	AATCAGTCACAAGTAAGGTAGGGTTTCCACGAGATGCGGCCCAAT T
ptsI H1 R	CCGGAGTCAGGGTAGACTTG
ptsI H2 F	AATTGGGCCGCATCTCGTGGAAACCCTACCTTACTTGTGACTGAT
ptsI H2 R	ACTGTATTGCGCTCTTCGTG
***ptsG* deletion**	
cat-sacB F	CACGCGTGAGAACGTAAAAAAAGCACCCATACTCAGGAGCACTCTCAATTT CGAGTGTGACGGAAGATCA
cat-sacB R	GTAAAAAAGGCAGCCATCTGGCTGCCTTAGTCTCCCCAACGTCTTACGGAT TAGCCATTTGCCTGCTTTT
*ptsG H1*F	CGGTTACTGGTGGAAACTGACTCAC
ptsG H1 R	CTTAGTCTCCCCAACGTCTTACGGAAATTGAGAGTGCTCCTGAGTATGGGT
ptsG H2 F	ACCCATACTCAGGAGCACTCTCAATTTCCGTAAGACGTTGGGGAGACTAAG
ptsG H2 R	GACAGTCAGTAAAGGGGTGGAATTTGAAC
***galP* deletion**	
cat-sacB F	TACTCACCTATCTTAATTCACAATAAAAAATAACCATATTGGAGGGCATCT CGAGTGTGACGGAAGATCA
cat-sacB R	GATGACTGCAAGAGGTGGCTTCCTCCGCGATGGGAGGAAGCTTGGGGAGA TTAGCCATTTGCCTGCTTTT
*galP H1*F	GGTCGTGAACATTTCCCGTGG
galP H1 R	TGGGAGGAAGCTTGGGGAGAGATGCCCTCCAATATGGTTATTTTTTATTGT GAAT
galP H2 F	ATTCACAATAAAAAATAACCATATTGGAGGGCATCTCTCCCCAAGCTTCCT CCCA
galP H2 R	CGGTAAGCTGATGCTCCTGG
***xylR* deletion & replacement**	
cat-sacB F	TCTCAAAGCCGGTTACGTATTACCGGTTTTGAGTTTTTGCATGATTCAGCTC GAGTGTGACGGAAGATCA
cat-sacB R	GATAAGGCTTTTGCTCGCATCAGGTGGCTGTGCTGAGTTCCCTGATGTGACC TTAGCCATTTGCCTGCT
tetA-sacB F	TTTGAGTTTTTGCATGATTCAGCAGGAAAAGAACCTCCTAATTTTTGTTGAC ACTCTATC
tetA-sacB R	GTTACCTGATGTGACGCCGACAATTCTCATCATCGATCAAAGGGAAAACTG TCCATATGC
*xylR H1*F	CTGTTACTCGGCGGAATGTT
xylR H1 R	GACGCCGACAATTCTCATCATCGGGTTCCTTTTCCTGCTGAATCATGC
xylR H2 F	GCATGATTCAGCAGGAAAAGAACCCGATGATGAGAATTGTCGGCGTC
xylR H2 R	CTTGCTTGAACGCGTAGACA
lacZ replacement	
cat-sacB F	TCACACAGGAAACAGCTATGACCATGATTACGGATTCACTGGCCGTCGTTT CGAGTGTGACGGAAGATCA
cat-sacB R	CATTCGCCATTCAGGCTGCGCAACTGTTGGGAAGGGCGATCGGTGCGGGCC CTTAGCCATTTGCCTGCT
glk replacement	
kan F	ATTTACAGTGTGAGAAAGAATTATTTTGACTTTAGCGGAGCAGTTGAAGAG TGTAGGCTGGAGCTGCTTC
kan R	TGATTTAAAAGATTATCGGGAGAGTTACCTCCCGATATAACAGGAAGGATC ATATGAATATCCTCCTTAGT

3.4.2 Cultivation Conditions

Monoculture and coculture batch fermentations were conducted in a pH (7.0) and temperature (37 °C) controlled vessel containing 300 mL of modified AM1 mineral salt medium[82,94] containing twice the ammonium phosphate (38.8 mM $(NH_4)_2H_2PO_4$ and 15.1 mM $(NH_4)H_2PO_4$) and 67 g L^{-1} glucose and 33 g L^{-1} xylose (Flores, Ayla et al. 2019; Martinez, Flores et al. 2019). pH was maintained by automatic addition of 6 M KOH for LA-producing cultures and a mixture of 6 M KOH and 3 M K_2CO_3 (1:4 ratio by volume) for SA-producing cultures, as previously described.[106] From -80 ºC frozen stocks, strains were streaked onto AM1 agar plates supplemented with 100 mM MOPS, and 20 g L^{-1} glucose or 20 g L^{-1} xylose. Agar plates were placed inside a sealed canister filled with argon gas and incubated at 37 °C for 16-24 h. Seed cultures were grown in AM1 medium containing 100 mM MOPS, 10 g L^{-1} glucose and 10 g L^{-1} xylose, and incubated at 37 °C with shaking at 120 rpm for approximately 12-16 h. Cells were harvested by centrifugation (5 min, 6750 x g, 4 °C) and resuspended in 300 mL fresh media. All monoculture and coculture fermentations were seeded using a total initial OD_{550mn} of 0.05 (approximately 0.022 gDCW L^{-1}).

3.4.3 Analytical Methods

Cell growth was quantified using a UV/Vis spectrophotometer (Beckman Coulter DU-730; Indianapolis, IN). Sugar and product concentrations were determined by high-performance liquid chromatography (HPLC; Thermo Fisher Scientific and UltiMate 3000, Waltham, MA) equipped with a refractive index detector. Analyte separation was performed using an Aminex HPX-87H column (Bio-Rad Laboratories, Hercules, CA)

maintained at 45 °C and a mobile phase consisting of 5 mM H_2SO_4 flowing at a constant rate of 0.4 mL min^{-1}. External standards prepared in house were used to quantify substrate and product concentrations. All experiments were performed in at least triplicates and the average and standard deviation is shown in figures and tables.

3.4 References

47 Eiteman, M. A., Lee, S. A. & Altman, E. A co-fermentation strategy to consume sugar mixtures effectively. *J Biol Eng* **2**, 3, doi:10.1186/1754-1611-2-3 (2008).

48 Eiteman, M. A., Lee, S. A., Altman, R. & Altman, E. A substrate-selective co-fermentation strategy with Escherichia coli produces lactate by simultaneously consuming xylose and glucose. *Biotechnol Bioeng* **102**, 822-827, doi:10.1002/bit.22103 (2009).

49 Xia, T., Altman, E. & Eiteman, M. A. Succinate production from xylose-glucose mixtures using a consortium of engineered Escherichia coli. *Eng Life Sci* **15**, 65-72, doi:10.1002/elsc.201400113 (2015).

68 Sievert, C. *et al.* Experimental evolution reveals an effective avenue to release catabolite repression via mutations in XylR. *Proc Natl Acad Sci U S A* **114**, 7349-7354, doi:10.1073/pnas.1700345114 (2017).

74 Chappell, T. C. & Nair, N. U. Co-utilization of hexoses by a microconsortium of sugar-specific E. coli strains. *Biotechnol Bioeng* **114**, 2309-2318, doi:10.1002/bit.26351 (2017).

76 Zhang, H., Pereira, B., Li, Z. & Stephanopoulos, G. Engineering Escherichia coli coculture systems for the production of biochemical products. *Proc Natl Acad Sci U S A* **112**, 8266-8271, doi:10.1073/pnas.1506781112 (2015).

82 Yomano, L. P., York, S. W., Shanmugam, K. T. & Ingram, L. O. Deletion of methylglyoxal synthase gene (mgsA) increased sugar co-metabolism in ethanol-producing Escherichia coli. *Biotechnol Lett* **31**, 1389-1398, doi:10.1007/s10529-009-0011-8 (2009).

92 Datsenko, K. A. & Wanner, B. L. One-step inactivation of chromosomal genes in Escherichia coli K-12 using PCR products. *Proc Natl Acad Sci U S A* **97**, 6640-6645, doi:10.1073/pnas.120163297 (2000).

93 Jantama, K. *et al.* Eliminating side products and increasing succinate yields in engineered strains of Escherichia coli C. *Biotechnol Bioeng* **101**, 881-893, doi:10.1002/bit.22005 (2008).

94 Martinez, A. *et al.* Low salt medium for lactate and ethanol production by recombinant Escherichia coli B. *Biotechnol Lett* **29**, 397-404 (2007).

95 Abdel-Rahman, M. A., Tashiro, Y. & Sonomoto, K. Recent advances in lactic acid production by microbial fermentation processes. *Biotechnol Adv* **31**, 877-902, doi:10.1016/j.biotechadv.2013.04.002 (2013).

96 Es, I. *et al.* Recent advancements in lactic acid production - a review. *Food Res Int* **107**, 763-770, doi:10.1016/j.foodres.2018.01.001 (2018).

97 Ahn, J. H., Jang, Y. S. & Lee, S. Y. Production of succinic acid by metabolically engineered microorganisms. *Curr Opin Biotechnol* **42**, 54-66, doi:10.1016/j.copbio.2016.02.034 (2016).

98 Jansen, M. L. & van Gulik, W. M. Towards large scale fermentative production of succinic acid. *Curr Opin Biotechnol* **30**, 190-197, doi:10.1016/j.copbio.2014.07.003 (2014).

99 Okano, K., Tanaka, T., Ogino, C., Fukuda, H. & Kondo, A. Biotechnological production of enantiomeric pure lactic acid from renewable resources: recent achievements, perspectives, and limits. *Appl Microbiol Biotechnol* **85**, 413-423, doi:10.1007/s00253-009-2280-5 (2010).

100 Abdel-Rahman, M. A., Tashiro, Y. & Sonomoto, K. Lactic acid production from lignocellulose-derived sugars using lactic acid bacteria: overview and limits. *J Biotechnol* **156**, 286-301, doi:10.1016/j.jbiotec.2011.06.017 (2011).

101 Lynd, L. R. The grand challenge of cellulosic biofuels. *Nat Biotechnol* **35**, 912-915, doi:10.1038/nbt.3976 (2017).

102 Nieves, L. M., Panyon, L. A. & Wang, X. Engineering Sugar Utilization and Microbial Tolerance toward Lignocellulose Conversion. *Front Bioeng Biotechnol* **3**, 17, doi:10.3389/fbioe.2015.00017 (2015).

103 Song, S. & Park, C. Organization and regulation of the D-xylose operons in Escherichia coli K-12: XylR acts as a transcriptional activator. *J Bacteriol* **179**, 7025-7032 (1997).

104 Wang, Q., Ingram, L. O. & Shanmugam, K. T. Evolution of D-lactate dehydrogenase activity from glycerol dehydrogenase and its utility for D-lactate production from lignocellulose. *Proc Natl Acad Sci U S A* **108**, 18920-18925 (2011).

105 Ishida, N. *et al.* D-lactic acid production by metabolically engineered Saccharomyces cerevisiae. *J Biosci Bioeng* **101**, 172-177, doi:10.1263/jbb.101.172 (2006).

106 Grabar, T. B., Zhou, S., Shanmugam, K. T., Yomano, L. P. & Ingram, L. O. Methylglyoxal bypass identified as source of chiral contamination in l(+) and d(-)-lactate fermentations by recombinant Escherichia coli. *Biotechnol Lett* **28**, 1527-1535 (2006).

107 Awasthi, D. *et al.* Metabolic engineering of Bacillus subtilis for production of D-lactic acid. *Biotechnol Bioeng* **115**, 453-463, doi:10.1002/bit.26472 (2018).

108 Litsanov, B., Kabus, A., Brocker, M. & Bott, M. Efficient aerobic succinate production from glucose in minimal medium with Corynebacterium glutamicum. *Microb Biotechnol* **5**, 116-128, doi:10.1111/j.1751-7915.2011.00310.x (2012).

109 Utrilla, J., Vargas-Tah, A., Trujillo-Martinez, B., Gosset, G. & Martinez, A. Production of d-lactate from sugarcane bagasse and corn stover hydrolysates using metabolic engineered Escherichia coli strains. *Bioresour Technol* **220**, 208-214, doi:10.1016/j.biortech.2016.08.067 (2016).

110 Sawisit, A. *et al.* Mutation in galP improved fermentation of mixed sugars to succinate using engineered Escherichia coli AS1600a and AM1 mineral salts medium. *Bioresour Technol* **193**, 433-441, doi:10.1016/j.biortech.2015.06.108 (2015).

111 Zhou, K., Qiao, K. J., Edgar, S. & Stephanopoulos, G. Distributing a metabolic pathway among a microbial consortium enhances production of natural products. *Nature Biotechnology* **33**, 377-U157, doi:10.1038/nbt.3095 (2015).

112 Jones, J. A. *et al.* Complete Biosynthesis of Anthocyanins Using E. coli Polycultures. *MBio* **8**, doi:10.1128/mBio.00621-17 (2017).

113 Camacho-Zaragoza, J. M. *et al.* Engineering of a microbial coculture of Escherichia coli strains for the biosynthesis of resveratrol. *Microb Cell Fact* **15**, 163, doi:10.1186/s12934-016-0562-z (2016).

114 Roell, G. W. *et al.* Engineering microbial consortia by division of labor. *Microb Cell Fact* **18**, 35, doi:10.1186/s12934-019-1083-3 (2019).

115 Lu, H., Villada, J. C. & Lee, P. K. H. Modular Metabolic Engineering for Biobased Chemical Production. *Trends Biotechnol* **37**, 152-166, doi:10.1016/j.tibtech.2018.07.003 (2019).

116 Wang, L., York, S. W., Ingram, L. O. & Shanmugam, K. T. Simultaneous fermentation of biomass-derived sugars to ethanol by a co-culture of an engineered Escherichia coli and Saccharomyces cerevisiae. *Bioresour Technol* **273**, 269-276, doi:10.1016/j.biortech.2018.11.016 (2019).

117 Flores, A. D., Ayla, E. Z., Nielsen, D. R. & Wang, X. Engineering a Synthetic, Catabolically Orthogonal Coculture System for Enhanced Conversion of Lignocellulose-Derived Sugars to Ethanol. *ACS Synth Biol* **8**, 1089-1099, doi:10.1021/acssynbio.9b00007 (2019).

118 Khunnonkwao, P., Jantama, S. S., Kanchanatawee, S. & Jantama, K. Re-engineering Escherichia coli KJ122 to enhance the utilization of xylose and xylose/glucose mixture for efficient succinate production in mineral salt medium. *Appl Microbiol Biotechnol* **102**, 127-141, doi:10.1007/s00253-017-8580-2 (2018).

119 Herre, E. A., Knowlton, N., Mueller, U. G. & Rehner, S. A. The evolution of mutualisms: exploring the paths between conflict and cooperation. *Trends Ecol Evol* **14**, 49-53 (1999).

120 Ponomarova, O. & Patil, K. R. Metabolic interactions in microbial communities: untangling the Gordian knot. *Curr Opin Microbiol* **27**, 37-44, doi:10.1016/j.mib.2015.06.014 (2015).

121 Scott, S. R. & Hasty, J. Quorum Sensing Communication Modules for Microbial Consortia. *ACS Synth Biol* **5**, 969-977, doi:10.1021/acssynbio.5b00286 (2016).

122 Li, X. T., Thomason, L. C., Sawitzke, J. A., Costantino, N. & Court, D. L. Positive and negative selection using the tetA-sacB cassette: recombineering and

P1 transduction in Escherichia coli. *Nucleic Acids Res* **41**, e204, doi:10.1093/nar/gkt1075 (2013).

CHAPTER 4

AN *ESCHERICHIA COLI* COCULTURE-COPROUDUCTION SYSTEM DESIGNED FOR ENHANCED CARBON CONSERVATION THROUGH INTER-STRAIN METABOLIC COOPERATION

Abstract

Carbon loss in the form of CO_2 is an intrinsic and persistent challenge faced during conventional and advanced biofuel production from biomass feedstocks. Nevertheless, current mechanisms for increasing carbon conservation typically require the provision of reduced co-substrates as additional reducing equivalents. This need can be circumvented, however, by exploiting the natural heterogeneity of lignocellulosic sugars mixtures and strategically using specific fractions to drive complementary CO_2 emitting vs. CO_2 fixing pathways. As a demonstration of concept, a coculture-coproduction system was developed by pairing two catabolically orthogonal *Escherichia coli* strains; one converting glucose to ethanol (G2E) and the other xylose to succinate (X2S). Using a sealed fermentation vessel and 2:1 (by mass) glucose-xylose mixture as model substrate, ^{13}C-labeling studies reveled that G2E+X2S cocultures were capable of recycling 24% of all evolved CO_2, corresponding to carbon conservation efficiency of 71%; significantly higher than the 64% achieved when all sugars are instead converted to just ethanol. Further tuning of the substrate ratio proved a facile mechanism for controlling the degree of CO_2 recycling, with a maximum carbon conservation efficiency of 77% being demonstrated using 3:7 glucose-xylose. Meanwhile, in addition to the expected inter-strain exchange of CO_2, more comprehensive analyses using different pairs of ^{13}C-labeled substrates and alternative bioreactor configurations revealed the unexpected exchange of pyruvate between strains, along with significant carbon rearrangement within X2S. The developed coculture-coproduction system represents an alternative and promising bioproduction paradigm that can be readily extended to improve carbon conservation for a range of feedstocks and bioproducts of interest.

Material presented in Chapter 4 have been submitted wholly to refereed journals.

Author contributions is as follows

Andrew D. Flores, Xuan Wang and David R. Nielsen conceived and designed experiments, analyzed data and wrote this chapter. Steven Holland, Apurv Mhatre and Aditya P. Sarnaik performed ^{13}C analysis. All authors are affiliated with Arizona State University.

4.1 Introduction

Chapters 2 and 3 illustrate how engineering catabolically-orthogonal sugar specialists is a flexible platform for efficient co-utilization of glucose-xylose mixtures. However, and as demonstrated in this chapter, the utility of catabolic division of labor can additionally be used to balance complementary CO_2 emitting vs CO_2 fixing pathways. Thereby increasing overall carbon conservation efficiency.

Biomass represents the most abundant feedstock for producing renewable biochemicals and biofuels and, with the future potential to produce one billion dry tons biomass annually, the U.S. could ultimately supplant up to ~30% of its total petroleum consumption in this manner [123]. The largest and most sustainable biomass sources are comprised of lignocellulose [124,125]; a complex matrix of polysaccharides and phenolic polymers [2,3]. Carbohydrates account for ~60-70% (dry wt.) of typical lignocellulosic biomass [2,102,124] and consist predominantly of D-glucose (sole cellulose monomer) and D-xylose (dominant hemicellulose monomer)) [2,3]. Owing to differing degrees of reduction, however, biofuel synthesis from carbohydrates is inevitably accompanied by significant carbon loss (~40-50% wt. of the substrate), typically in the form of CO_2[126,127]. Inefficient conversion of feedstock carbon constitutes an intrinsic limitation that plagues the production of ethanol as well that of other advanced biofuels, all of whose biosynthetic pathways rely upon decarboxylation steps for precursor generation (e.g., acetaldehyde for ethanol [128]; acetolactate for isobutanol [129]; acetyl-CoA for n-butanol [130,131], farnesene [132] and fatty acids [133]). When scaled to meet demand, byproduct CO_2 generation is a very significant problem. For example, in the U.S. alone in 2016, 216 biorefineries produced at a total capacity of 16 billion gallons ethanol [134], resulting in the co-generation of 45.7 million metric tons of CO_2

[135]. Since most fermentation facilities simply emit their CO_2-rich off-gases, the majority of this carbon is currently lost to and accumulates in the atmosphere [136].

To address this persistent, fundamental challenge, recent studies have explored diverse strategies to reduce CO_2 loss during biofuel production, including via the engineering of synthetic glycolytic pathways [137]. Non-oxidative glycolysis (NOG), for example, offers the potential for greater carbon conservation (i.e., 3 acetyl-CoA produced per glucose, rather than just 2); however, insufficient generation of reducing equivalents requires the provision of a reduced co-substrate (e.g., methanol) as additional electron donor [126]. Alternatively, enhanced utilization of feedstock carbon can instead be realized by recycling and subsequently fixing evolved CO_2; as has been achieved, for example, by equipping heterotrophs with (photo)autotrophic enzymes/pathways, resulting in a form of synthetic mixotrophy [138-146]. Since low heterologous enzyme activities can be a common challenge to this approach, others have recently explored how the same net, mixotrophic effect can be realized via the engineering of synthetic microbial communities incorporating natural CO_2-fixing species. For example, heterotrophic *Clostridium acetobutylicum* and autotrophic *C. ljungdahlii* were recently combined in a synthetic coculture that displayed enhance carbon conservation during acetone-butanol-ethanol fermentations [147]. In this case, however, the fermentation required significant supplementation with H_2 (which is poorly water soluble) since the Wood-Ljungdahl pathway requires eight electrons to fix two molecules of CO_2 into one acetyl-CoA [145].

Though often overlooked relative to autotrophs, all heterotrophs also naturally fix CO_2, in this case via numerous carboxylase-dependent pathways [148,149]. Among these, anaplerotic carboxylases, which incorporate CO_2 into TCA cycle intermediates, have been

proposed to have a low overall energy cost and suitable kinetic parameters for CO_2 fixation [150,151]. To date, however, such mechanisms have not been thoroughly investigated as a robust strategy for carbon conservation through CO_2 recycling. This is likely because anaplerotic carboxylases are typically responsible for capturing only a limited amount of CO_2 [149]; equal to an estimated 2-8% of the total carbon in a cell [148]. For such mechanisms to constitute a significant pathway for recycling evolved CO_2 would require: (i) a non-biomass product to serve as a less complex and easily accumulated fixed carbon sink. (ii) an ample source of carboxylase precursors, and (iii) abundant reducing equivalents.

Here we report on the systematic development of a synthetic coculture-coproduction system that enables efficient recycling of evolved CO_2 via inter-strain metabolic cooperation. In particular, the above key requirements are uniquely addressed by exploiting the heterogeneous nature of lignocellulosic sugars, allowing feedstock carbon/electrons to be readily partitioned across and used to drive complementary CO_2 emitting vs. CO_2 fixing pathways; an approach that importantly avoids the need to supply cultures with additional external reducing equivalents. As proof of concept, this general approach is demonstrated for the case of ethanol and succinate coproduction by two engineered *Escherichia coli* specialist strains in a single, sealed vessel. Once established, the extent of carbon conservation by inter-strain CO_2 recycling was characterized via comprehensive ^{13}C-labeling studies, which further revealed the additional yet unexpected exchange of pyruvate. The developed strategy provides a promising avenue for strategic feedstock management in support of increased carbon conservation during lignocellulosic biofuel production, with the potential to improve overall economics through value-added coproduct biosynthesis.

4.2 Results and Discussion

4.2.1 Designing a Heterotrophic Coculture-CoProduction System for *in situ* CO_2 Recycling

A synthetic coculture capable of recycling CO_2 evolved during ethanol fermentation and fixing it in support of succinate coproduction was first engineered in a 'bottom-up' manner. To overcome carbon catabolite repression, prevent substrate competition, and facilitate feedstock distribution across complementary biocatalytic roles, each strain was engineered to be 'catabolically-orthogonal' (i.e., capable of using just one unique sugar as substrate); a coculture design strategy previously shown to promote rapid and efficient co-utilization of biomass sugar mixtures [47,117,152]. As lignocellulosic biomass is typically composed of about 2:1 glucose:xylose (by mass), glucose was specified for ethanol production to ensure abundant and non-limiting CO_2 availability (1 mole CO_2 evolved per mole ethanol produced via the Pdc pathway). Xylose, therefore, was reserved solely for succinate production, serving as the source of both the requisite endogenous precursor for CO_2 assimilation (i.e., phosphoenolpyruvate; PEP) and all necessary reducing equivalents; thereby eliminating the need to supply additional, reduced co-substrates. Orthogonal sugar catabolism was engineered in the respective strains by i) deleting *xylR* (a required transcriptional activator) to block xylose catabolism in a previously-engineered ethanologenic strain [82,83] resulting in G2E ('glucose-to-ethanol') [117]; and ii) disrupting major glucose transport and phosphorylation systems (Δ*ptsI* Δ*galP* Δ*glk*) in a previously-engineered succinogenic strain that also displays enhanced xylose utilization (LP001, a derivative of KJ122) [93,153], resulting in X2S ('xylose-to-succinate'). Strain X2S furthermore carries a mutant copy of PEP-carboxykinase (*pck**) that displays increased

transcriptional and enzyme activity; both critical for CO_2 fixation into the reductive branch of TCA cycle (rTCA) and, ultimately, succinate production (**Figure 4.1A**) [154]. With

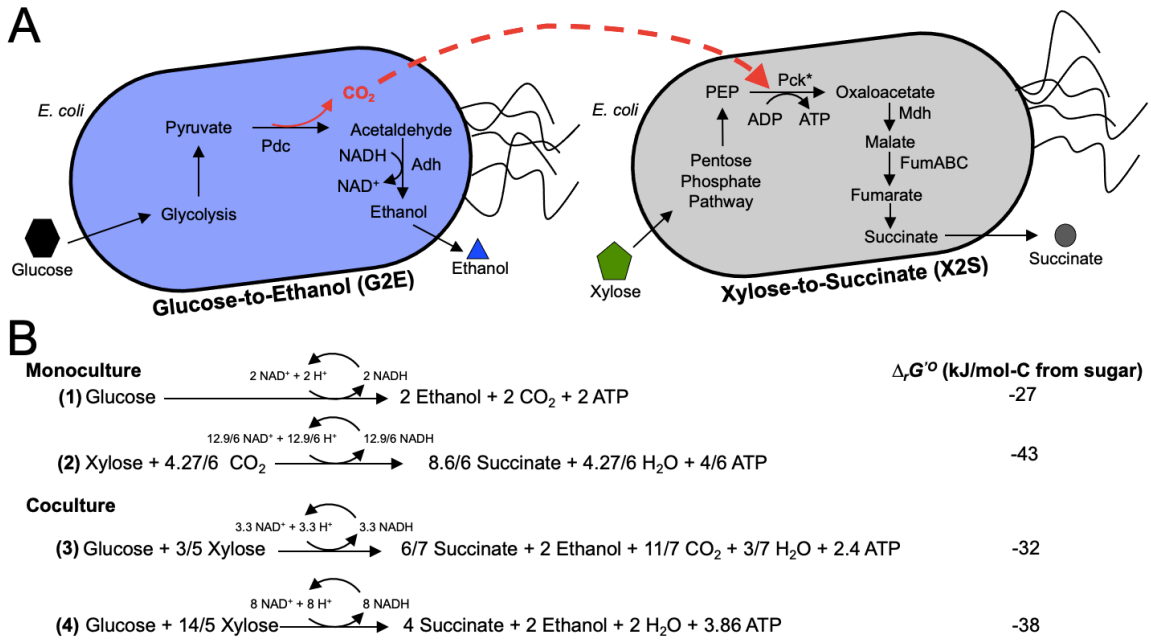

Figure 4.1 Construction of a catabolically-orthogonal, CO_2-recycling coculture for the coproduction of ethanol and succinate from glucose and xylose, respectively.

(A) A schematic representing the key metabolic features of the 'glucose-to-ethanol' (G2E) and 'xylose-to-succinate' (X2S) E. coli strains and their role in the evolution and subsequent fixation of CO_2. Pdc, pyruvate decarboxylase; Adh, alcohol dehydrogenase; PEP, phosphoenolpyruvate; Pck, phosphoenolpyruvate carboxykinase (* indicates a mutant with a G to A change at position -64 relative to start codon); Mdh, malate dehydrogenase; FumABC, fumarase. (B) Equations (1) and (2) represent the stoichiometry of ethanol and succinate production by G2E and X2S from glucose and xylose, respectively. Equation (3) represents the physiological scenario of a lignocellulosic feedstock consisting of a 2:1 (by mass) glucose:xylose mixture and the corresponding CO_2 recycling potential. Equation (4) represents the stoichiometry of ethanol and succinate coproduction by a G2E+X2S coculture and the feedstock composition that would be necessary to recycle 100% of CO_2 evolved during ethanol production. The standard Gibbs free energy of reaction ($\Delta_r G'^{O}$; at pH 7 and ionic strength of 0.1 M) for each scenario was calculated using eQuilibrator (http://equilibrator.weizmann.ac.il/) with consideration of inherent redox balance for fermentative production and transport energy expenditure of the sugars (i.e., $EIIBC^{Glc}$-based PTS for glucose and XylFGH for xylose).*

succinate fermentation the only remaining pathway available for net ATP generation and achieving redox balance, as expected, growth of X2S stringently depends upon CO_2 availability under strictly anaerobic conditions (**Figure 4.2** and **4.3**). Alternatively, it was hypothesized that this requirement could instead be met via a coculturing strategy where, in a closed system, CO_2 emitted by G2E would be available for fixation and reutilization by X2S (**Figure 4.1*A***). In this case, succinate production via the Pck-mediated route alone provides a mechanism for *in situ* CO_2 reutilization that is both redox balanced and strongly thermodynamically favorable (**Figure 4.1*B*** and **Figure 4.4**). Ultimately, however, the total possible extent of CO_2 recycling is controlled in such a coculture system by both the net fixation potential of X2S and the relative feedstock sugar composition. That said, X2S is theoretically capable of fixing 0.5 mol-CO_2 mol-succinate^{-1}; with its performance capped by and inherent redox limitation that enables only up to 71% of PEP to proceed via rTCA, with the remainder proceeding via the NADH regenerating, but CO_2-emitting oxidative branch [155]. Considering this, with a feedstock consisting of 2:1 (by mass) glucose:xylose, a G2E+X2S coculture would have the potential to fix up to ~21% of all evolved CO_2 in support of succinate coproduction, whereas complete CO_2 recycling would only be possible using a feed mixture minimally consisting of 1:2.8 (by mass) glucose:xylose (**Figure 4.1*B***).

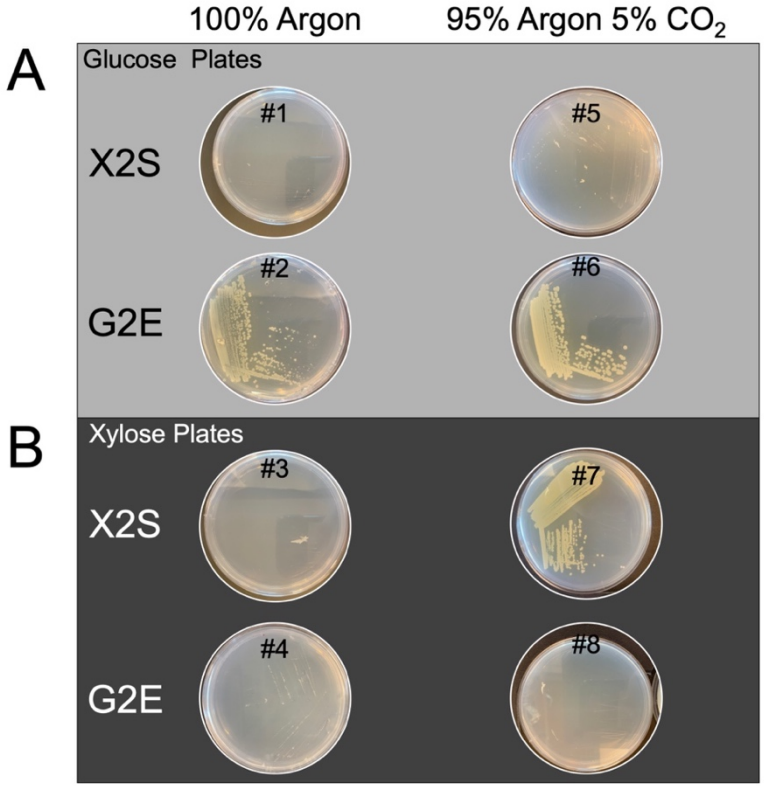

Figure 4.2 Demonstrating the catabolically-orthogonal nature of G2E and X2S, as well as the importance of CO_2 availability for X2S growth.

Cells were grown on AM1 mineral media agar plates supplemented with 100 mM MOPS and (A) 20 g L^{-1} glucose or (B) 20 g L^{-1} xylose as the sole organic carbon source. From -80℃ frozen stocks, strains were streaked onto agar plates and placed inside a BD BBL™ GasPack™ jar with a headspace consisting of either 100% argon or a mixture of 95% argon and 5% CO_2, after which they were sealed and incubated at 37℃ for 48 h. BD BBL™ GasPack™ anaerobic indicators were placed inside the jars prior to sealing to confirm anaerobic conditions were maintained throughout. G2E is unable to grow on plates containing just xylose, however, grows on plates containing just glucose. Conversely, X2S is unable to grow on plates containing just glucose, however, grows on plates containing just xylose. Furthermore, X2S cannot grow when the headspace does not include CO_2.

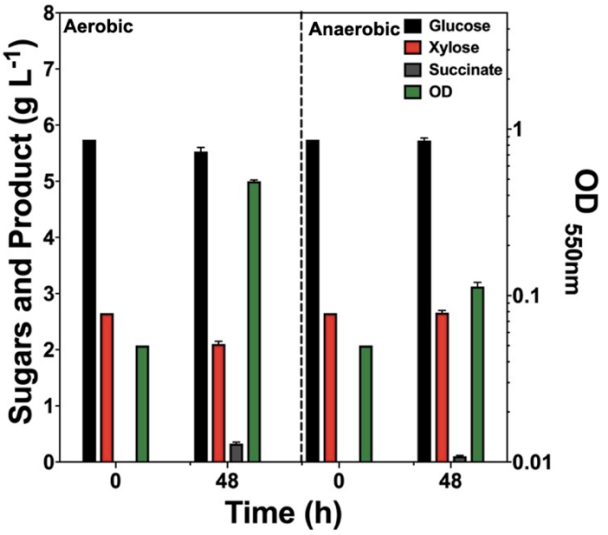

Figure 4.3 Batch fermentation of X2S on a glucose-xylose sugar mixture (10 g L^{-1} total, 2:1 glucose: xylose by mass) in sealed vessels under (left) initially aerobic and (right) fully anaerobic conditions.

For initially aerobic conditions, the bioreactor headspace initially consisted of air. In this case, a limited amount of CO_2 was first produced via respiration which, being retained in the sealed vessel, could subsequently be reassimilated in support of limited succinate fermentation. For anaerobic conditions, a gentle stream of argon gas was bubbled through the media for ~15 min in order to displace air from the headspace prior to inoculation and sealing. Concentrations of glucose (black bar), xylose (red bar), and succinate (grey bar), as well as cell growth (as OD_{550nm}; green bar), were measured at 0 and 48 h. While no glucose was utilized by X2S under both conditions, strictly anaerobic conditions lead to significant decreases in xylose utilization (0.55 ± 0.04 vs. 0.07 ± 0.03 g L^{-1} for initially aerobic vs. anaerobic conditions, respectively), growth (with just one biomass doubling under fully anaerobic conditions), and succinate production.

Succinate Production from Xylose (with xylose transport via XylFGH)

Transport and Activation

6 xylose + 6 ATP + 6 H_2O → 6 xylose + 6 ADP + 6 P_i + 6 H^+

6 xylose → 6 xylulose

6 xylulose + 6 ATP → 6 xylulose 5-phosphate + 6 ADP + 6 H^+

Pentose Phosphate Pathway

2 xylulose 5-phosphate → 2 ribose 5-phosphate

2 xylulose 5-phosphate + 2 ribose 5-phosphate → 2 glyceraldehyde-3-phoshpate + 2 sedaheptulose 7-phosphate

2 glyceraldehyde-3-phoshpate + 2 sedaheptulose 7-phosphate → 2 fructose 6-phosphate + 2 erythrose 4-phosphate

2 xylulose 5-phosphate + 2 erythrose 4-phosphate → 2 glyceraldehyde-3-phoshpate + 2 fructose-6-phosphate

Net from PPP

6 xylulose 5-phosphate → 2 glyceraldehyde-3-phoshpate + 4 fructose-6-phosphate

Glycolysis

4 fructose-6-phosphate + 4 ATP → 8 glyceraldehyde-3-phoshpate + 4 ADP + 4H^+

10 glyceraldehyde-3-phoshpate + 10 Pi + 10 NAD^+ → 10 1,3-bisphophoglycerate +10 NADH + 10 H+

10 1,3-bisphophoglycerate + 10 ADP → 10 3-phosphoglycerate + 10 ATP

10 3-phosphoglycerate → 10 2-phophoglycerate

10 2-phophoglycerate → 10 PEP + 10 H_2O

Overall to PEP

6 Xylose + 6 ATP + 10 NAD → 10 PEP + 6 ADP +10 NADH

Reductive TCA

7.136 PEP + 7.136 CO_2 + 7.14 ADP → 7.136 oxaloacetate + 7.136 ATP

5.712 oxaloacetate + 5.712 NADH → 5.712 malate + 5.712 NAD^+

5.712 malate → 5.712 fumarate + 5.712 H_2O

5.712 fumarate + 2 NADH → 5.712 succinate + 2 NAD^+

Oxidative TCA

1.424 oxaloacetate + 1.424 acetyl-CoA + 1.424 H_2O → 1.424 citrate

1.424 citrate → 1.424 isocitrate

1.424 isocitrate → 1.424 succinate + 1.424 glyoxylate

Glyoxylate Bypass

2.864 PEP + 2.864 ADP → 2.864 pyruvate + 2.864 ATP

2.864 pyruvate → 2.864 acetyl-CoA + 2.864 CO_2 + 2.864 NADH

1.44 acetyl-CoA + 1 glyoxylate → 1.44 malate

1.44 malate → 1.44 fumarate + 1.44 H_2O

1.44 fumarate + 1 NADH → 1.44 succinate +1.44 NAD^+

Overall to Succinate

6 Xylose + 4.27 CO_2 + 12.86 NAD^+ + 12.86 NADH + 4 ADP → 8.57 Succinate + 4.27 H_2O + 12.86 NAD^+ + 12.86 NADH + 4 ATP

Figure 4.4 Stoichiometrically-balanced equations representing succinate production from xylose by *E. coli* X2S.

4.2.2 Establishing a CO_2 Recycling Coculture for Increased Carbon Conservation

Following construction, G2E and X2S were next individualized characterized (i.e., as monocultures) with respect to their CO_2 evolution/fixation behaviors and overall performance. To ensure complete retention of fermentation gases and facilitate carbon balancing, all fermentations were performed using custom-made, sealed pressure vessels as bioreactors; each equipped with a digital pressure sensor to indirectly monitor fermentation progress via gas accumulation (**Figure 4.5*A***). Consistent with its inability to grow using xylose as sole carbon source **(Figure 4.2),** when

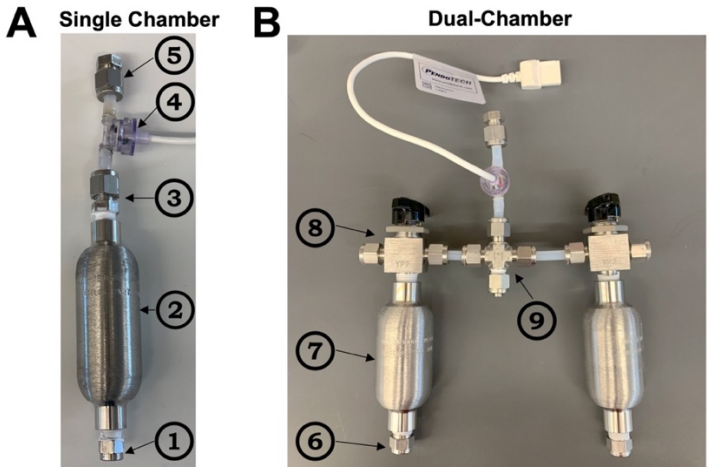

Figure 4.5 Custom-made, stainless-steel pressure vessels designed and used as sealed bioreactors for retaining fermentation gases in support of *in situ* CO_2 recycling.

System pressures were monitored via an integrated digital pressure sensor. All stainless-steel parts were purchased from Swagelok Southwest-Arizona (Phoenix Arizona). (A) Single chamber fermentation vessel used for monoculture and coculture fermentation, consisting of: [1] stainless steel 1/8 inch pipe plug MNPT (Part No.SS-2-P), [2] 40 mL 304L stainless steel double ended sample cylinder with 1/8 inch FNPT (Part No. 304L-HDF2-40), [3] stainless steel tube fitting, male connector with 1/4 inch tube OD and 1/8 inch MNPT (Part No. SS-400-1-2), [4] single use pressure sensors with polysulfone 1/8 inch hose barb (Part No. PREPS-N-012; PendoTECH, Princeton, NJ), [5] Stainless steel cap for 1/4 inch OD tubing (Part No. SS-400-C). (B) Dual-chamber bioreactor configuration that enables physical separation between strains while connecting the headspaces of both vessels to promote exchange of fermentation gases, consisting of: [6] stainless steel 1/4 inch pipe plug MNPT (Part No.SS-4-P), [7] 50 mL 304L stainless steel double ended sample cylinder (Part No. 304L-HDF4-50), [8] stainless steel 1-piece 40G series 3-way ball valve with 1/4 inch MNPT and 1/4 inch OD tube fitting (Part No. SS-43GXS4-S4-M4), [9] stainless steel union cross with 1/4 inch OD tube fitting (Part No. SS-400-4).

provided with a 2:1 (by mass) glucose-xylose mixture (9 g L^{-1} total), G2E utilized all glucose but no xylose (i.e., 67% of total sugars) during a 96 h fermentation (**Figure 4.6*A***). Overall, 59% of consumed glucose carbon was used for ethanol production (2.2 ± 0.1 g L^{-1} final titer, 0.45 ± 0.03 g-ethanol g-glucose^{-1} yield; **Figure 4.6*A***, **Table 4.1**) which was accompanied by significant CO_2 accumulation, causing the vessel pressure to reach and

sustain 7.6 pounds per square inch gauge (psig) by 36 h (likely occurring alongside glucose exhaustion; **Figure 4.6*C***).

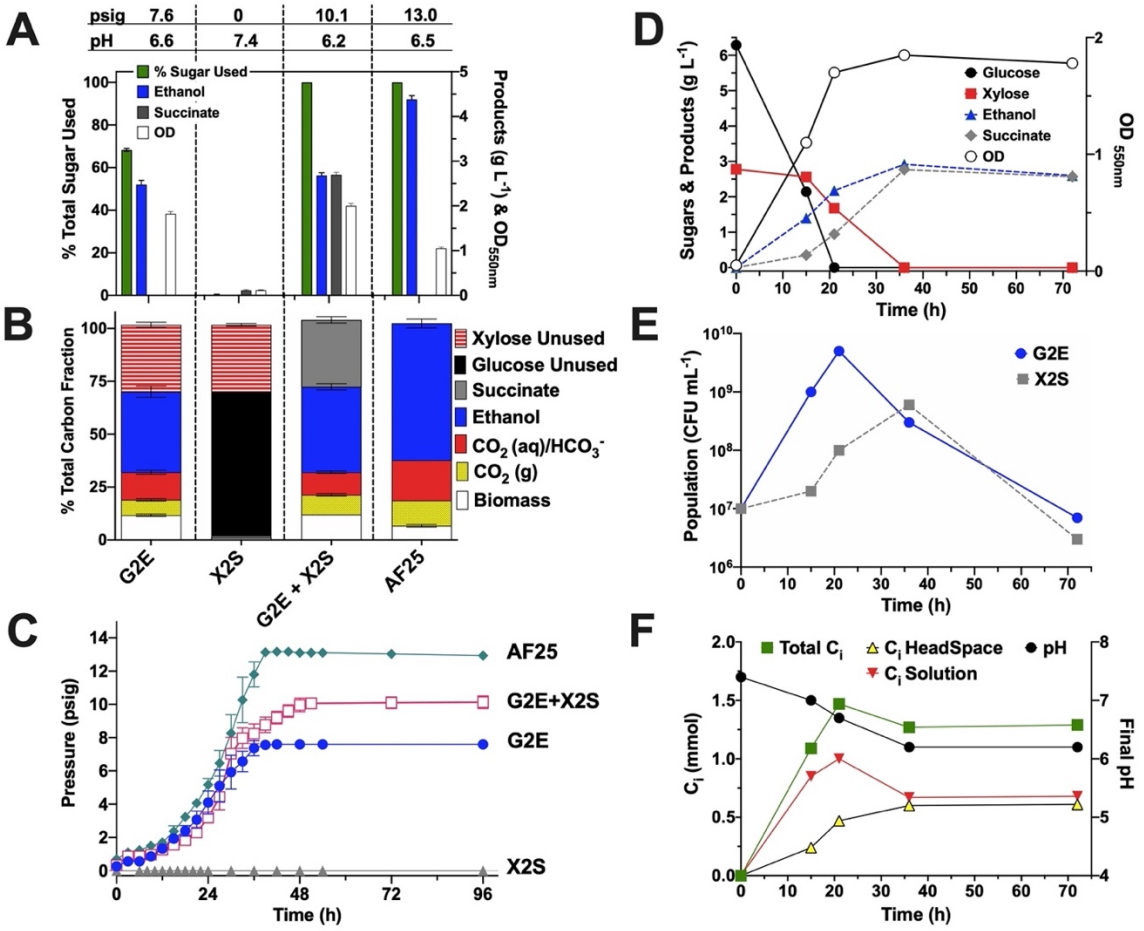

Figure 4.6 Comparing monoculture (G2E, X2S and AF25) and coculture (G2E+X2S) fermentations in sealed fermentation vessels.

(A) Concentrations of glucose, xylose, ethanol, and succinate in fermentation broths, as well as optical densities at 550 nm (OD_{550nm}). In all cases, cultures were inoculated at an initial OD_{550nm} of 0.05, where for the G2E+X2S coculture a 1:1 inoculum ratio was used with the same total initial OD_{550nm} (i.e., OD_{550nm} of 0.025 for each strain). Fermentation vessels remained sealed throughout, only being opened for sampling after 96 h. (B) Distribution of total system carbon between unused sugars, growth, products, and inorganic carbon, as represented by the percent total carbon fraction (i.e., moles carbon in each species divided by total moles carbon supplied initially as sugars). (C) Pressure accumulation profiles during monoculture and coculture cultivations, including X2S (red triangle), G2E (black circles), G2E+X2S (white squares), and AF25 (blue diamonds). A series of identical G2E+X2S fermentations were performed and sacrificed at the indicated time points in order to enable dynamic characterization of: (D) sugar and

product concentrations, (E) the population profile between G2E and X2S, and (F) inorganic carbon species and pH changes. Colony forming units (CFU) of G2E and X2S were measured during the experiment via plate counting using LB agar plates containing (40 mg mL^{-1}) chloramphenicol or (60 mg mL^{-1}) kanamycin for G2E and X2S, respectively. Error bars represent the standard error from biological triplicates.

Assuming CO_2 vapor-liquid equilibrium and accounting for pH, total dissolved levels of inorganic carbon (C_i) were estimated (equations 1-3 in section 4.3.4) which, when combined with measured levels of product biosynthesis and cell growth (equations 4 in section 4.3.4) enabled the steady-state carbon distribution to be elucidated (**Figure 4.6*B***, **Table 4.1**). This revealed that, in total, 32% of all consumed glucose carbon terminally accumulated as C_i between both the headspace (as CO_2(g)) and medium (predominantly HCO_3^- at pH 6.6), which translates to a molar yield of CO_2 equivalents ($Y_{CO2\text{-}eq/S\text{-}tot}$) of 1.88 ± 0.12 mol-$CO_2$-eq mol-sugar consumed^{-1} (**Table 4.1**).

Table 4.1. Comparing the performance of different *E. coli* strains as monocultures or cocultures, as well as the distribution of carbon among major organic and inorganic fermentation products.

All cultures were grown at 37℃ in AM1 mineral salts medium initially at pH 7.4 and supplied with ~9 g L^{-1} of total sugars (2:1 glucose:xylose by mass) in a sealed vessel with 21 mL total liquid volume. Errors represent the standard error from biological triplicates. 'NR' indicates 'not reported', in this case due to the fact that X2S did not utilize any sugar, significantly grow, or generate pressure within the sealed vessel.[A] Includes $CO_{2(aq)}$ and HCO_3^-. At pH values < 8, CO_3^{2-} levels are negligible and were thus omitted. Abbreviations: HS, headspace; Soln, solution. [B] pH of the culture medium measured at 96 h. Major dissolved inorganic carbon species estimated via Equations 6-9 in methods section. [C] $Y_{P/S}$ denotes the overall molar yield coefficient of each product per specific substrate utilized.[D] $Y_{P\text{-}tot/S\text{-}tot}$ denotes the overall molar yield coefficient of total products per total substrates utilized on a carbon basis.[E] $Y_{CO2\text{-}eq/S\text{-}tot}$ denotes the overall molar yield coefficient of total CO_2 equivalents produced per total substrates utilized, including those accumulated in both the headspace and dissolved in the medium.

Strain(s)	Initial Substrate Carbon (mmol) Glucose Xylose	Total Inorganic Carbon, Final (mmol)[A] HS	Soln	Total	pH, Dissolved C_i Ratio (CO_2(aq)/HCO_3^-)[B]	Product Carbon (mmol)[E] Ethanol Succinate	$Y_{P/S}$ (mol mol^{-1})[C] Ethanol Succinate	$Y_{P\text{-}tot/S\text{-}tot}$ (mol-C mol-C^{-1})[D]	$Y_{CO2\text{-}eq/S\text{-}tot}$ (mol mol^{-1})[E]
G2E	3.76 ± 0.15 2.02 ± 0.10	0.42 ±0.03	0.76 ±0.05	1.18 ±0.06	6.6 0.56 ± 0.01	2.2 ± 0.1 0 ± 0	1.76 ± 0.12 0 ± 0	0.59 ± 0.04	1.88 ± 0.12
X2S	3.92 ± 0.15 1.81 ± 0.10	NR	NR	NR	NR	NR	NR	NR	NR
G2E+X2S	4.10 ± 0.15 1.85 ± 0.10	0.56 ±0.04	0.63 ±0.04	1.19 ±0.06	6.2 1.4 ± 0.1	2.4 ± 0.1 1.9 ± 0.1	1.76 ± 0.39 1.26 ± 0.05	0.72 ± 0.03	1.13 ± 0.07
AF25	4.07 ± 0.15 1.95 ± 0.10	0.71 ±0.01	1.1 ± 0.1	1.81 ±0.10	6.5 0.71 ± 0.01	3.9 ± 0.1 0 ± 0	1.79 ± 0.04 0 ± 0	0.64 ± 0.01	1.70 ± 0.11

When compared with molar yield of ethanol from glucose (1.76 ± 0.12 mol mol^{-1}; **Table 4.1**), this result follows the expected 1:1 CO_2:ethanol stoichiometry; validating the relationships used in the system carbon balance. Under the same conditions, meanwhile, without supplying an exogenous C_i source, X2S was unable to grow (consistent with **Figure 4.2** and **Figure 4.3)**, leading to no sugar utilization or pressure generation (**Figure 4.6*A-C***); noting, however, that full xylose conversion as well as robust growth and succinate production were possible when the same sealed vessel was instead initially

charging with 30 psig CO_2(g) (**Figure 4.7**). In contrast, by coculturing it together with G2E (at a 1:1 initial inoculum ratio), X2S growth was indeed rescued as a result of the C_i made available via CO_2 evolution by G2E; with the resulting G2E+X2S coculture achieving complete utilization of both sugars in support of ethanol and succinate coproduction (2.7 ± 0.1 g L^{-1} final titer for both) (**Figure 4.6*A*-*C***). Notably, the overall yield of succinate from xylose (0.99 ± 0.04 g-succinate g-xylose^{-1}) was consistent with past studies involving exogenous HCO_3^- addition[118], indicating that C_i availability did not limit X2S when solely supplied as CO_2 from G2E. Similar rates of pressure generation between G2E and G2E+X2S, meanwhile, further suggest that the fitness of G2E was not inhibited (nor improved) by the presence of X2S (**Figure 4.6*C***).

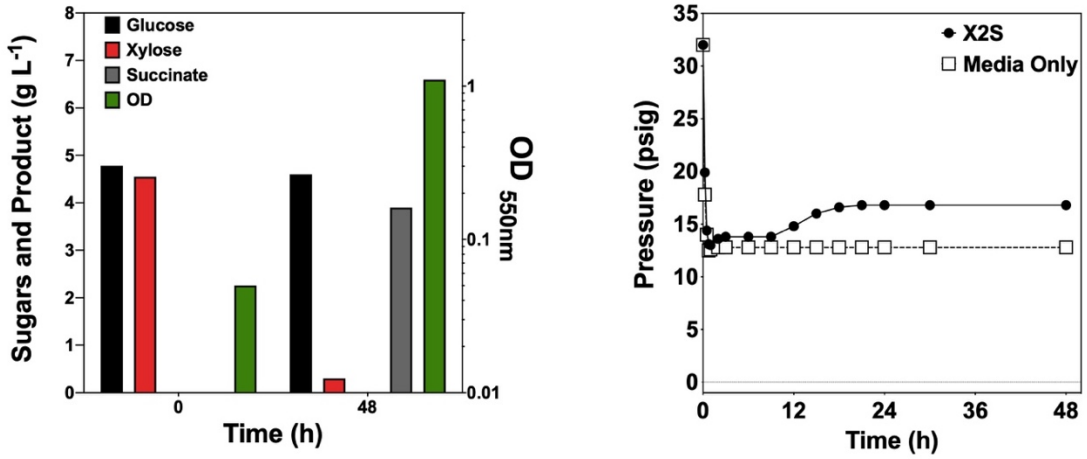

Figure 4.7 Batch fermentation of X2S using a 10 g L^{-1} glucose-xylose sugar mixture (1:1 by mass) with CO_2 pre-charged into the sealed vessel at 30 psig initially.

(*A) Concentrations of glucose (black bar), xylose (red bar), OD_{550nm} (green bar), and succinate (grey bar) were measured in the fermentation broth at 0 and 48 h, revealing that nearly all supplied xylose was converted to succinate while glucose remained unused and no ethanol was detected. (B) Vessel pressure during X2S monoculture cultivation (closed circles) compared with an abiotic (i.e., media only) control (open squares).*

As a comparison, with the ability to co-ferment both glucose and xylose [156], ethanologenic *E. coli* AF25 was analogously cultured by itself where, as expected, it entirely consumed both substrates (**Figure 4.6*A***) and generated a correspondingly higher final ethanol titer (4.4 ± 0.1 g L^{-1}) while achieving similar yields of both ethanol and CO_2 equivalents relative to G2E (**Table 4.1**). Compared with the above cultures, AF25 accumulated the highest final system pressure, exceeding that of G2E by 50% due to its ability to also co-ferment xylose (**Figure 4.6*A***, ***C***). Meanwhile, although the final system pressure of G2E+X2S actually exceeded that of G2E, this largely resulted due to the pH-lowering effect of succinate accumulation (**Figure 4.6*A***), which caused a ~3-fold shift in dissolved C_i equilibrium towards CO_2 (**Table 4.1**) and its increased headspace accumulation. However, in terms of final accumulation total C_i, a 34% reduction was indeed observed for G2E+X2S relative to AF25 (**Table 4.1**), whereas $Y_{CO2\text{-}eq/S\text{-}tot}$ for G2E+X2S was similarly reduced (by 35-40%; 1.13 ± 0.07 mol mol^{-1}) relative to both AF25 and G2E (1.70 ± 0.11 and 1.88 ± 0.12 mol mol^{-1}, respectively). Overall, with significantly reduced total C_i accumulation, these results suggest that succinate coproduction represents a robust strategy for *in situ* CO_2 recycling. Furthermore, as a result of this approach, 72% of all supplied substrate carbon was conserved and converted into final products (i.e., ethanol or succinate), compared to just 64% when both sugars were co-utilized to produce just ethanol by AF25. Lastly, enhanced carbon conversion efficiency was achieved here without need to supply additional reducing equivalents by rationing and allocating specific portions of the feedstock between complementary metabolic functions; an approach greatly facilitated by using an engineered coculture.

4.2.3 Characterizing the Dynamic Behavior of a CO_2-Recycling Coculture

A series of fermentations were next performed to understand the dynamic behaviors of the individual members comprising the G2E+X2S coculture. Despite using a 1:1 initial inoculum ratio (with each strain seeded at 10^7 CFU mL^{-1}), G2E grew more rapidly, consuming all glucose within the first 21 h, at which point the final ethanol titer reached 2.6 g L^{-1} and G2E comprised more than 99% of the total population ($5.6x10^9$ vs $1.1x10^7$ CFU mL^{-1} for G2E and X2S, respectively; **Figure 4.6*D*, *E***). Rapid glucose consumption in turn led to a sharp increase in pressure and Ci accumulation (**Figure 4.8**, **Table 4.2**) and decline in pH (7.4 to 6.7) (**Figure 4.6*F***). Meanwhile, following an initial lag of

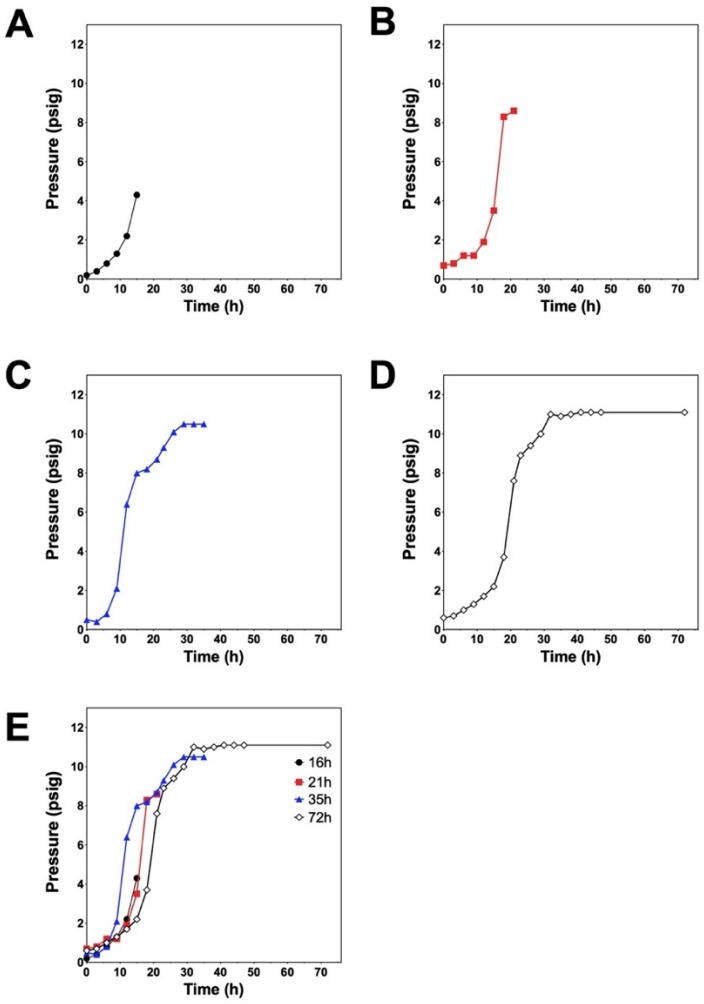

Figure 4.8 Pressure profiles generated during a series of parallel G2E+X2S fermentations initially supplied with a 2:1 (by mass) glucose-xylose mixture (9 g L^{-1} total) and seeded at a 1:1 initial inoculum ratio.

Each vessel was sacrificed at a different time in order to assay the fermenter internals, including at: (A) 16 h (black circles), (B) 21 h (red squares), (C) 35 h (blue triangles), and (D) 72 h (open diamonds). (E) An overlay of the pressure profiles for all 4 vessels.

~16 h (**Figure 4.6*E***), X2S then began to grow and completely consumed all xylose by 35 h, resulting in a final succinate titer of 2.8 g L^{-1} (**Figure 4.6*D***), further medium acidification (to pH 6.2; **Figure 4.6*F***), and corresponding additional increase in pressure (reaching ~11 psig; **Figure 4.8**). Meanwhile, by 35 h the population had dramatically shifted, with X2S

now accounting for 66% of total viable cells (**Figure 4.6*E***). Since X2S is relieved from glucose catabolite repression and thus capable of utilizing xylose in the presence of glucose (**Figure 4.7**), the observed lag was attributed to the initial lack of available C_i, which then only became as G2E fermented glucose to ethanol. By the end of the lag (i.e., 16 h), dissolved C_i was estimated as 0.85 mmol, which later peaked at 1.0 mmol by 21 h (corresponding with glucose exhaustion) before declining to 0.67 mmol by 35 h (**Figure 4.6*F***, **Table 4.2**). These results further demonstrate the essential dependence of X2S on G2E for provision of C_i and how succinate coproduction can be used to recycle CO_2 byproduct, while also illustrating how this coculture itself is naturally capable of responding to changing conditions within the sealed bioreactor system.

Table 4.2. Time-dependent performance of the G2E+X2S coculture and the distribution of carbon among major organic and inorganic fermentation products.

All cultures were grown at 37℃ in AM1 mineral salts medium initially at pH 7.4 and supplied with ~9 g L^{-1} of total sugars in a sealed vessel with 21 mL total liquid volume. Only overall yields are reported. Errors represent the standard error from biological triplicates. 'NR' indicates 'not reported', in this case due to the fact that the sealed vessel was initially at atmospheric pressure and anaerobic conditions. [A] *Includes $CO_{2(aq)}$ and HCO_3^-. At pH values < 8, CO_3^{2-} levels are negligible and were thus omitted. Abbreviations: HS, headspace; Soln, solution.* [B] *pH of the culture medium measured at 96 h. Major dissolved inorganic carbon species estimated via Equations 6-9 in methods section.* [C] *$Y_{P/S}$ denotes the overall molar yield coefficient of each product per specific substrate utilized.* [D] *$Y_{P\text{-}tot/S\text{-}tot}$ denotes the overall molar yield coefficient of total products per total substrates utilized on a carbon basis.* [E] *$Y_{CO2\text{-}eq/S\text{-}tot}$ denotes the overall molar yield coefficient of total CO_2 equivalents produced per total substrates utilized, including those accumulated in both the headspace and dissolved in the medium.*

Time (h)	Initial Substrate Carbon (mmol) Glucose Xylose	Total Inorganic Carbon, Final (mmol)[A] HS	Soln	Total	pH, Dissolved C_i Ratio (CO_2(aq)/HCO_3^-)[B]	Product Carbon (mmol)[E] Ethanol Succinate
0	4.3 1.9	NR	NR	NR	7.4 NR	0 0
16	1.46 1.75	0.24	0.85	1.1	7.0 0.23	1.3 0.3
21	0 1.15	0.47	1.0	1.5	6.7 0.45	1.9 0.66
35	0 0	0.60	0.67	1.3	6.2 1.4	2.6 1.9
72	0 0	0.61	0.68	1.3	6.2 1.4	2.4 1.8

4.2.4 ^{13}C-Labeling and Fingerprinting Analyses Confirm Inter-Strain CO_2-Recycling While Revealing Additional Metabolite Exchange Behaviors

To provide a direct and quantitative measure of the extent of inter-strain CO_2 recycling within G2E+X2S cocultures, a series of ^{13}C-labeling studies were next performed; in this case being greatly facilitated by the catabolically-orthogonal nature of the individual member strains. More specifically, since each strain can utilize only one but not both

sugars, using glucose-xylose mixtures composed of one uniformly labeled and one unlabeled sugar, inter-strain CO_2 exchange could be easily resolved by determining the mass isotopomer distribution (MID) of succinate. First, the natural isotopic abundance of carbons in the test system of interest (2:1 glucose-xylose mixture by mass; 9 g L^{-1} total) was determined by providing both unlabeled sugars, from which it was found that less than 4% of succinate isotopomers were labeled as M+1 (where M+N is the mass fraction of succinate containing N number of ^{13}C atoms in its structure) (**Figure 4.9*A***, **Table 4.3**). In contrast, when providing [U-^{13}C]glucose and unlabeled xylose, the major succinate isotopomer was then M+1 (47% of all isotopomers); proving that [^{13}C]CO_2 released by G2E during ethanol fermentation from [U-^{13}C]glucose was in fact significantly fixed and reutilized by X2S to produce succinate. Meanwhile, in light of the inherent redox limitations of X2S, 71% of PEP produced during xylose catabolism can theoretically enter rTCA and be carboxylated to OAA, whereas the remaining 29% would be converted to pyruvate and then decarboxylated by PDH (yielding the required reducing equivalents for succinate production in the process; **Figure 4.9*A***). In this case, up to 83% of succinate molecules formed by X2S could be synthesized by recycling CO_2 derived from G2E (where 35% of succinate would be generated via the combined glyoxylate bypass and oxidative TCA (**Figure 4.4**). Here, if considering just M+1, it can be concluded that 12% of all succinate carbons (10.5 mM) came from recycling [^{13}C]CO_2 evolved during ethanol fermentation; equal to 57% of the theoretical maximum (i.e., 21% of all succinate carbons from CO_2 recycling). With a final ethanol production by G2E reaching 2.0 g L^{-1} total ethanol produced (corresponding to 43.4 mM co-produced CO_2), in this case, again based solely on M+1 succinate, the G2E+X2S coculture effectively recycled 24% of evolved

CO_2, which translates to a carbon conservation efficiency of 71% (**Table 4.3**). With theoretical carbon conversion efficiency topping out at 82.6% for a 2:1 (by mass) glucose-xylose mixture (**Table 4.4**), this represents 86% of the maximum possible performance.

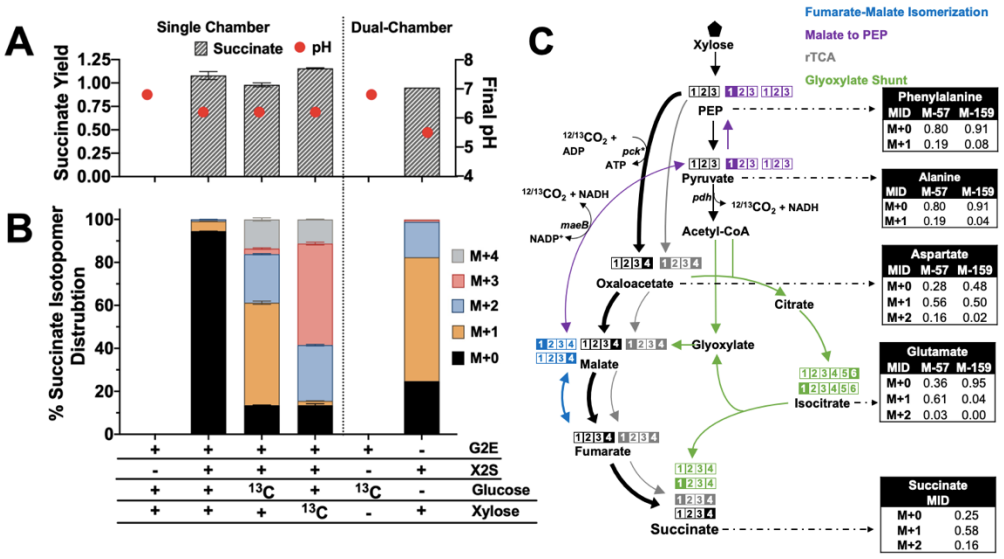

Figure 4.9 Confirming and understanding inter-strain CO_2 and other metabolite exchange behaviors via ^{13}C-labeling and fingerprinting analyses.

Different mixtures of ^{13}C-labeled and unlabeled glucose and xylose were supplied to G2E+X2S cocultures in order to track and quantify CO_2 assimilation by X2S by determining the resultant effect on the succinate mass isotopomer distribution (MID). In all cases, cultures were initially supplied with 2:1 (by mass) glucose:xylose mixture. (A) Comparing the yield of succinate and final culture pH for each fermentation. (B) Comparing the resulting succinate MID, as determined by liquid chromatography-mass spectroscopy (LC-MS). '+' and '-' indicate the presence and absence of each strain/sugar in the experiment, respectively, while '^{13}C' indicates where the form of sugar used was [U-^{13}C]. In the dual-chamber study, while the headspace between both chambers was connected, the first chamber contained only G2E and glucose (left column in A and B) while the second chamber (right column in A and B) contained only X2S and xylose. (C) Schematic of the relevant labeling routes in the dual-chamber experiment, where ^{13}C carbons and their labeling positions are indicated by filled/colored boxes. MID of select amino acid fragment ions are also shown for X2S biomass. Error bars represent the standard error from biological triplicates.

Along with M+1, however, additional succinate isotopomers, including M+0, M+2, M+3, and M+4, were also detected, with relative abundances reaching 13%, 22%, 3%, and

14%, respectively (**Figure 4.9**). Taken together, these additional isotopomers suggested the total abundance of labeled

Table 4.3. G2E+X2S coculture performance and succinate mass isotope distribution during fermentations in single and dual-chamber vessels.

All cultures were grown at 37℃ in AM1 mineral salts medium initially supplied with different mixtures of ^{13}C-labeled and unlabeled glucose and xylose. Errors represent the standard error from biological triplicates. 'NR' indicates 'not reported', in this case due to the fact that G2E did not produce any succinate. [A] ^{13}C indicates universally labeled glucose or xylose was used during fermentations. [B] $Y_{P/S}$ denotes the overall mass yield coefficient of each product per specific substrate utilized. [C] Average concentrations of each succinate isotopomer, as calculated from the succinate MID percentages determined via LC-MS. [D] $Y_{P\text{-}tot/S\text{-}tot}$ denotes the overall molar yield coefficient of total products per total substrates utilized on a carbon basis.

Strain	Initial Substrate[A] (g L^{-1})	$Y_{P/S}$[B] (g g^{-1})	Final Titer (g L^{-1})	$Y_{P\text{-}tot/S\text{-}tot}$ (mol-C mol-C^{-1})[D]	Succinate Isotope Contribution (g L^{-1})[C]				
	Glucose Xylose	Ethanol Succinate	Ethanol Succinate		M+0	M+1	M+2	M+3	M+4
Single Chamber									
G2E	5.5 ± 0.1 2.9 ± 0.1	0.45 ± 0.03 NR	2.5 ± 0.2 NR	0.59 ± 0.05	NR	NR	NR	NR	NR
G2E+X2S	6.76 ± 0.1 2.96 ± 0.1	0.39 ± 0.01 1.08 ± 0.03	2.7 ± 0.1 3.2 ± 0.1	0.70 ± 0.04	3.0 ± 0.1	0.15 ± 0.01	0.05 ± 0.1	0 ± 0	0 ± 0
G2E+X2S	4.6 ± 0.1 (^{13}C) 2.8 ± 0.1	0.42 ± 0.02 0.98 ± 0.01	2.0 ± 0.1 2.6 ± 0.1	0.71 ± 0.05	0.35 ± 0.01	1.2 ± 0.1	0.59 ± 0.01	0.07 ± 0.01	0.36 ± 0.01
G2E+X2S	6.1 ± 0.1 2.3 ± 0.1 (^{13}C)	0.41 ± 0.02 1.16 ± 0.01	2.5 ± 0.1 2.7 ± 0.1	0.71 ± 0.03	0.36 ± 0.01	0.05 ± 0.01	0.70 ± 0.01	1.30 ± 0.01	0.30 ± 0.01
G2E+X2S	2.8 ± 0.1 (^{13}C) 6.4 ± 0.1	0.43 ± 0.1 0.85 ± 0.01	1.2 ± 0.1 5.7 ± 0.1	0.82 ± 0.02	2.6 ± 0.1	2.3 ± 0.2	0.48 ± 0.01	0.08 ± 0.01	0.24 ± 0.01
Dual Chamber									
G2E	10.8 ± 0.1 (^{13}C) 0	0.50 NR	5.5 NR	0.76	NR	NR	NR	NR	NR
X2S	0 5.4 ± 0.1	NR 0.95	NR 5.1		1.26	2.9	0.84	0.05	0.007

carbons in succinate was in fact closer to 38.5%; a finding which, by exceeding the theoretical maximum potential, suggested the unexpected exchange of additional

metabolites and/or significant carbon rearrangement within X2S. In particular, M+0 succinate can be produced by two main metabolic routes: 1) assimilation of CO_2 derived from xylose catabolism by X2S itself and/or 2) labeled carbon arrangement by isocitrate splitting through the glyoxylate cycle (as illustrated in **Figure 4.10**). Meanwhile, M+2 succinate, can putatively be produced by: 1) incorporation of two $[^{13}C]CO_2$ into one succinate and/or 2) as a result of exchanging an additional metabolite(s) that could also serve as a succinate precursor. To investigate the latter mechanism, supernatant

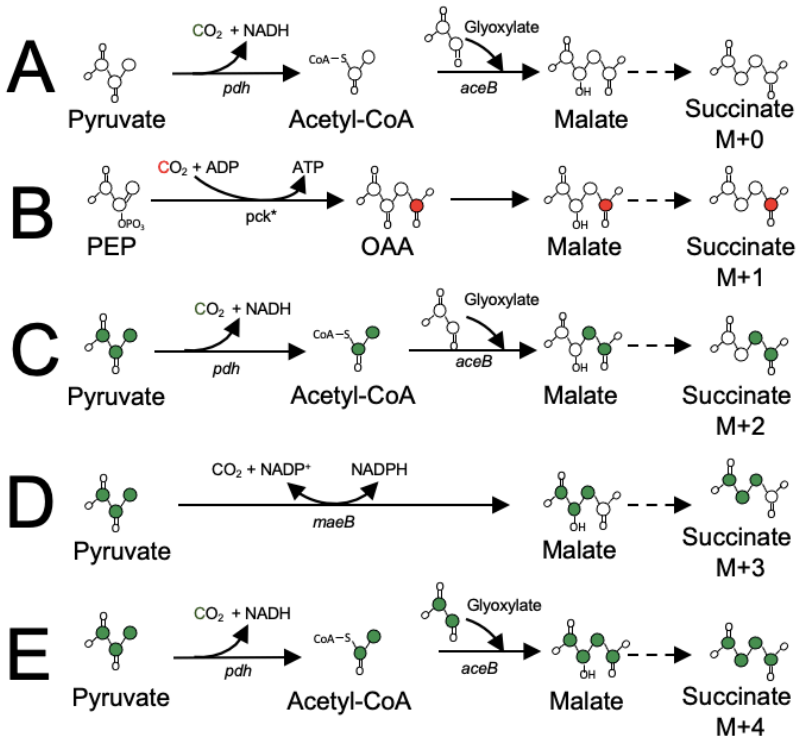

Figure 4.10 Schematic representation of the predominant pathways associated with succinate fermentation in the single chamber bioreactor and the resulting succinate labeling patterns.

White circles are ^{12}C carbons and derived from xylose; Red and green circles are ^{13}C carbons and derived from glucose in the form of CO_2 and pyruvate, respectively.

samples from the first G2E+X2E coculture experiment (shown in **Figure 4.6**) were revisited and thoroughly analyzed across the time course by HPLC, revealing the appearance of pyruvate at 21 h and its subsequent disappearance by 35 h; timepoints that again correspond with the depletion of glucose and xylose, respectively (**Figure 4.11**). Thus, we hypothesized that, as a result overflow metabolism in the presence of abundant [U-^{13}C]glucose, [U-^{13}C]pyruvate was secreted from G2E and subsequently scavenged by X2S. Once assimilated, [U-^{13}C]pyruvate could be converted to [^{13}C]CO_2 and [2-^{13}C]acetyl-CoA via pyruvate dehydrogenase (active in X2S), the latter of which could then enter the

glyoxylate cycle, yielding not only M+2 succinate but also the M+4 isotopomer (**Figure 4.10**). Finally, the M+3 succinate isotopomer was a minor product, likely resulting from

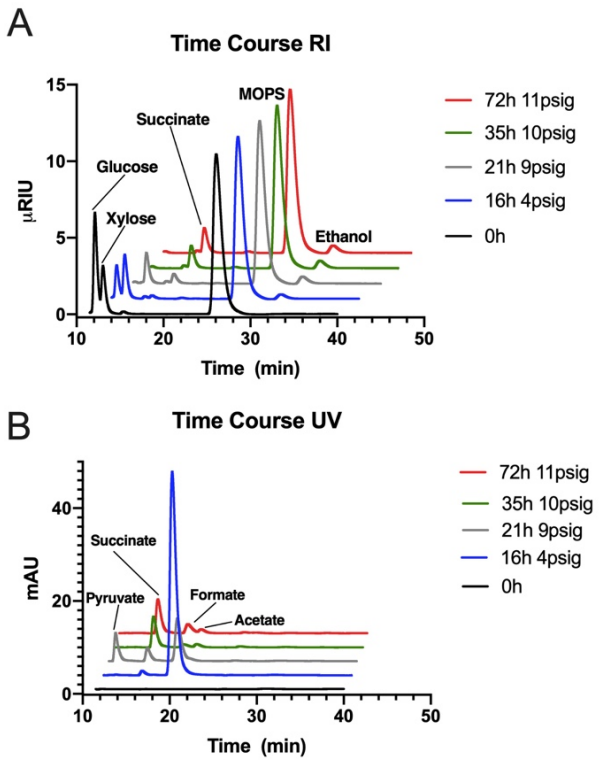

Figure 4.11 Comparing HPLC chromatograms from the G2E+X2S fermentation as a function of fermentation time.

The coculture was initially supplied with a 2:1 (by mass) glucose-xylose mixture (9 g L^{-1} total) and seeded at a 1:1 initial inoculum ratio. Raw outputs from the (A) refractive index detector [glucose (12.1 min), xylose (13.1 min), succinate (16.3 min), MOPS (26.1 min), ethanol (31.1 min)] and (B) UV-Vis detector [pyruvate (12.3 min), succinate (16 min), formate (19.5 min), acetate (20.1 min)]. A peak corresponding to pyruvate uniquely appears at 21 h before then disappearing by 35 h

inefficient pyruvate carboxylation by MaeA [154]. Assuming our hypothesis to be true (i.e., M+4 mainly derived from [U-^{13}C]pyruvate), based on M+3 and M+4, at least 15% of the total carbon in all produced succinate would have come from assimilated [U-^{13}C]pyruvate which, with 2.6 g L^{-1} succinate produced, would have required the total exchange of ~590 mg L^{-1} pyruvate throughout the fermentation. Assimilated pyruvate may have contributed to an enhanced CO_2 recycling capacity in X2S by contributing precursors for additional

PEP synthesis and/or by shifting the redox status to allow more PEP to serve as Pck substrate and enter rTCA; prospective phenomena that are difficult to untangle but worthy of future investigation. Lastly, to complement and validate these findings, G2E+X2E was also alternatively provided with a mixture of [U-^{13}C]xylose and unlabeled glucose; in this case resulting in a near mirror image succinate isotopomer distribution (14%, 2%, 26%, and 47%, 11% for M+0, M+1, M+2, M+3, and M+4, respectively) (**Figure 4.9*B***), confirming the occurrence of significant CO_2 recycling along with other, potential modes of metabolite exchange.

Table 4.4. Theoretical maximum carbon conservation efficiency of G2E+X2S cocultures, as predicted for different initial glucose-xylose mixtures (by mass).

Analysis assumes the maximum CO_2 fixation potential of X2S is 0.5 mol CO_2 fixed per mol succinate produced. [A] CO_2 produced per mol of total sugar mixture utilized. [B] Predicted values >100% indicate a deficit for inorganic carbon, where full xylose conversion would not be possible without additional C_i supplementation.

Initial Sugar Mixture Glucose:Xylose	CO_2 Produced (mol mol-substrate^{-1})[A]	CO_2 Fixed (mol mol-substrate^{-1})[A]	Carbon Conservation Efficiency (%)[B]
9:1	1.77	0.08	71.4
7:3 (2.33:1)	1.32	0.24	81.0
6:3 (2:1)	1.25	0.27	82.6
5:5 (1:1)	0.91	0.39	90.5
3:7 (1:2.33)	0.53	0.53	100.1
1:9	0.17	0.65	109.6

To further investigate the relative contributions of CO_2 recycling vs. other potential metabolite exchanges, a dual-chamber sealed bioreactor system was developed to provide physical separation between individual strains (and their exometabolomes) while enabling CO_2 gas exchange via connected headspaces (**Figure 4.5*B***). One chamber contained G2E and [U-^{13}C]glucose and the other X2S and xylose. During fermentation, both sugars were fully consumed in their respective chambers (**Figure 4.12*A***), and the same total pressure was achieved throughout (5 psig final; **Figure 4.12*B***). Final pH, however, differed greatly between chambers (pH 6.8 and 5.6, respectively; **Figure 4.9*B***) owing to ethanol vs. succinate production. As expected, M+1 remained the major succinate isotopomer (57%; **Figure 4.9*B***). Meanwhile, by blocking the potential for pyruvate exchange, we expected to observe significant reductions in both M+2 and M+4 succinate, leading also to a reduction in total carbons labeled. As expected, by physically separating these two strains, the abundance of labeled carbons amongst all succinate carbon dropped from 38.5% to 22%; confirming that metabolite exchanges beyond just CO_2 recycling were significant in

G2E+X2S cocultures. Interestingly, while the succinate MID no longer included M+4 (supporting the likelihood that pyruvate was indeed the exchanged species in the single chamber system), significant (16%) M+2 still remained. Since this indicates that two [^{13}C]CO_2 molecules were in fact being incorporated into succinate, we sought to better understand this mechanism by determining the MID of proteinogenic amino acids in X2S biomass (**Figure 4.9*C***, **Table 4.5**). The first observation was that the labeling pattern

Table 4.5. Mass isotopomer distribution of amino acid fragment ions obtained from X2S biomass.

The biomass of X2S was harvested from the dual-chamber bioreactor where G2E was supplied with [U-^{13}C]glucose in the first chamber and X2S was supplied with unlabeled xylose in the second chamber. ^{A} *M-57 fragment excludes* C_4H_9 ^{B} *M-159 fragment excludes C(O)-O-TBDMS* ^{C} *M-15 fragment excludes* CH_3 ^{D} *M-85 fragment excludes* C_4H_9*-CO*

	Mass Isotopomer Distribution				Ion fragments
Amino Acid	**M+0**	**M+1**	**M+2**	**M+3**	**M-57^{A}** **M-159^{B}** **M-15^{C}** **M-85^{D}**
Isoleucine	0.27	0.54	0.16	0.00	M-15
	0.50	0.46	0.03	0.00	M-159
Methionine	0.26	0.54	0.18	0.00	M-57
	0.46	0.50	0.04	0.00	M-159
Threonine	0.22	0.58	0.15	0.01	M-57
	0.49	0.50	0.00	0.00	M-85
Aspartate	0.28	0.56	0.16	0.00	M-57
	0.48	0.50	0.02	0.00	M-159
Lysine	0.34	0.51	0.12	0.00	M-57
	0.45	0.52	0.02	0.00	M-159
Alanine	0.80	0.19	0.00	0.00	M-57
	0.91	0.04	0.04	0.00	M-159
Serine	0.87	0.12	0.00	0.00	M-57
	0.97	0.02	0.00	0.00	M-159
Phenylalanine	0.80	0.19	0.00	0.00	M-57
	0.91	0.08	0.00	0.00	M-159
Glutamate	0.36	0.61	0.03	0.00	M-57
	0.95	0.04	0.00	0.00	M-159

of aspartate (56% M+1 and 16% M+2), which is also synthesized from oxaloacetate (OAA), was very similar to that of succinate (57% M+1, 16% M+2); indicating that the majority of succinate was synthesized via rTCA under this condition. Furthermore, a decrease in M+2 from 16% for the M-57 fragment to 2% for the M-159 fragment of aspartate confirms the labeling was present at both the 1st and 4th positions of OAA. The labeling profile of alanine indicated that pyruvate had significant one carbon

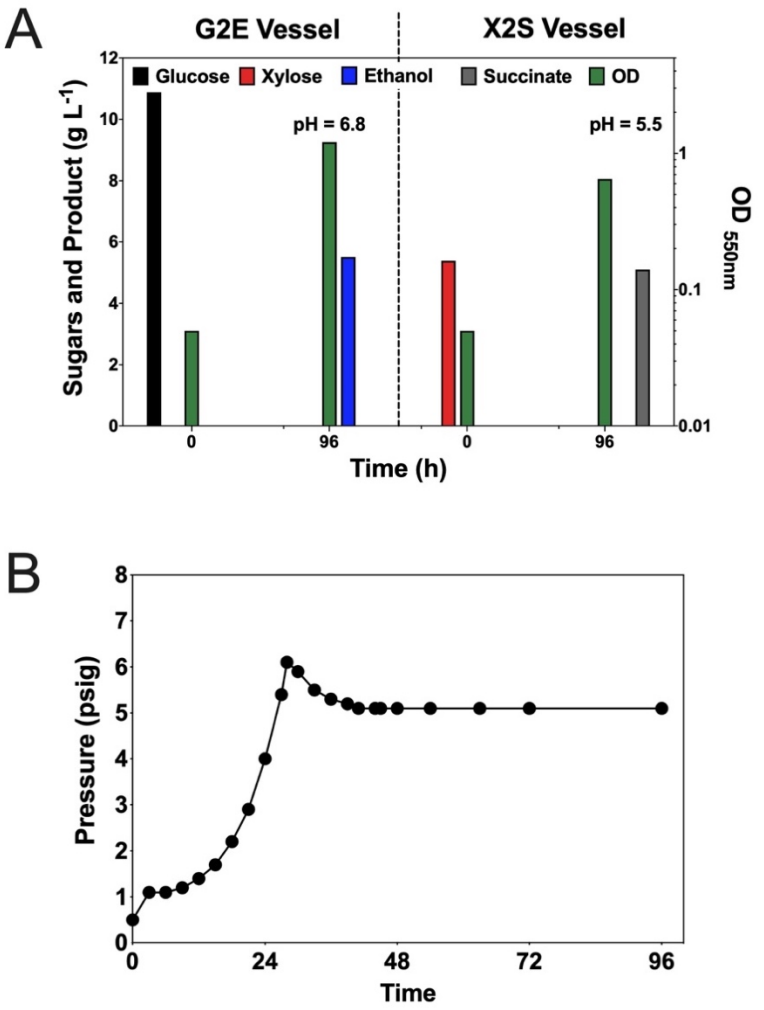

Figure 4.12 Co-cultivation of G2E and X2S in separate chambers of the dual-chamber bioreactor.

(A) Concentrations of glucose (black bar), xylose (red bar), OD_{550nm} (green bar), and succinate (grey bar) as measured in both chambers at 0 h and 96 h. Final pH values were also measured in each vessel. G2E was cultured in the first chamber containing AM1 mineral media supplemented with 100 mM MOPS and [^{13}C]glucose, whereas X2S was cultured in the second chamber containing AM1 mineral media supplemented with 100 mM MOPS and unlabeled xylose. Total initial sugar concentration was increased to 16 g L^{-1} to account for the larger total headspace volume of this configuration, while still maintaining a 2:1 glucose:xylose mass ratio. (B) System pressure profile generated within the dual-chamber bioreactor over the course of the fermentation.

labeling (83% M+0 and 16% M+1). For a labeled pyruvate to be synthesized via the cataplerotic pathway, malate must be labeled at its 1st position. However, PEP

carboxylation of labeled CO_2 yields OAA labeled at its 4th position (**Figure 4.9*C***). Pathway analysis suggested at least the following two routes by which malate and thereby OAA would have obtained their 1st position labeled carbon: 1) since fumarate is a diastereomer, as [4-^{13}C]fumarate reverts back to malate via the TCA cycle it can form either [1-^{13}C] or [4-^{13}C]malate [157]; 2) likewise, [6-^{13}C]citrate can form either [1-^{13}C] or [6-^{13}C] isocitrate via isomerization (**Figure 4.13**). The resulting [1-^{13}C] isocitrate can then form [1-^{13}C]malate via the glyoxylate shunt. Once malate is labelled at the 1st position, this labeled carbon passes on to pyruvate via the cataplerotic pathway. Phenylalanine MID confirms that the M+1 fraction of PEP is identical to that of pyruvate, confirming the conversion of pyruvate to PEP. Carboxylation of pyruvate or PEP with [^{13}C]CO_2 yields malate labelled at 1st and 4th position which, in turn, yields succinate labeled at 1st and 4th position (**Figure 4.9*C***). The surprising discovery that two $^{13}CO_2$ molecules were ultimately assimilated into one succinate indicates the previously unrealized CO_2 recycling potential of anaplerotic carboxlylation reactions. Taken together, these results confirm that M+2 succinate isotopomers were generated by the G2E+X2S coculture in the single chamber fermenter via two main routes: incorporation of additional [^{13}C]CO_2 and exchange of [U-^{13}C]pyruvate.

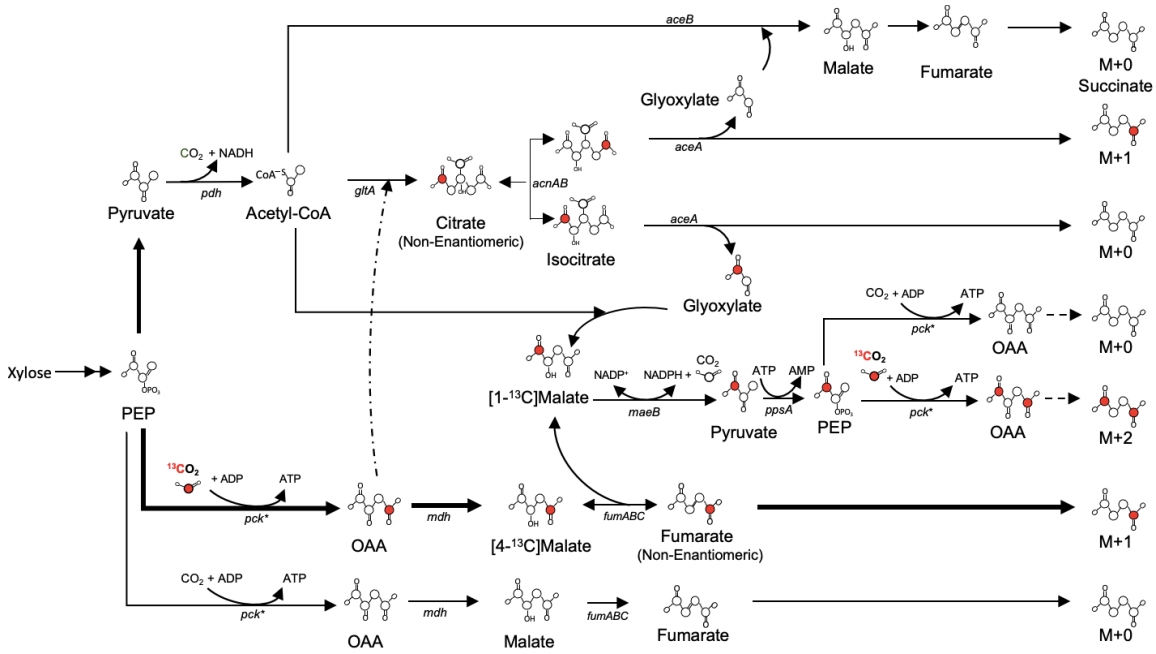

Figure 4.13 Schematic representation of the predominant pathways associated with succinate fermentation in the dual-chamber bioreactor and the resulting succinate labeling patterns.

The primary route for succinate M+1 is pck assimilating [^{13}C]CO_2 to generate [4-^{13}C]OAA. [4-^{13}C]OAA is then converted to succinate M+1 via the reductive TCA cycle. Succinate M+1, along with M+0, can also be generated via the glyoxylate cycle In the glyoxylate cycle, acetyl-CoA combines with [4-^{13}C]OAA to generate [1-^{13}C]citrate via citrate synthase (encoded by gltA). Citrate is a non-enantiomeric molecule, both [1-^{13}C]isocitrate and [4-^{13}C]isocitrate are generated aconitase. Succinate M+1 and M+0is then formed during glyoxylate regeneration as isocitrate undergoes aldol cleavage by isocitrate lyase (encoded by aceA). M+2 labeling routes are achieved via two pathways: (1) labeled glyoxylate combines with unlabeled acetyl-CoA to generate [1-^{13}C]malate and (2) [1-^{13}C]fumarate reversibly converts to [1-^{13}C]malate. Malic enzyme can then convert [1-^{13}C]malate to [1-^{13}C]pyruvate then to [1-^{13}C]PEP. Leading to [1,4-^{13}C]OAA and hence, [1,4-^{13}C]succinte. Genes and enzymes: xylE, D-xylose H^+ transporter; xylFGH, ATP-dependent xylose transporter; xylA, xylose isomerase; xylB, xylulokinase; pyk, pyruvate kinase; pdh, pyruvate dehydrogenase; pck*, PEP-carboxykinase; mdh, malate dehydrogenase; fumABC, fumarase; frdABCD, fumarate reductase; maeB, maleic dehydrogenase, aceA, isocitrate lyase; aceB, malate synthase A; gltA, citrate synthase; acnAB, aconitase; and icd, isocitrate dehydrogenase.*

4.2.5 Controlling Substrate Stoichiometry to Maximize CO_2-Recycling and Carbon Conservation

As discussed, the relative glucose:xylose abundance in the feedstock determines possible extent of CO_2 recycling by the G2E+X2S coculture (**Figure 4.1*A***) and, therefore, the maximum achievable carbon conservation efficiency of the system (**Table 4.4**). To this point, while the focus has been on model sugar mixtures representing the native, 2:1 glucose:xylose ratio of lignocellulosic biomass, alternative ratios were lastly examined in an effort to maximize carbon conservation by the developed coculture system. A series of G2E+X2S cocultures were performed, each supplied with 10 g L^{-1} total sugars according to the following glucose:xylose mass ratios: 9:1, 7:3, 5:5, 3:7 and 1:9. As predicted (see Eqn. 3 in **Figure 4.1*A*** and **Table 4.4**) complete fixation of CO_2 evolved during ethanol production is theoretically possible using a glucose:xylose mixture 1:2.8 molar ratio, or ~3:7 by mass. Expectedly, as xylose abundance increased, so too did succinate production, with a corresponding reduction in ethanol production; in both cases by stoichiometric amounts (**Figure 4.14A**, **Table 4.6**). Though estimated to reach 1.20-1.30 mmol for each of the 9:1, 7:3, and 5:5 glucose:xylose mixtures, total accumulated C_i sharply dropped (by >50%) to just 0.53 ± 0.04 mmol in the case of the 3:7 glucose:xylose mixture (**Table 4.6**). Under this condition, while the system pressure initially peaked at about 24 h (typical of glucose exhaustion) a brief decline then also uniquely followed, presumably as a result of elevated net CO_2 assimilation by X2S, after which the pressure later increased as succinate production resulted in a further pH decline (**Figure 4.14A** and **Figure 4.15**). Further shifting the glucose:xylose ratio to 1:9 proved detrimental, likely since C_i then became insufficiently available to support robust growth of X2S (**Figure 4.15**); as indicated by low final succinate production (**Table 4.6**) and poor xylose consumption (84% unused; **Figure 4.14*B***). Thus, as predicted, the 3:7 glucose:xylose mixture supported the greatest extent of

CO_2 recycling, allowing carbon conversion efficiency 77% (**Table 4.6**); the highest level achieved in this study.

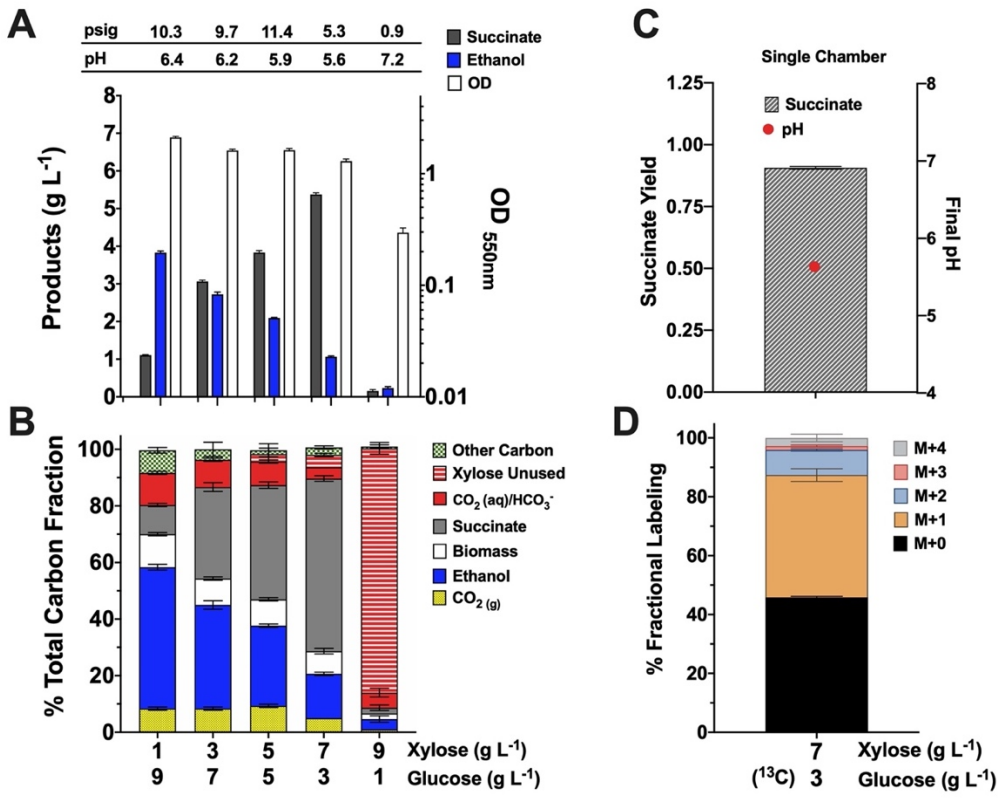

Figure 4.14 Tuning of the feedstock composition enables facile optimization of CO_2 recycling and carbon conversion efficiency.

G2E+X2S cocultures were fermented using different glucose-xylose mixtures across a range of relative concentrations while maintaining the total initial sugar concentration constant at 10 g L^{-1}. In all cases, cocultures were inoculated at a total initial OD_{550nm} of 0.05 using a 1:1 inoculum ratio (i.e., OD_{550nm} of 0.025 for each strain). Fermentation vessels remained sealed throughout, only being opened for sampling after 48 h. (A) Comparing final product titers, cell growth (as OD_{550}), pH, and system pressure for each coculture. (B) Distribution of total system carbon between unused sugars, growth, product and inorganic carbon, as represented by the percent total carbon fraction (i.e., moles carbon in each species divided by total moles carbon supplied initially as sugars). For the case of 3:7 glucose-xylose (by mass), labeling experiments were also performed using [U-^{13}C]glucose and unlabeled xylose in order to track and quantify CO_2 assimilation by X2S, as assessed by (C) final succinate yield (g-succinate g-xylose^{-1}) and pH, as well as (D) succinate mass isotopomer distribution (MID). Error bars represent the standard error from biological triplicates.

Lastly, ^{13}C-labeling was again revisited using [U-^{13}C]glucose and unlabeled xylose at this optimum, 3:7 glucose:xylose ratio. In this case, M+2 and M+4 succinate isotopomers

were 2.7- and 4.3-fold lower, respectively, when compared with the G2E+X2S coculture grown using the 2:1 glucose-xylose mixture (**Figure 4.14*C*,*D*** and **Table 4.3**). With less glucose available, these reductions were likely a result of: 1) reduced rates of overflow metabolism by G2E, leading to lower levels of [U-^{13}C]pyruvate and thus less assimilation by X2S; as well as 2) less [^{13}C]CO_2 generation by G2E which, in turn, reduced the occurrence by which two [^{13}C]CO_2 were assimilated into a single succinate molecule. Interestingly, M+0 tripled in abundance (from ~13% to ~45% for 7:3 and 3:7, respectively), which suggests the possibility that X2S had an improved ability to self-assimilate CO_2 derived from xylose catabolism under these conditions (**Figure 4.14*C*,*D*** and **Table 4.3**). Thus, these results further support the notion that, while CO_2 may represent the most significant inter-strain interaction within the G2E+X2S coculture, the overall process is more complex than it initially appears.

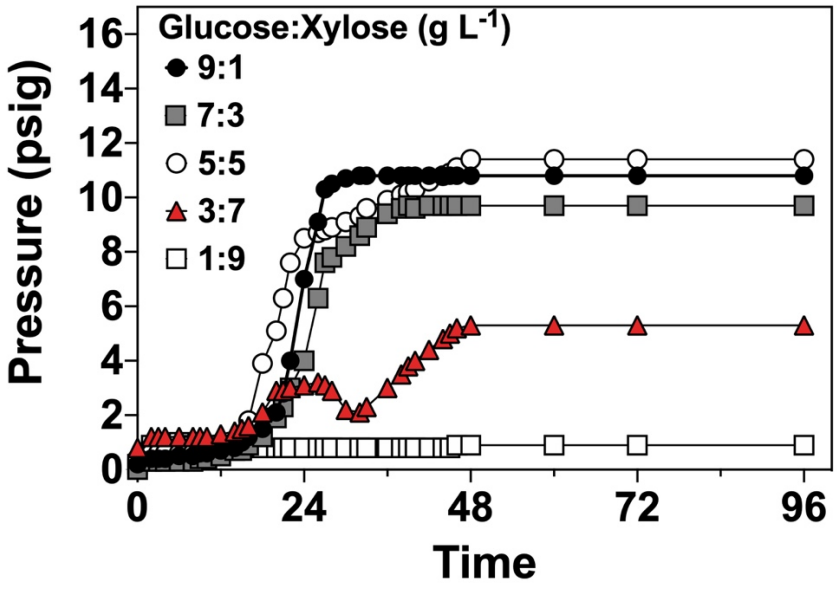

Figure 4.15 System pressure profiles generated over the course G2E+X2S fermentations.

G2E+X2S fermentations were performed using glucose:xylose mass ratios of: 9:1(black circles), 7:3 (grey squares), 5:5 (white circles), 3:7 (red triangle), and 1:9 (white squares). In each case, cultures were initially supplied with 10 g L^{-1} total sugars.

4.3 Conclusion

Overall, this study demonstrates how, through judicious selection of complementary metabolic pathways and a catabolic mechanism allowing them to be driven by distinctly allocated feedstock components, carbon conversion efficiency of lignocellulosic feedstocks can be significantly enhanced through *in situ* recycling of evolved CO_2 by a cooperative, coculture-coproduction system. Ultimately, lessoned learned here have the potential to be applied to other consortia and used to convert diverse feedstocks to a range of coproducts of interest with improved efficiency and less waste.

Table 4.6. Comparing the fermentation performance of G2E+X2S cocultures across a range of different glucose-xylose sugar mixtures.

All cultures were grown at 37℃ in AM1 mineral salts medium initially supplied with ~10 g L^{-1} total sugars at different glucose:xylose mass ratios in a sealed vessel with 21 mL total liquid volume. Errors represent the standard error from biological triplicates. [A] *Includes $CO_{2(aq)}$ and HCO_3^-. At pH values < 8, CO_3^{2-} levels are negligible and were thus omitted. Abbreviations: HS, headspace; Soln, solution.* [B] *pH of the culture medium measured at 96 h. Major dissolved inorganic carbon species estimated via Equations 6-9 in methods section.* [C] *$Y_{P/S}$ denotes the overall molar yield coefficient of each product per specific substrate utilized.* [D] *$Y_{P\text{-}tot/S\text{-}tot}$ denotes the overall molar yield coefficient of total products per total substrates utilized on a carbon basis.* [E] *$Y_{CO2\text{-}eq/S\text{-}tot}$ denotes the overall molar yield coefficient of total CO_2 equivalents produced per total substrates utilized, including those accumulated in both the headspace and dissolved in the medium*

Glucose-Xylose Mass Ratio	Initial Substrate Carbon (mmol) Glucose Xylose	Total Inorganic Carbon, Final (mmol)[A]			pH, Dissolved C_i Ratio (CO_2(aq)/HCO_3^-)[B]	Product Carbon (mmol)[E] Ethanol Succinate	$Y_{P/S}$ (mol mol^{-1})[C] Ethanol Succinate	$Y_{P\text{-}tot/S\text{-}tot}$ (mol-C mol-C^{-1})[D]	$Y_{CO2\text{-}eq/S\text{-}tot}$ (mol mol^{-1})[E]
		HS	Soln	Total					
9-1	6.9 ± 0	0.57 ±0.02	0.76 ± 0.02	1.30 ± 0.10	6.4 0.97 ± 0.03	3.4 ± 0.1 0.70 ± 0.02	1.72 ± 0.04 1.09 ± 0.03	0.60 ± 0.01	1.2 ± 0.1
7-3	6.4 ± 0	0.56 ±0.03	0.64 ± 0.03	1.20 ± 0.10	6.2 1.4 ± 0.1	2.4 ± 0.1 2 .2 ± 0.1	1.56 ± 0.08 1.33 ± 0.05	0.69 ± 0.02	1.0 ± 0.1
5-5	6.5 ± 0	0.62 ±0.02	0.55 ±0.03	1.20 ± 0.10	5.9 3.1 ± 0.4	1.9 ± 0.1 2.7 ± 0.1	1.68 ± 0.04 1.08 ± 0.06	0.69 ± 0.01	1.0 ± 0.1
3-7	6.1 ± 0	0.30 ±0.02	0.23 ±0.02	0.53 ± 0.04	5.6 5.3 ± 0.7	0.95 ± 0.03 3.7 ± 0.1	1.56 ± 0.04 1.16 ± 0.01	0.77 ± 0.01	0.47 ± 0.04
1-9	6.0 ± 0	0.06 ±0.01	0.33 ± 0.07	0.39 ± 0.08	7.2 0.14 ± 0.01	0.21 ± 0.06 0.11 ± 0.05	1.25 ± 0.35 0.41 ± 0.02	0.05 ± 0.02	2.6 ± 0.6

4.4 Methods

4.4.1 Strains and Fermentation Conditions

All strains and plasmids used in this study are listed in **Table 4.7**. All fermentations were conducted without antibiotics at 37°C in AM1 mineral salts medium [158] buffered with 100 mM MOPS (pH 7.4) and supplemented glucose-xylose mixtures at different relative concentrations. A 1:1 working medium volume to headspace volume was used throughout. Monoculture and coculture fermentations were inoculated using a total initial OD_{550nm} of

0.05 (~0.022 gDCW L^{-1}). Unless otherwise stated, and prior to sealing the fermentation vessel, a gentle stream of argon gas was bubbled in the media for ~15 min to displace air from the headspace, facilitating the onset of anaerobic conditions.

Table 4.7. List of strains and plasmids constructed and/or used in Chapter 4.

[A]pck denotes a mutated form of pck (G to A at position -64 relative to the ATG start codon).[B]ptsI* denotes a mutated form of ptsI (single base deletion at position 1,673 causing a frameshift mutation in the carboxyl-terminal region).*

Strains and Plasmids	Relevant Characteristics	Source
Strains		
G2E	LY180 Δ*xylR* Δ*lacZ::cat-sacB* adapted in glucose-xylose mixture; previously referred to as LYglc1	117
KJ122	ATCC 8739 *pck**[A] *ptsI**[B] Δ*ldhA* Δ*adhE* Δ*ackA*, Δ(*focA-pflB*) Δ*mgsA* Δ*poxB* Δ*tdcDE* Δ*citF* Δ*aspC* Δ*sfcA*	118
LP001	KJ122 isolate adapted for ~60 generations in 100 g L^{-1} xylose	153
X2S	LP001 Δ*galP* Δ*ptsI* Δ*glk*::*kan*^{R}	This Study
Plasmids		
pXW001	The *cat-sacB* cassette with the *sacB* native terminator cloned into a modified vector pLOI4162	71
pKD46	λ-Red recombinase, temperature sensitive replication (repA101ts), *bla*	92

4.4.2 Bioreactor Design and Configuration

The configuration and part numbers associated with the developed and employed sealed bioreactors are shown and described **Figure 4.5.** A digital pressure monitor (PMAT4A) and pressure sensors with polysulfone 1/8" hose barb (PREP-N-012) were purchased from PendoTECH (Princeton, NJ) and used to collect system pressure data

4.4.3 Detection of Extracellular Metabolites and ^{13}C-Labeling Experiments

Concentrations of sugars, organic acid, and alcohols in fermentation broth were determined via high performance liquid chromatography (HPLC; Thermo Fisher Scientific UltiMate 3000, Waltham, MA) equipped with a refractive index detector (RID; operated at 45°C), and UV-Vis detector. Analyte separation was achieved using an Aminex HPX-87H column (Bio-Rad Laboratories, Hercules, CA) maintained at 45°C and a mobile phase that consisted of 5 mM H_2SO_4 at a constant flow rate of 0.4 mL min^{-1}.

For ^{13}C labeling experiments, working stocks of [U-^{13}C]glucose and [U-^{13}C]xylose (Cambridge Isotope Laboratories, Inc., Tewksbury, MA) were prepared and filter sterilized

prior to addition. Mass isotopomer distributions of succinate were analyzed by liquid chromatography mass spectrometry (LC-MS). Analytes were separated on a Cogent Diamond Hydride column (4 μ, 100 Å; MicroSolv Technology Corporation) using a modified version of the manufacturer's protocol (Application Note AA-00687). Running buffer A consisted of 50% methanol, 50% DI water, and 10 mM ammonium acetate. Running buffer B consisted of 90% acetonitrile, 10% DI water, and 10 mM ammonium acetate. Samples were diluted 1:1 using a 1:1 mixture of A:B solvents. For analysis, 5 μL of each sample was injected at a constant solvent flow rate of 300 μL/min according to the following schedule: 0-5 min, 100% B; 5-8 min, linear gradient from 100% to 50% B; 8-10 min, 50% B; 10-12 min, linear gradient from 50% to 100% B; 12-15 min, 100% B. Eluent flow was fed into a Bruker micrOTOF$_Q$ mass spectrometer and ionized using electrospray ionization with compounds then detected in the negative-ion mode. Relevant instrument settings were as follows: capillary, +3700 V; end plate offset, +500 V; funnels 1 and 2 RFs, 200 Vpp; hexapole RF, quadrupole ion energy, 5 eV; low mass 55 m/z; collision energy, 10 eV; 100 Vpp; transfer time, 148 μs; prepulse storage, 7 μs. MS data were processed using Bruker Data Analysis 4.2 software. Isotope abundance was determined by measuring succinate mass intensities (117.0164, 118.0185, 119.0196, 120.0275, and 121.0287) at the peak retention time (~3.2 min).

Biomass proteins were hydrolyzed to corresponding amino acids using 6M HCl. Amino acids were then derivatized using N-(tert-butyldimethylsilyl)-N-methyl-trifluoroacetamide (TBDMS) according to previously reported protocols [159,160]. Derivatized amino acids were analyzed by GC-MS (7890 GC system and 5975 MS detector; Agilent Technologies) equipped with a DB5-MS column (J&W Scientific) to

identify the abundance of all amino acid isotopomers [159,161]. The derivatized sample (1 μL) was injected at a 1:5 split ratio using H_2 as carrier gas. Initially, the column was held at 150°C for 2 min, before being increased at 3°C per min to 250°C and then further increased at 8°C per min to 300°C, after which it was held at 300°C for 5 min. The $[M-57]^+$ m/z ion was used to calculate the ^{13}C mass fraction of entire intact amino acids (where M is the molecular mass of the derivatized amino acids). $[M-15]^+$ was used for leucine and isoleucine alone since their $[M-57]^+$ overlaps with other mass peaks [162]. $[M-159]^+$ or $[M-85]^+$, which contain information of the amino acid after loss of its first carbon, were also used for isotopic tracing. The MID for each fragment of the amino acids were represented by M+0, M+1, M+2, etc., indicating the unlabeled, singly labeled, doubly labeled mass isotopomer fractions of the amino acids and so on, respectively. The natural abundance of isotopes, including ^{13}C (1.13%), ^{18}O (0.20%), ^{29}Si (4.70%), and ^{30}Si (3.09%) contributes noise to the mass isotopomer spectrum. This background noise was rectified in MID calculations using a published algorithm and detailed correction protocol

4.4.4 Equation and Sample Calculations

Stoichiometric equations for aqueous dissociation of CO_2 to dissolved inorganic carbon species. Following absorption into an aqueous solution, $CO_{2(aq)}$ becomes hydrated and then readily dissociates into HCO_3^- and CO_3^{2-} according to the following sequence of equilibrium relationships:

$$CO_2(g) \leftrightarrow CO_2(aq) \quad \textbf{(Equation 1)}$$
$$CO_2(aq) + H_2O \leftrightarrow H_2CO_3 \quad \textbf{(Equation 2)}$$
$$H_2CO_3 \leftrightarrow H^+ + HCO_3^- \quad \textbf{(Equation 3)}$$
$$HCO_3^- \leftrightarrow H^+ + CO_3^{2-} \quad \textbf{(Equation 4)}$$
$$H_2O \leftrightarrow H^+ + OH^- \quad \textbf{(Equation 5)}$$

Calculating concentrations of dissolved inorganic carbon species is as follows. Based on the concentration of CO_2(g) in the headspace, represented as pCO_2 (partial pressure of CO_2, in units of atm) the concentration of dissolved $CO_{2(aq)}$ can be calculated using Henry's Law:

$$CO_2(aq) = K_H pCO_2 \quad \textbf{(Equation 6)}$$

K_H is Henry's law constant (in units of mol L^{-1} atm^{-1}), equal to $10^{-1.61}$ mol L^{-1} atm^{-1} at 37°C [163]. Equilibrated concentrations of HCO_3^- in solution were then estimated according to the following relationship:

$$log(HCO_3^-) = pH - pK_a + log\big(CO_2(aq)\big) \quad \textbf{(Equation 7)}$$

pK_a is an equilibrium constant, equal to 4.45 x 10^{-7} [163]. Since levels of CO_3^{2-} are negligible at acidic to neutral pH, these were omitted from all calculations. Total dissolved inorganic carbon was then determined as the sum of $CO_{2(aq)}$ and HCO_3^-.

Calculating total carbon from CO_2(g) generated in the headspace is as follows. Moles of CO_2 in the headspace can be calculated using the ideal gas law,

$$PV = nRT \quad \textbf{(Equation 8)}$$

P is the partial pressure of CO_2 detected in headspace (in units atm), V is the volume of headspace (in this study, equal to 20.5 mL when the aqueous volume was 20.5 mL), n is the number of moles in the headspace, R is the gas constant (0.08206 L atm mol^{-1} K^{-1}) and

T is the temperature (in this study, 310 K). To convert psi to atm, a conversion factor of 14.7 psi = 1 atm was used. As an example, if the pCO_2 is 11.1 psi (0.76 atm) then moles of CO_2(g) can be calculated as:

$n = (0.76 \text{ atm} \times 20.5 \text{ mL}) \times (0.08206 \text{ L atm mol}^{-1} \text{ K}^{-1} \times 310 \text{ K})^{-1} = 0.56$ mmol CO_2 = 0.56 mmol C **(Equation 9)**

Calculating total carbon in biomass is as follows. Biomass dry cell weight (DCW) values were calculated using a conversion factor of 0.44 g-DCW L^{-1} = 1 OD_{550}. For example, if OD_{550} is 1.6 and the fermentation working volume is 20.5 mL, the total biomass DCW can be calculated as:

$$1.6 \text{ OD}_{550} \times 20.5 \text{ mL} \times (0.44 \text{ g-DCW L}^{-1} \text{ OD}_{550}^{-1}) = 15 \text{ mg-DCW} \quad \textbf{(Equation 10)}$$

The carbon fraction of biomass was then estimated assuming an empirical chemical formula of $CH_{1.8}O_{0.5}N_{0.2}$ for *Escherichia coli* biomass, which corresponds to a molecular weight of 24.6 g mol^{-1}.

Carbon Conservation Efficiency was calculated as the following. For a glucose-xylose sugar mixture of 5 g L^{-1} each (total 10 g L^{-1}), the total substrate carbon and product carbon were calculating as the following.

$$[5 \text{ g L}^{-1} \text{ glucose} / (\text{molar mass of glucose})] \times (6 \text{ mol-C/mol glucose}) = 0.167 \text{ mol-C L}^{-1} \quad \textbf{(Equation 11)}$$

Since theoretically 1 mole of glucose can be converted 2 mole ethanol, a maximum of 0.055 mol L^{-1} ethanol (0.11 mol-C L^{-1}) can be produced from 5 g L^{-1} glucose. Now for xylose

$$[5\ g\ L^{-1}\ xylose\ /(molar\ mass\ of\ xylose)]\ x\ (5\ mol\text{-}C/mol\ xylose) = 0.167\ mol\text{-}C\ L^{-1} \quad \textbf{(Equation 12)}$$

Therefore, the total substrate carbon provided was 0.333 mol-C L^{-1}. And since theoretically 1 mole of xylose can produce 1.43 moles of succinate, a maximum of 0.190 mol-C L^{-1} can be converted to succinate from 5 g L^{-1} xylose. Therefore, the theoretical substrate carbon recovery is calculated as

$$(0.112\ mol\text{-}C\ L^{-1} + 0.190\ mol\text{-}C\ L^{-1})/\ (0.333\ mol\text{-}C\ L^{-1})\ *100\% = 90.5\%\ carbon\ conserved \quad \textbf{(Equation 13)}$$

4.4 References

2 Saha, B. C. Hemicellulose bioconversion. *J Ind Microbiol Biotechnol* **30**, 279-291 (2003).

3 Girio, F. M. *et al.* Hemicelluloses for fuel ethanol: A review. *Bioresour Technol* **101**, 4775-4800, doi:10.1016/j.biortech.2010.01.088 (2010).

47 Eiteman, M. A., Lee, S. A. & Altman, E. A co-fermentation strategy to consume sugar mixtures effectively. *J Biol Eng* **2**, 3, doi:10.1186/1754-1611-2-3 (2008).

82 Yomano, L. P., York, S. W., Shanmugam, K. T. & Ingram, L. O. Deletion of methylglyoxal synthase gene (mgsA) increased sugar co-metabolism in ethanol-producing Escherichia coli. *Biotechnol Lett* **31**, 1389-1398, doi:10.1007/s10529-009-0011-8 (2009).

83 Miller, E. N. *et al.* Silencing of NADPH-dependent oxidoreductase genes (yqhD and dkgA) in furfural-resistant ethanologenic Escherichia coli. *Appl Environ Microbiol* **75**, 4315-4323, doi:10.1128/AEM.00567-09 (2009).

92 Datsenko, K. A. & Wanner, B. L. One-step inactivation of chromosomal genes in Escherichia coli K-12 using PCR products. *Proc Natl Acad Sci U S A* **97**, 6640-6645, doi:10.1073/pnas.120163297 (2000).

93 Jantama, K. *et al.* Eliminating side products and increasing succinate yields in engineered strains of Escherichia coli C. *Biotechnol Bioeng* **101**, 881-893, doi:10.1002/bit.22005 (2008).

102 Nieves, L. M., Panyon, L. A. & Wang, X. Engineering Sugar Utilization and Microbial Tolerance toward Lignocellulose Conversion. *Front Bioeng Biotechnol* **3**, 17, doi:10.3389/fbioe.2015.00017 (2015).

117 Flores, A. D., Ayla, E. Z., Nielsen, D. R. & Wang, X. Engineering a Synthetic, Catabolically Orthogonal Coculture System for Enhanced Conversion of Lignocellulose-Derived Sugars to Ethanol. *ACS Synth Biol* **8**, 1089-1099, doi:10.1021/acssynbio.9b00007 (2019).

123 Langholtz MH, S. B., & Eaton LM Vol. 1 (Oak Ridge National Laboratory, Oak Ridge, TN, (Energy USDo), 2016).

124 Lynd, L. R. Large-Scale Fuel Ethanol from Lignocellulose - Potential, Economics, and Research Priorities. *Appl Biochem Biotech* **24-5**, 695-719 (1990).

125 Blaschek, Z. L. L. a. H. P. *Biomass to biofuels: strategies for global industries.*, (2010).

126 Bogorad, I. W., Lin, T. S. & Liao, J. C. Synthetic non-oxidative glycolysis enables complete carbon conservation. *Nature* **502**, 693-697, doi:10.1038/nature12575 (2013).

127 Jarboe, L. R., Grabar, T. B., Yomano, L. P., Shanmugan, K. T. & Ingram, L. O. Development of ethanologenic bacteria. *Adv Biochem Eng Biotechnol* **108**, 237-261, doi:10.1007/10_2007_068 (2007).

128 Ingram, L. O., Conway, T., Clark, D. P., Sewell, G. W. & Preston, J. F. Genetic engineering of ethanol production in Escherichia coli. *Appl Environ Microbiol* **53**, 2420-2425 (1987).

129 Atsumi, S., Hanai, T. & Liao, J. C. Non-fermentative pathways for synthesis of branched-chain higher alcohols as biofuels. *Nature* **451**, 86-89, doi:10.1038/nature06450 (2008).

130 Shen, C. R. *et al.* Driving forces enable high-titer anaerobic 1-butanol synthesis in Escherichia coli. *Appl Environ Microbiol* **77**, 2905-2915, doi:10.1128/AEM.03034-10 (2011).

131 Bond-Watts, B. B., Bellerose, R. J. & Chang, M. C. Enzyme mechanism as a kinetic control element for designing synthetic biofuel pathways. *Nat Chem Biol* **7**, 222-227, doi:10.1038/nchembio.537 (2011).

132 Meadows, A. L. *et al.* Rewriting yeast central carbon metabolism for industrial isoprenoid production. *Nature* **537**, 694-697, doi:10.1038/nature19769 (2016).

133 Lennen, R. M. & Pfleger, B. F. Engineering Escherichia coli to synthesize free fatty acids. *Trends in biotechnology* **30**, 659-667, doi:10.1016/j.tibtech.2012.09.006 (2012).

134 Davis, S. C., Williams, S. E. & Boundy, R. G. Vol. 36th Ed. (Oak Ridge National Lab, 2017).

135 Xu, Y., Isom, L. & Hanna, M. A. Adding value to carbon dioxide from ethanol fermentations. *Bioresour Technol* **101**, 3311-3319, doi:10.1016/j.biortech.2010.01.006 (2010).

136 Kheshgi, H. S. & Prince, R. C. Sequestration of fermentation CO2 from ethanol production. *Energy* **30**, 1865-1871, doi:10.1016/j.energy.2004.11.004 (2005).

137 Francois, J. M., Lachaux, C. & Morin, N. Synthetic Biology Applied to Carbon Conservative and Carbon Dioxide Recycling Pathways. *Front Bioeng Biotechnol* **7**, 446, doi:10.3389/fbioe.2019.00446 (2019).

138 Mattozzi, M., Ziesack, M., Voges, M. J., Silver, P. A. & Way, J. C. Expression of the sub-pathways of the Chloroflexus aurantiacus 3-hydroxypropionate carbon fixation bicycle in E. coli: Toward horizontal transfer of autotrophic growth. *Metab Eng* **16**, 130-139, doi:10.1016/j.ymben.2013.01.005 (2013).

139 Guadalupe-Medina, V. *et al.* Carbon dioxide fixation by Calvin-Cycle enzymes improves ethanol yield in yeast. *Biotechnol Biofuels* **6**, 125, doi:10.1186/1754-6834-6-125 (2013).

140 Gong, F. *et al.* Quantitative analysis of an engineered CO2-fixing Escherichia coli reveals great potential of heterotrophic CO2 fixation. *Biotechnol Biofuels* **8**, 86, doi:10.1186/s13068-015-0268-1 (2015).

141 Li, Y. H., Ou-Yang, F. Y., Yang, C. H. & Li, S. Y. The coupling of glycolysis and the Rubisco-based pathway through the non-oxidative pentose phosphate pathway to achieve low carbon dioxide emission fermentation. *Bioresour Technol* **187**, 189-197, doi:10.1016/j.biortech.2015.03.090 (2015).

142 Papapetridis, I. *et al.* Optimizing anaerobic growth rate and fermentation kinetics in Saccharomyces cerevisiae strains expressing Calvin-cycle enzymes for improved ethanol yield. *Biotechnol Biofuels* **11**, 17, doi:10.1186/s13068-017-1001-z (2018).

143 Xia, P. F. *et al.* Recycling Carbon Dioxide during Xylose Fermentation by Engineered Saccharomyces cerevisiae. *ACS Synth Biol* **6**, 276-283, doi:10.1021/acssynbio.6b00167 (2017).

144 Fast, A. G., Schmidt, E. D., Jones, S. W. & Tracy, B. P. Acetogenic mixotrophy: novel options for yield improvement in biofuels and biochemicals production. *Curr Opin Biotechnol* **33**, 60-72, doi:10.1016/j.copbio.2014.11.014 (2015).

145 Jones, S. W. *et al.* CO2 fixation by anaerobic non-photosynthetic mixotrophy for improved carbon conversion. *Nat Commun* **7**, 12800, doi:10.1038/ncomms12800 (2016).

146 Gleizer, S. *et al.* Conversion of Escherichia coli to Generate All Biomass Carbon from CO2. *Cell* **179**, 1255-1263.e1212 (2019).

147 Charubin, K. & Papoutsakis, E. T. Direct cell-to-cell exchange of matter in a synthetic Clostridium syntrophy enables CO2 fixation, superior metabolite yields, and an expanded metabolic space. *Metab Eng* **52**, 9-19, doi:10.1016/j.ymben.2018.10.006 (2019).

148 Spona-Friedl, M. *et al.* Substrate-dependent CO2 fixation in heterotrophic bacteria revealed by stable isotope labelling. *FEMS Microbiol Ecol* **96**, doi:10.1093/femsec/fiaa080 (2020).

149 Erb, T. J. Carboxylases in natural and synthetic microbial pathways. *Appl Environ Microbiol* **77**, 8466-8477, doi:10.1128/AEM.05702-11 (2011).

150 Bar-Even, A., Noor, E., Lewis, N. E. & Milo, R. Design and analysis of synthetic carbon fixation pathways. *Proc Natl Acad Sci U S A* **107**, 8889-8894, doi:10.1073/pnas.0907176107 (2010).

151 Bar-Even, A., Noor, E. & Milo, R. A survey of carbon fixation pathways through a quantitative lens. *J Exp Bot* **63**, 2325-2342, doi:10.1093/jxb/err417 (2012).

152 Flores, A. D. *et al.* Catabolic Division of Labor Enhances Production of D-Lactate and Succinate From Glucose-Xylose Mixtures in Engineered Escherichia coli Co-culture Systems. *Front Bioeng Biotechnol* **8**, 329, doi:10.3389/fbioe.2020.00329 (2020).

153 Kurgan, G. *et al.* Parallel experimental evolution reveals a novel repressive control of GalP on xylose fermentation in Escherichia coli. *Biotechnol Bioeng* **116**, 2074-2086, doi:10.1002/bit.27004 (2019).

154 Zhang, X. *et al.* Metabolic evolution of energy-conserving pathways for succinate production in Escherichia coli. *Proc Natl Acad Sci U S A* **106**, 20180-20185, doi:10.1073/pnas.0905396106 (2009).

155 Vemuri, G. N., Eiteman, M. A. & Altman, E. Effects of growth mode and pyruvate carboxylase on succinic acid production by metabolically engineered strains of Escherichia coli. *Appl Environ Microb* **68**, 1715-1727 (2002).

156 Martinez, R., Flores, A. D., Dufault, M. E. & Wang, X. The XylR variant (R121C and P363S) releases arabinose-induced catabolite repression on xylose fermentation and enhances coutilization of lignocellulosic sugar mixtures. *Biotechnol Bioeng* **116**, 3476-3481, doi:10.1002/bit.27144 (2019).

157 Lindsay, R. T. *et al.* A model for determining cardiac mitochondrial substrate utilisation using stable 13C-labelled metabolites. *Metabolomics* **15**, 154, doi:10.1007/s11306-019-1618-y (2019).

158 Martinez, A. *et al.* Low salt medium for lactate and ethanol production by recombinant Escherichia coli B. *Biotechnol Lett* **29**, 397-404, doi:10.1007/s10529-006-9252-y (2007).

159 You, L. *et al.* Metabolic Pathway Confirmation and Discovery Through 13C-labeling of Proteinogenic Amino Acids. *J. Vis. Exp.*, e3583, doi:doi:10.3791/3583 (2012).

160 Varman, A. M., He, L., You, L., Hollinshead, W. & Tang, Y. J. Elucidation of intrinsic biosynthesis yields using ^{13}C-based metabolism analysis. *Microb Cell Fact* **13**, 42, doi:10.1186/1475-2859-13-42 (2014).

161 Varman, A. M., Xiao, Y., Pakrasi, H. B. & Tang, Y. J. Metabolic engineering of Synechocystis sp. Strain PCC 6803 for isobutanol production. *Appl Environ Microbiol* **79**, doi:10.1128/aem.02827-12 (2012).

162 Wahl, S. A., Dauner, M. & Wiechert, W. New tools for mass isotopomer data evaluation in (13)C flux analysis: mass isotope correction, data consistency

checking, and precursor relationships. *Biotechnol Bioeng* **85**, 259-268, doi:10.1002/bit.10909 (2004).

163 Butler, J. N. *Carbon dioxide equilibria and their applications*. (Addison-Wesley, 1982).

CHAPTER 5

FURTURE DIRECTIONS AND CONCLUSIONS

5.1 Introduction

Previous chapters illustrate the latent potential for synthetic coculture systems, both in terms of enhancing sugar utilization as well as improving carbon conservation efficiency. With the ability to overcome challenging and complex metabolic tasks, many researchers have and continue to leverage division of labor and explore engineering synthetic microbial communities to enhance the performance of engineered bioprocesses [50,71,164]. However, to date many examples (including those presented in Chapters 2, 3, and 4) lack fundamental knowledge regarding the nature and degree of metabolic interactions that may also be taking place between community members, particularly at the metabolic level. For synthetic microbial communities to further mature as a rigorous bioproduction strategy, improved fundamental understanding of inter-strain metabolite exchange, communication/signallings, and behaviors are needed. This chapter will discuss the challenges associated with capturing and revealing the full scope and complexity of naturally occurring and synthetically engineered microbial communities. And how developing a novel experimental apparatus and analytical platform could be a versatile tool in advancing fundamental understandings of microbial communities.

5.2 Natural and Synthetic Ecosystems are Complex

In nature, microorganisms rarely exist alone as pure species, but rather occupy different environmental niches as part of diverse communities where, by performing complementary functions, they play key roles in shaping intricate ecosystems and in numerous processes affecting human health [165]. Within communities, functional differentiation and collaboration between different specialists leads to beneficial chemical interactions that enhances the survivability, robustness and/or overall fitness.

Understanding metabolic interactions occurring within a microbial community is critical for further optimization of culture performance. However, detailed characterization of metabolite exchange is rarely performed. This is mainly due to the complexity and uncontrolled function of many individual community members. Strategies to tune and control the population-level of individual community members include modulating or delaying the initial inoculum and metabolic cross-feeding [166]. Typical measurements used to track individual members in a cocultures system rely on a combination of absorbance, fluorescence, fluorescence-activated cell sorting (FACS) and qPCR [166]. The aforementioned methods are not ideal to comprehensively investigate community interactions at the molecular level due to the inherent variability of gene expression and slow and tedious methodology.

5.3 Preliminary Results

5.3.1 Development of a Novel, Two-Chamber Inter-Loop Membrane Bioreactor

To address these limitations, we developed a novel, two-chamber inter-loop membrane bioreactor system (**Figure 5.1**). This two-chamber inter-loop membrane bioreactor employs dedicated tangential flow filter (TFF) membrane cassettes (see methods section for details) to confine individual strains to their own dedicated vessel, all the while actively mixing and distributing the same culture media throughout the system. As shown in **Figure 5.1**, the system includes control of mixing, pH, and temperature. Tube lengths and membrane hold-up (<2mL) are also minimal, to avoid additional mass transfer limitations. Additionally, the two-chamber inter-loop membrane bioreactor vessel-in-vessel design allows scaling-down of the total volume (from 750 mL to 50 mL; conserving costly ^{13}C substrates). Several ports are available for sampling/additions and to supply N_2 or air to

facilitate anaerobic or aerobic conditions. Overall, this two-chamber inter-loop membrane bioreactor system enables mimicry of coculture behaviors of fully-mixed, single vessels, while providing access to each cell population for focal sampling of its biomass. This design uniquely enables the ability to easily and repeatedly sample biomass at any time point, and in significant quantities.

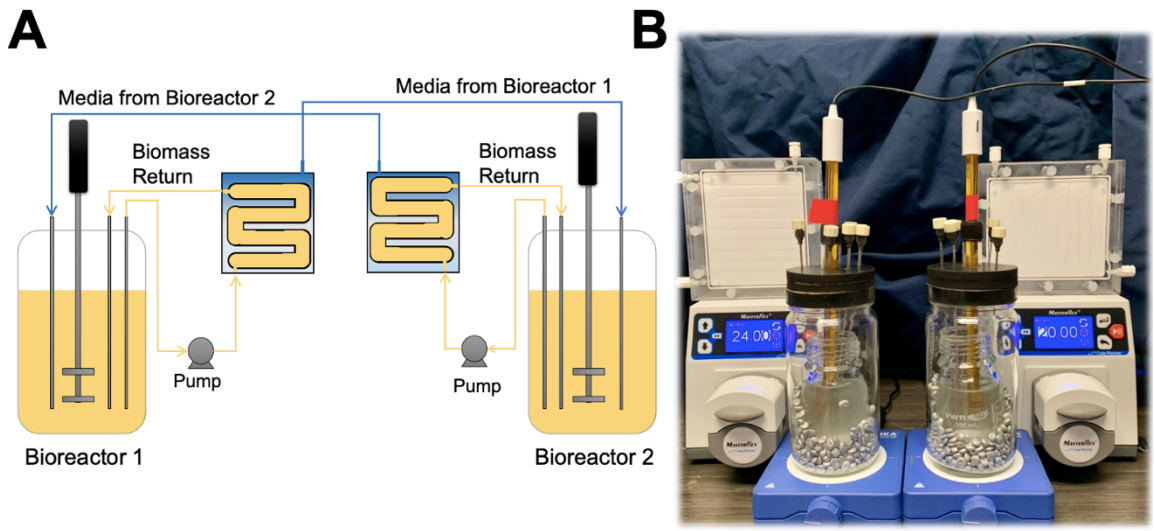

Figure 5.1 A novel, two-chamber inter-loop membrane bioreactor system.

A) Schematic depiction of the novel, two-chamber inter-loop membrane bioreactor system *that confines individual strains to dedicated vessels while distributing a shared medium. B) Fully operational* two-chamber inter-loop membrane bioreactor system demonstrating *vessel-in-vessel design (reducing working volume to 100 mL).*

5.3.2 Characterization of Two-Chamber Inter-Loop Membrane Bioreactor System Using Wild-Type Derived Sugar Specialists

To establish if the two-chamber inter-loop membrane bioreactor design imposes any significant, negative consequence toward the growth of or sugar utilization by individual sugar specialists, the system was first operated as a single-vessel membrane bioreactor (i.e., cycling and returning retentate and filtrate back to bioreactor) and under identical conditions was compared to bioreactor with no TFF. To minimize cross-catabolic activities, we first evaluated a complementary pair of wild-type derived *E. coli* glucose and xylose sugar specialist strains, WTglc and WTxyl4, respectively, developed in Chapter 2 (**Figure 2.1**) [117]. Since WTxyl4 still utilized a minor amounts of glucose (12% when supplied with 66 g L^{-1} glucose and 33 g L^{-1} xylose; **Figure 2.1**) glucokinase (*glk*) was

inactivated to abolish glucose catabolism, yielding the strain herein called WTxyl. As shown in **Figure 5.2**, and consistent with their previous performance, WTglc and WTxyl each preferentially utilized only one sugar when fermented in mineral salt media supplemented with 10 g L^{-1} glucose and 2 g L^{-1} xylose. In both experimental conditions (with TFF and without TFF) WTglc utilized 100 % of the supplied glucose within 9 h, all while leaving all the initially supplied xylose unused. In a similar manner, WTxyl, utilized 100 % of the supplied by 12 h and no glucose. Growth of WTxyl, was significantly less than that of WTglc (maximum OD_{550nm} of 2 compared to 6 for WTxyl and WTglc, respectively; **Figure 5.2A** and **B**) as expected since less total sugar is available/utilizable for the WTxyl along with lower energy yield of xylose fermentation relative to that of glucose fermentation. Relative to their respective performance as a pure culture without TFF, no apparent hinder in growth was observed. Together, these promising results demonstrate the latent potential of the two-chamber inter-looped bioreactor.

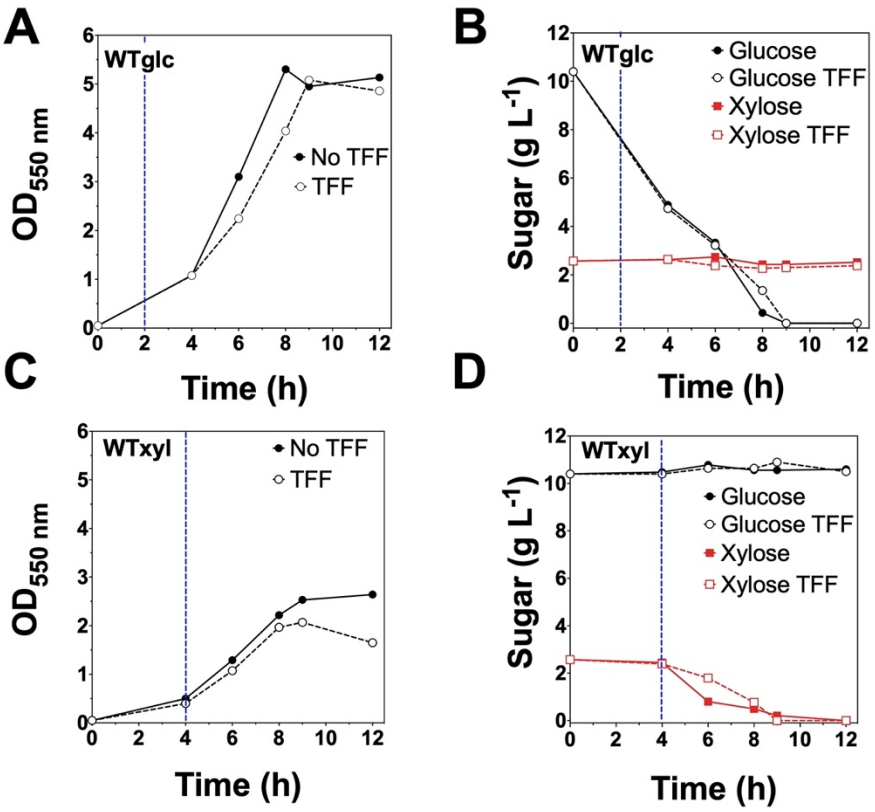

Figure 5.2 Characterizing wild-type derived *E. coli* sugar specialist in single-vessel membrane bioreactor.

A) Optical density and B) residual sugar remaining in the fermentation broths for glucose specialist strain WTglc. C) optical density and d) residual sugar remaining in the fermentation broth for xylose specialist Open symbols indicate cells were subject to tangential flow filtration (TFF). Each vessel initially contained 10 g L^{-1} of glucose and 2 g L^{-1} xylose.

5.3.3 Fermentation Performance of Coculture Sugar Specialist in Two-Chamber Inter-Loop Membrane Bioreactor

Given their promising performance in the single-vessel membrane bioreactor and no appreciative cross-catabolic activities, WTglc and WTxyl were next used as a selected pair of catabolically-orthogonal sugar specialists with which to fully operate and evaluate the two-chamber inter-loop membrane bioreactor. An operational advantage of the unique membrane bioreactor system is sampling each individual strain/vessel at different growth

phases (e.g., early-, mid-, late-exponential, stationary) is possible. As shown in **Figure 5.3**, when grown as a segregated coculture, growth of and sugar utilization by each individual specialist reflected that of pure cultures (**Figure 5.2;** maxium OD_{550} of ~5 and ~2 for WTglc and WTxyl, respectively), whereas sugar concentrations were identical across both vessels at all times. Complete co-utilization of the supplied 10 g L^{-1} glucose and 2 g L^{-1} xylose was achieved by 14 h. The novel two-chamber inter-loop membrane bioreactor described successfully mimics fully-mixed, single vessel and allows for easy access to each strain for analyses into metabolic exchanges. Future directions using this transformative platform are presented next.

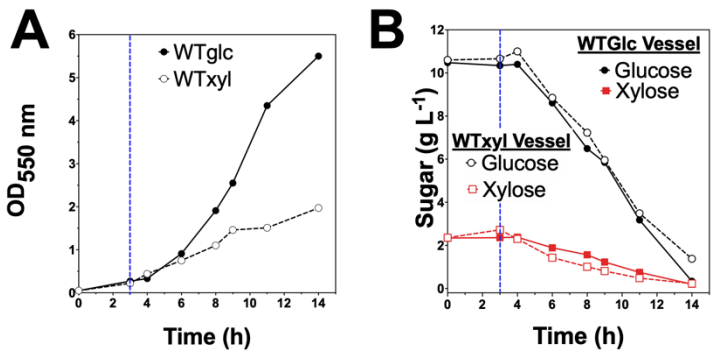

Figure 5.3 Co-utilization of a glucose-xylose mixture using wild-type derived *E. coli* sugar specialist in segregated membrane bioreactor system.

A) Optical density of each specialist in their respective vessel. B) Residual sugar remaining in the fermentation broth for each vessel (solid symbols indicate the vessel containing the glucose specialist and open symbols indicate the vessel containing the xylose specialist). Each vessel initially contained 10 g L^{-1} of glucose and 2 g L^{-1} xylose.

5.4 Future Directions

5.4.1 Deciphering Metabolic Interactions in *E. coli-E. coli* Cocultures Via ^{13}C-Fingerprinting

With the two catabolically-orthogonal sugar specialist strains in Sections 5.3 serving as two previously non-interacting, prototrophic *E. coli* strains, the two-chamber inter-loop membrane bioreactor system can be used to comprehensively elucidate bidirectional metabolic cross-feeding behaviors via ^{13}C-fingerprinting analysis (**Figure 5.4)**. Characterization of bidirectional metabolite exchanges requires the ability to generate uniquely distinguishable exometabolomes for each strain and this *E. coli*-*E. coli* coculture will serve an initial and baseline model.

First, analogous to the experiment presented in Section 5.3.3, the wild-type *E. coli* coculture can be grown aerobically with minimal media containing mixtures of [U-^{13}C]glucose-xylose and glucose-[U-^{13}C]xylose. By alternating between labeled substrates, bidirectional metabolite exchange behaviors will be enabled and allow for identifying and tracking reciprocal metabolite exchanges (**Figure 5.4;** also the technique was applied in Chapter 4).

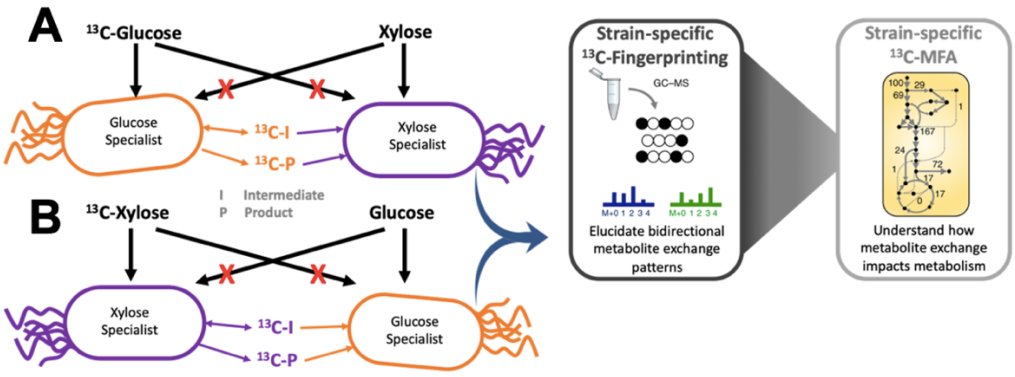

Figure 5.4 Schematic of elucidate bidirectional metabolite exchange via alternating ^{13}C-labeled substrates with sugar specialist.

Using catabolically-orthogonal sugar specialist and (A) [U-^{13}C]glucose-xylose or (B) glucose-[U-^{13}C]xylose sugar mixture to elucidate bidirectional metabolite exchange patterns and to understand how metabolite exchange impacts metabolism.

We anticipate that the type and degree of exchanged metabolites changes during the fermentation time-course. At each growth phase, individual biomass samples will be removed for ^{13}C-fingerprinting analysis (a technique used in Chapter 4). Exometabolomes of each strain can be characterized via LC-MS and GC-MS (as described by others [167-170]) to enable differentiation between amino acids that are directly assimilated vs. produced from other assimilated precursors. This will further enable us to also identify potential 'missed opportunities' (i.e., metabolites secreted but not subsequently assimilated by the partner strain). Collectively, these experiments will provide new and comprehensive understandings of the prevalence of metabolic interactions arising between two prototrophic *E. coli* strains, including with respect to their bidirectional and possible dynamic behaviors.

5.4.2 Investigating Metabolic Interactions Across Inter-Species Cocultures

Since exometabolomes can vary significantly across species [171], we expect that specific inter-species pairings may naturally be better poised to establish and support beneficial intercellular metabolic interactions. Accordingly, and expanding on the knowledge learned from Section 5.4.1, metabolite exchange behaviors vary across cocultures composed of different prototrophic species can be explored; focusing specifically on those commonly employed as bioproduction hosts.

As discussed in Sections 5.4.1, and to reemphasize again, to attain uniquely labeled exometabolomes for each species is important that coculture pairs remain catabolically-orthogonal. Numerous industrial microbial hosts, for example are incapable of utilizing xylose, including *S. cerevisiae*, *B. subtilis*, and *C. glutamicum*.[172]. These naturally occurring glucose specialists can each be individually paired with our previously engineered wild-type *E. coli* xylose specialist (WTxyl, from Chapter 2) to establish a series of synthetic cocultures (i.e., *E. coli*-*B. subtilis*, *E. coli*-*S. cerevisiae*, *E. coli*-*C. glutamicum*). As a preliminary result, we have confirmed that *S. cerevisiae* W303 grows normally in our typical *E. coli* mineral salts media (i.e. AM1) and, as expected, cannot utilize xylose after 24 h for both glucose-xylose mixtures and xylose only media. (**Figure 5.4**). Future work will initially involve evaluating media compatibility for *B. subtilis* and *C. glutamicum*. Followed by rigorous ^{13}C-labeling studies as described in section 5.4.1 to investigate if specific metabolites are commonly traded (i.e., donated and successfully taken up).

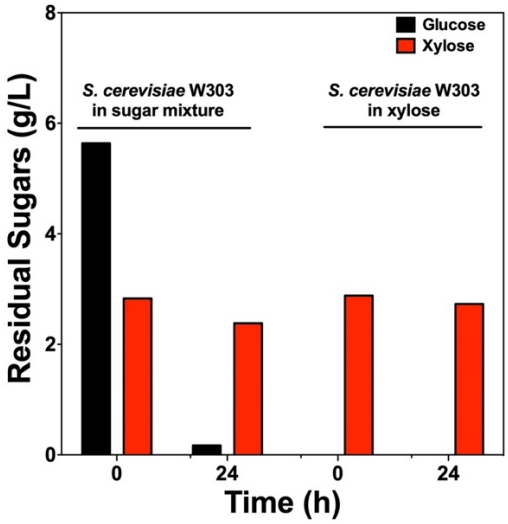

Figure 5.5 Co-utilization of a glucose-xylose mixture using *S. cerevisiae*.

Residual sugar remaining in the fermentation broth for S. cerevisiae in a glucose-xylose sugar mixture and xylose only media. 250 mL Erlenmeyer shake flask containing 100 mL of AM1 mineral media supplemented with 6 g L^{-1} of glucose and 3 g L^{-1} xylose.

5.4.3 Investigating Environmental Influences on Metabolic Interactions

Environmental conditions and nutrient availability can dynamically influence the behavior and biochemical interactions occurring within microbial communities [173-177]. With section 5.4.1 and 5.4.2 serving as baseline interactions, this hypothesis can be tested by comparing/contrasting the outcomes of with those from analogous cocultures grown under different nutritional or environmental stresses. In do so, bidirectional metabolic interactions may be altered for different pairs in response to different stresses, including: O_2 limitation (i.e., microaerobic and anaerobic conditions), high temperature, nitrogen limitation, and phosphate limitation. Meanwhile, as high substrate levels exacerbate overflow metabolism, different initial glucose-xylose concentrations can also be studied. For each unique coculture, it is expected to that the profile of exchanged metabolites will vary as a function of the specific stressor. Understanding how these factors shape and

influence microbial communities gain be used to gain insight into fundamental principles and can be leveraged into creating interactions and communities with desired characteristics and functionality

5.5 Conclusion

The novel experimental apparatus and analytical platform, segregated membrane bioreactor system, developed will uniquely enable the full spectrum of metabolic interactions occurring between strains to be determined. This system enables both strain-specific ^{13}C-fingerprinting information and an understanding of exchanged metabolites. Taken together, key outcomes of implementing this unique analytical apparatus will include an improved understanding of how different strains pairs interact at the molecular level, as well as what impact these interactions have on both individual and community metabolism. In the long-term, these insights could aid in establishing more holistic design rules and 'synthetic ecology' approaches for engineering efficient, robust, and stable communities for industrial bioprocesses [170,178,179].

5.6 Methods

5.6.1 Strains, Culture Conditions and Analytics

Strains and plasmids used in Chapter 5 are listed in **Table 5.1**. All strains were fermented in AM1 minimal salt medium [94] supplemented with either a glucose-xylose mixture or xylose only. Vessel-in-vessel design utili All monoculture and coculture batch fermentations were inoculated using a total initial OD_{550nm} of 0.05 (approximately 0.022 g dry cell weight (DCW) L^{-1}) and cells were grown at 37 °C in a fermentation vessel with pH maintained at 7.0 (except shake flask experiments) by manual addition of 2.0 M KOH

base. Analytics to quantify residual sugar and optical density are the same as Chapters 2 and Chapter 3.

Table 5.1 List of strains and plasmids used to construct strains in Chapter 5.

Strains and Plasmids	Relevant Characteristics	Source
Strains		
E. coli W	wild-type	ATCC
WTglc	*E. coli* W Δ*xylR*	117
WTxyl4	*E. coli* W *xylR*::*xylR** Δ*ptsI* Δ*ptsG* Δ*galP*	117
WTxyl	WTxyl4 *glk::Kan*^{R} (Kan^R)	This Study
Plasmids		
XW001	*The cat-sacB* cassette with the *sacB* native terminator cloned into a modified vector pLOI4162	71
pKD46	Red recombinase, temperature-conditional, *bla*	175

5.6.2 Segregated Bioreactor Design and Configuration

The Vivaflow 200 reusable crossflow cassette with a sizeable cutoff of 0.2 μm polyethersulfone (PES) and 200 cm^2 filtration area (main housing material acrylic; Sartorius Product No. VF20P7) was employed as a tangential flow filtration system. This module included a pressure indicator (Sartorius Product No. VFA020), polypropylene flow restrictor and size 16 silicon peristaltic tubing and fittings. Masterflex L/S Digital miniflex pump systems recirculated culture broth at 168 mL/min, turnover and mixing the fermentation broth in each vessel at least 2 per hour.

References

50 Chen, Y. Development and application of co-culture for ethanol production by co-fermentation of glucose and xylose: a systematic review. *J Ind Microbiol Biotechnol* **38**, 581-597, doi:10.1007/s10295-010-0894-3 (2011).

71 Song, H., Ding, M. Z., Jia, X. Q., Ma, Q. & Yuan, Y. J. Synthetic microbial consortia: from systematic analysis to construction and applications. *Chem Soc Rev* **43**, 6954-6981, doi:10.1039/c4cs00114a (2014).

94 Martinez, A. *et al.* Low salt medium for lactate and ethanol production by recombinant Escherichia coli B. *Biotechnol Lett* **29**, 397-404 (2007).

117 Flores, A. D., Ayla, E. Z., Nielsen, D. R. & Wang, X. Engineering a Synthetic, Catabolically Orthogonal Coculture System for Enhanced Conversion of Lignocellulose-Derived Sugars to Ethanol. *ACS Synth Biol* **8**, 1089-1099, doi:10.1021/acssynbio.9b00007 (2019).

164 Goers, L., Freemont, P. & Polizzi, K. M. Co-culture systems and technologies: taking synthetic biology to the next level. *J R Soc Interface* **11**, doi:10.1098/rsif.2014.0065 (2014).

165 Johns, N. I., Blazejewski, T., Gomes, A. L. & Wang, H. H. Principles for designing synthetic microbial communities. *Curr Opin Microbiol* **31**, 146-153, doi:10.1016/j.mib.2016.03.010 (2016).

166 Kerner, A., Park, J., Williams, A. & Lin, X. N. A programmable Escherichia coli consortium via tunable symbiosis. *PLoS One* **7**, e34032, doi:10.1371/journal.pone.0034032 (2012).

167 Bolten, C. J., Kiefer, P., Letisse, F., Portais, J. C. & Wittmann, C. Sampling for metabolome analysis of microorganisms. *Anal Chem* **79**, 3843-3849, doi:10.1021/ac0623888 (2007).

168 Canelas, A. B. *et al.* Leakage-free rapid quenching technique for yeast metabolomics. *Metabolomics* **4**, 226-239, doi:10.1007/s11306-008-0116-4 (2008).

169 Taymaz-Nikerel, H. *et al.* Development and application of a differential method for reliable metabolome analysis in Escherichia coli. *Anal Biochem* **386**, 9-19, doi:10.1016/j.ab.2008.11.018 (2009).

170 Kosina, S. M. *et al.* Exometabolomics Assisted Design and Validation of Synthetic Obligate Mutualism. *Acs Synth Biol* **5**, 569-576, doi:10.1021/acssynbio.5b00236 (2016).

171 Paczia, N. *et al.* Extensive exometabolome analysis reveals extended overflow metabolism in various microorganisms. **11**, 122, doi:10.1186/1475-2859-11-122 (2012).

172 Kawaguchi, H., Vertès, A. A., Okino, S., Inui, M. & Yukawa, H. Engineering of a xylose metabolic pathway in Corynebacterium glutamicum. *Appl Environ Microbiol* **72**, 3418-3428, doi:10.1128/AEM.72.5.3418-3428.2006 (2006).

173 Ponomarova, O. & Patil, K. R. Metabolic interactions in microbial communities: untangling the Gordian knot. *Current Opinion in Microbiology* **27**, 37-44, doi:10.1016/j.mib.2015.06.014 (2015).

174 Zampieri, M. & Sauer, U. Model-based media selection to minimize the cost of metabolic cooperation in microbial ecosystems. *Bioinformatics* **32**, 1733-1739, doi:10.1093/bioinformatics/btw062 (2016).

175 Bull, J. J. & Harcombe, W. R. Population dynamics constrain the cooperative evolution of cross-feeding. *Plos One* **4**, e4115, doi:10.1371/journal.pone.0004115 (2009).

176 Callaway, R. M. *et al.* Positive interactions among alpine plants increase with stress. *Nature* **417**, 844-848, doi:DOI 10.1038/nature00812 (2002).

177 Hoek, T. A. *et al.* Resource Availability Modulates the Cooperative and Competitive Nature of a Microbial Cross-Feeding Mutualism. *Plos Biol* **14**, e1002540, doi:10.1371/journal.pbio.1002540 (2016).

178 Fredrickson, J. K. Ecological communities by design. *Science* **348**, 1425-1427, doi:10.1126/science.aab0946 (2015).

179 Minty, J. J. *et al.* Design and characterization of synthetic fungal-bacterial consortia for direct production of isobutanol from cellulosic biomass. *P Natl Acad Sci USA* **110**, 14592-14597, doi:10.1073/pnas.1218447110 (2013).

COMPLETE REFERENCES

1 Clark, J. H. *et al.* Green chemistry and the biorefinery: A partnership for a sustainable future. *Green Chemistry* **8**, 853-860 (2006).

2 Saha, B. C. Hemicellulose bioconversion. *J Ind Microbiol Biotechnol* **30**, 279-291 (2003).

3 Girio, F. M. *et al.* Hemicelluloses for fuel ethanol: A review. *Bioresour Technol* **101**, 4775-4800, doi:10.1016/j.biortech.2010.01.088 (2010).

4 Singh, A. & Mishra, P. *Microbial Pentose UtilizatJon*. (Elsevier, 1995).

5 Geddes, C. C. *et al.* Optimizing the saccharification of sugar cane bagasse using dilute phosphoric acid followed by fungal cellulases. *Bioresour Technol* **101**, 1851-1857 (2010).

6 Kim, S. R., Ha, S. J., Wei, N., Oh, E. J. & Jin, Y. S. Simultaneous co-fermentation of mixed sugars: a promising strategy for producing cellulosic ethanol. *Trends in Biotechnology* **30**, 274-282 (2012).

7 Doran-Peterson, J. *et al.* Simultaneous saccharification and fermentation and partial saccharification and co-fermentation of lignocellulosic biomass for ethanol production. *Methods Mol Biol* **581**, 263-280 (2009).

8 Kim, J. H., Block, D. E. & Mills, D. A. Simultaneous consumption of pentose and hexose sugars: an optimal microbial phenotype for efficient fermentation of lignocellulosic biomass. *Appl Microbiol Biot* **88**, 1077-1085 (2010).

9 Kolb, A., Busby, S., Buc, H., Garges, S. & Adhya, S. Transcriptional Regulation by Camp and Its Receptor Protein. *Annual Review of Biochemistry* **62**, 749-795 (1993).

10 Deutscher, J. The mechanisms of carbon catabolite repression in bacteria. *Curr Opin Microbiol* **11**, 87-93 (2008).

11 Gorke, B. & Stulke, J. Carbon catabolite repression in bacteria: many ways to make the most out of nutrients. *Nat Rev Microbiol* **6**, 613-624, doi:10.1038/nrmicro1932 (2008).

12 Toivari, M. H., Salusjarvi, L., Ruohonen, L. & Penttila, M. Endogenous xylose pathway in Saccharomyces cerevisiae. *Appl Environ Microbiol* **70**, 3681-3686, doi:10.1128/AEM.70.6.3681-3686.2004 (2004).

13 Jeffries, T. W. Utilization of xylose by bacteria, yeasts, and fungi. *Adv Biochem Eng Biotechnol* **27**, 1-32 (1983).

14 Jeffries, T. W. & Shi, N. Q. Genetic engineering for improved xylose fermentation by yeasts. *Adv Biochem Eng Biotechnol* **65**, 117-161 (1999).

15 Stulke, J. & Hillen, W. Carbon catabolite repression in bacteria. *Curr Opin Microbiol* **2**, 195-201, doi:10.1016/S1369-5274(99)80034-4 (1999).

16 Kotrba, P., Inui, M. & Yukawa, H. Bacterial phosphotransferase system (PTS) in carbohydrate uptake and control of carbon metabolism. *J Biosci Bioeng* **92**, 502-517 (2001).

17 Tchieu, J. H., Norris, V., Edwards, J. S. & Saier, M. H., Jr. The complete phosphotransferase system in Escherichia coli. *J Mol Microbiol Biotechnol* **3**, 329-346 (2001).

18 Postma, P. W., Lengeler, J. W. & Jacobson, G. R. Phosphoenolpyruvate:carbohydrate phosphotransferase systems of bacteria. *Microbiol Rev* **57**, 543-594 (1993).

19 Stock, J. B., Waygood, E. B., Meadow, N. D., Postma, P. W. & Roseman, S. Sugar transport by the bacterial phosphotransferase system. The glucose receptors of the Salmonella typhimurium phosphotransferase system. *J Biol Chem* **257**, 14543-14552 (1982).

20 Misset, O., Blaauw, M., Postma, P. W. & Robillard, G. T. Bacterial phosphoenolpyruvate-dependent phosphotransferase system. Mechanism of the transmembrane sugar translocation and phosphorylation. *Biochemistry* **22**, 6163-6170 (1983).

21 Horazdovsky, B. F. & Hogg, R. W. High-affinity L-arabinose transport operon. Gene product expression and mRNAs. *J Mol Biol* **197**, 27-35 (1987).

22 Sumiya, M., Davis, E. O., Packman, L. C., McDonald, T. P. & Henderson, P. J. Molecular genetics of a receptor protein for D-xylose, encoded by the gene xylF, in Escherichia coli. *Receptors Channels* **3**, 117-128 (1995).

23 Jojima, T., Omumasaba, C. A., Inui, M. & Yukawa, H. Sugar transporters in efficient utilization of mixed sugar substrates: current knowledge and outlook. *Applied microbiology and biotechnology* **85**, 471-480, doi:10.1007/s00253-009-2292-1 (2010).

24 Davis, E. O. & Henderson, P. J. The cloning and DNA sequence of the gene xylE for xylose-proton symport in Escherichia coli K12. *The Journal of biological chemistry* **262**, 13928-13932 (1987).

25 Maiden, M. C., Jones-Mortimer, M. C. & Henderson, P. J. The cloning, DNA sequence, and overexpression of the gene araE coding for arabinose-proton symport in Escherichia coli K12. *The Journal of biological chemistry* **263**, 8003-8010 (1988).

26 Liu, M. Z. *et al.* Global transcriptional programs reveal a carbon source foraging strategy by Escherichia coli. *Journal of Biological Chemistry* **280**, 15921-15927, doi:10.1074/jbc.M414050200 (2005).

27 Blencke, H. M. *et al.* Transcriptional profiling of gene expression in response to glucose in Bacillus subtilis: regulation of the central metabolic pathways. *Metabolic engineering* **5**, 133-149 (2003).

28 Moreno, M. S., Schneider, B. L., Maile, R. R., Weyler, W. & Saier, M. H., Jr. Catabolite repression mediated by the CcpA protein in Bacillus subtilis: novel modes of regulation revealed by whole-genome analyses. *Molecular microbiology* **39**, 1366-1381 (2001).

29 Yoshida, K. *et al.* Combined transcriptome and proteome analysis as a powerful approach to study genes under glucose repression in Bacillus subtilis. *Nucleic Acids Res* **29**, 683-692 (2001).

30 Escalante, A., Salinas Cervantes, A., Gosset, G. & Bolivar, F. Current knowledge of the Escherichia coli phosphoenolpyruvate-carbohydrate phosphotransferase system: peculiarities of regulation and impact on growth and product formation. *Applied microbiology and biotechnology* **94**, 1483-1494, doi:10.1007/s00253-012-4101-5 (2012).

31 Nelson, S. O., Wright, J. K. & Postma, P. W. The mechanism of inducer exclusion. Direct interaction between purified III of the phosphoenolpyruvate:sugar phosphotransferase system and the lactose carrier of Escherichia coli. *EMBO J* **2**, 715-720 (1983).

32 Osumi, T. & Saier, M. H., Jr. Regulation of lactose permease activity by the phosphoenolpyruvate:sugar phosphotransferase system: evidence for direct binding of the glucose-specific enzyme III to the lactose permease. *Proceedings of the National Academy of Sciences of the United States of America* **79**, 1457-1461 (1982).

33 Geng, H. F. & Jiang, R. R. cAMP receptor protein (CRP)-mediated resistance/tolerance in bacteria: mechanism and utilization in biotechnology. *Appl Microbiol Biot* **99**, 4533-4543 (2015).

34 Gosset, G. Improvement of Escherichia coli production strains by modification of the phosphoenolpyruvate:sugar phosphotransferase system. *Microb Cell Fact* **4**, 14, doi:10.1186/1475-2859-4-14 (2005).

35 Dien, B. S., Nichols, N. N. & Bothast, R. J. Fermentation of sugar mixtures using Escherichia coli catabolite repression mutants engineered for production of L-lactic acid. *J Ind Microbiol Biotechnol* **29**, 221-227, doi:10.1038/sj.jim.7000299 (2002).

36 Dien, B. S., Nichols, N. N. & Bothast, R. J. Recombinant Escherichia coli engineered for production of L-lactic acid from hexose and pentose sugars. *Journal of industrial microbiology & biotechnology* **27**, 259-264, doi:10.1038/sj/jim/7000195 (2001).

37 Nichols, N. N., Dien, B. S. & Bothast, R. J. Use of catabolite repression mutants for fermentation of sugar mixtures to ethanol. *Applied microbiology and biotechnology* **56**, 120-125 (2001).

38 Flores, N., Xiao, J., Berry, A., Bolivar, F. & Valle, F. Pathway engineering for the production of aromatic compounds in Escherichia coli. *Nature biotechnology* **14**, 620-623, doi:10.1038/nbt0596-620 (1996).

39 Hernandez-Montalvo, V., Valle, F., Bolivar, F. & Gosset, G. Characterization of sugar mixtures utilization by an Escherichia coli mutant devoid of the phosphotransferase system. *Applied microbiology and biotechnology* **57**, 186-191 (2001).

40 Hernandez-Montalvo, V. *et al.* Expression of galP and glk in a Escherichia coli PTS mutant restores glucose transport and increases glycolytic flux to fermentation products. *Biotechnology and bioengineering* **83**, 687-694, doi:10.1002/bit.10702 (2003).

41 Balderas-Hernandez, V. E., Hernandez-Montalvo, V., Bolivar, F., Gosset, G. & Martinez, A. Adaptive evolution of Escherichia coli inactivated in the phosphotransferase system operon improves co-utilization of xylose and glucose under anaerobic conditions. *Applied biochemistry and biotechnology* **163**, 485-496, doi:10.1007/s12010-010-9056-3 (2011).

42 Chiang, C. J. *et al.* Systematic Approach To Engineer Escherichia coli Pathways for Co-utilization of a Glucose-Xylose Mixture. *J Agr Food Chem* **61**, 7583-7590 (2013).

43 Kim, J., Adhya, S. & Garges, S. Allosteric changes in the cAMP receptor protein of Escherichia coli: hinge reorientation. *Proc Natl Acad Sci U S A* **89**, 9700-9704 (1992).

44 Cirino, P. C., Chin, J. W. & Ingram, L. O. Engineering Escherichia coli for xylitol production from glucose-xylose mixtures. *Biotechnol Bioeng* **95**, 1167-1176 (2006).

45 Ji, X. J. *et al.* Elimination of carbon catabolite repression in Klebsiella oxytoca for efficient 2,3-butanediol production from glucose-xylose mixtures. *Appl Microbiol Biotechnol* **89**, 1119-1125, doi:10.1007/s00253-010-2940-5 (2011).

46 Khankal, R., Chin, J. W., Ghosh, D. & Cirino, P. C. Transcriptional effects of CRP* expression in Escherichia coli. *J Biol Eng* **3**, 13, doi:10.1186/1754-1611-3-13 (2009).

47 Eiteman, M. A., Lee, S. A. & Altman, E. A co-fermentation strategy to consume sugar mixtures effectively. *J Biol Eng* **2**, 3, doi:10.1186/1754-1611-2-3 (2008).

48 Eiteman, M. A., Lee, S. A., Altman, R. & Altman, E. A substrate-selective co-fermentation strategy with Escherichia coli produces lactate by simultaneously consuming xylose and glucose. *Biotechnol Bioeng* **102**, 822-827, doi:10.1002/bit.22103 (2009).

49 Xia, T., Altman, E. & Eiteman, M. A. Succinate production from xylose-glucose mixtures using a consortium of engineered Escherichia coli. *Eng Life Sci* **15**, 65-72, doi:10.1002/elsc.201400113 (2015).

50 Chen, Y. Development and application of co-culture for ethanol production by co-fermentation of glucose and xylose: a systematic review. *J Ind Microbiol Biotechnol* **38**, 581-597, doi:10.1007/s10295-010-0894-3 (2011).

51 Lakshmanaswamy, A., Rajaraman, E., Eiteman, M. A. & Altman, E. Microbial removal of acetate selectively from sugar mixtures. *Journal of industrial microbiology & biotechnology* **38**, 1477-1484, doi:10.1007/s10295-010-0932-1 (2011).

52 Xia, T., Eiteman, M. A. & Altman, E. Simultaneous utilization of glucose, xylose and arabinose in the presence of acetate by a consortium of Escherichia coli strains. *Microb Cell Fact* **11**, 77, doi:10.1186/1475-2859-11-77 (2012).

53 Zhang, H. & Stephanopoulos, G. Co-culture engineering for microbial biosynthesis of 3-amino-benzoic acid in Escherichia coli. *Biotechnol J* **11**, 981-987, doi:10.1002/biot.201600013 (2016).

54 Zhang, H. R., Pereira, B., Li, Z. J. & Stephanopoulos, G. Engineering Escherichia coli coculture systems for the production of biochemical products. *Proceedings of the National Academy of Sciences of the United States of America* **112**, 8266-8271, doi:10.1073/pnas.1506781112 (2015).

55 Jones, J. A. *et al.* Experimental and computational optimization of an Escherichia coli co-culture for the efficient production of flavonoids. *Metabolic engineering* **35**, 55-63, doi:10.1016/j.ymben.2016.01.006 (2016).

56 Willrodt, C., Hoschek, A., Buhler, B., Schmid, A. & Julsing, M. K. Coupling limonene formation and oxyfunctionalization by mixed-culture resting cell fermentation. *Biotechnology and bioengineering* **112**, 1738-1750, doi:10.1002/bit.25592 (2015).

57 Zhang, H. & Wang, X. Modular co-culture engineering, a new approach for metabolic engineering. *Metabolic engineering* **37**, 114-121, doi:10.1016/j.ymben.2016.05.007 (2016).

58 Saini, M., Li, S. Y., Wang, Z. W., Chiang, C. J. & Chao, Y. P. Systematic engineering of the central metabolism in Escherichia coli for effective production of n-butanol. *Biotechnology for biofuels* **9**, 69, doi:10.1186/s13068-016-0467-4 (2016).

59 Saini, M., Hong Chen, M., Chiang, C. J. & Chao, Y. P. Potential production platform of n-butanol in Escherichia coli. *Metabolic engineering* **27**, 76-82, doi:10.1016/j.ymben.2014.11.001 (2015).

60 Saini, M., Chiang, C. J., Li, S. Y. & Chao, Y. P. Production of biobutanol from cellulose hydrolysate by the Escherichia coli co-culture system. *FEMS microbiology letters* **363**, doi:10.1093/femsle/fnw008 (2016).

61 Minty, J. J. *et al.* Design and characterization of synthetic fungal-bacterial consortia for direct production of isobutanol from cellulosic biomass. *Proceedings of the National Academy of Sciences of the United States of America* **110**, 14592-14597, doi:10.1073/pnas.1218447110 (2013).

62 Gilbert, E. S., Walker, A. W. & Keasling, J. D. A constructed microbial consortium for biodegradation of the organophosphorus insecticide parathion. *Applied microbiology and biotechnology* **61**, 77-81, doi:10.1007/s00253-002-1203-5 (2003).

63 Zhou, K., Qiao, K., Edgar, S. & Stephanopoulos, G. Distributing a metabolic pathway among a microbial consortium enhances production of natural products. *Nature biotechnology* **33**, 377-383, doi:10.1038/nbt.3095 (2015).

64 Minami, H. *et al.* Microbial production of plant benzylisoquinoline alkaloids. *Proceedings of the National Academy of Sciences of the United States of America* **105**, 7393-7398, doi:10.1073/pnas.0802981105 (2008).

65 Wang, E. X., Ding, M. Z., Ma, Q., Dong, X. T. & Yuan, Y. J. Reorganization of a synthetic microbial consortium for one-step vitamin C fermentation. *Microbial cell factories* **15**, 21, doi:10.1186/s12934-016-0418-6 (2016).

66 Kumar, R., Singh, S. & Singh, O. V. Bioconversion of lignocellulosic biomass: biochemical and molecular perspectives. *J Ind Microbiol Biotechnol* **35**, 377-391, doi:10.1007/s10295-008-0327-8 (2008).

67 Jeffries, T. W. Engineering yeasts for xylose metabolism. *Curr Opin Biotechnol* **17**, 320-326, doi:10.1016/j.copbio.2006.05.008 (2006).

68 Sievert, C. *et al.* Experimental evolution reveals an effective avenue to release catabolite repression via mutations in XylR. *Proc Natl Acad Sci U S A* **114**, 7349-7354, doi:10.1073/pnas.1700345114 (2017).

69 Geddes, C. C. *et al.* Simplified process for ethanol production from sugarcane bagasse using hydrolysate-resistant Escherichia coli strain MM160. *Bioresour Technol* **102**, 2702-2711, doi:10.1016/j.biortech.2010.10.143 (2011).

70 Sawisit, A. *et al.* Mutation in galP improved fermentation of mixed sugars to succinate using engineered Escherichia coli AS1600a and AM1 mineral salts medium. *Bioresource Technol* **193**, 433-441 (2015).

71 Song, H., Ding, M. Z., Jia, X. Q., Ma, Q. & Yuan, Y. J. Synthetic microbial consortia: from systematic analysis to construction and applications. *Chem Soc Rev* **43**, 6954-6981, doi:10.1039/c4cs00114a (2014).

72 Lu, H., Villada, J. C. & Lee, P. K. H. Modular Metabolic Engineering for Biobased Chemical Production. *Trends Biotechnol*, doi:10.1016/j.tibtech.2018.07.003 (2018).

73 Hays, S. G., Patrick, W. G., Ziesack, M., Oxman, N. & Silver, P. A. Better together: engineering and application of microbial symbioses. *Curr Opin Biotechnol* **36**, 40-49, doi:10.1016/j.copbio.2015.08.008 (2015).

74 Chappell, T. C. & Nair, N. U. Co-utilization of hexoses by a microconsortium of sugar-specific E. coli strains. *Biotechnol Bioeng* **114**, 2309-2318, doi:10.1002/bit.26351 (2017).

75 Maleki, N., Safari, M. & Eiteman, M. A. Conversion of glucose-xylose mixtures to pyruvate using a consortium of metabolically engineered Escherichia coli. *Eng Life Sci* **18**, 40-47, doi:10.1002/elsc.201700109 (2018).

76 Zhang, H., Pereira, B., Li, Z. & Stephanopoulos, G. Engineering Escherichia coli coculture systems for the production of biochemical products. *Proc Natl Acad Sci U S A* **112**, 8266-8271, doi:10.1073/pnas.1506781112 (2015).

77 Zhang, H., Li, Z., Pereira, B. & Stephanopoulos, G. Engineering E. coli-E. coli cocultures for production of muconic acid from glycerol. *Microb Cell Fact* **14**, 134, doi:10.1186/s12934-015-0319-0 (2015).

78 Zhang, H. R. & Wang, X. N. Modular co-culture engineering, a new approach for metabolic engineering. *Metab Eng* **37**, 114-121 (2016).

79 Shin, H. D., McClendon, S., Vo, T. & Chen, R. R. Escherichia coli binary culture engineered for direct fermentation of hemicellulose to a biofuel. *Appl Environ Microbiol* **76**, 8150-8159, doi:10.1128/AEM.00908-10 (2010).

80 Monk, J. M. *et al.* Multi-omics Quantification of Species Variation of Escherichia coli Links Molecular Features with Strain Phenotypes. *Cell Syst* **3**, 238-251 e212, doi:10.1016/j.cels.2016.08.013 (2016).

81 Saha, B. C., Iten, L. B., Cotta, M. A. & Wu, Y. V. Dilute acid pretreatment, enzymatic saccharification, and fermentation of rice hulls to ethanol. *Biotechnol Prog* **21**, 816-822, doi:10.1021/bp049564n (2005).

82 Yomano, L. P., York, S. W., Shanmugam, K. T. & Ingram, L. O. Deletion of methylglyoxal synthase gene (mgsA) increased sugar co-metabolism in ethanol-producing Escherichia coli. *Biotechnol Lett* **31**, 1389-1398, doi:10.1007/s10529-009-0011-8 (2009).

83 Miller, E. N. *et al.* Silencing of NADPH-dependent oxidoreductase genes (yqhD and dkgA) in furfural-resistant ethanologenic Escherichia coli. *Appl Environ Microbiol* **75**, 4315-4323, doi:10.1128/AEM.00567-09 (2009).

84 Yomano, L. P., York, S. W., Zhou, S., Shanmugam, K. T. & Ingram, L. O. Re-engineering Escherichia coli for ethanol production. *Biotechnol Lett* **30**, 2097-2103 (2008).

85 McDonald, T. P., Walmsley, A. R. & Henderson, P. J. Asparagine 394 in putative helix 11 of the galactose-H+ symport protein (GalP) from Escherichia coli is associated with the internal binding site for cytochalasin B and sugar. *J Biol Chem* **272**, 15189-15199 (1997).

86 Brenner, K., You, L. & Arnold, F. H. Engineering microbial consortia: a new frontier in synthetic biology. *Trends Biotechnol* **26**, 483-489, doi:10.1016/j.tibtech.2008.05.004 (2008).

87 Shong, J., Jimenez Diaz, M. R. & Collins, C. H. Towards synthetic microbial consortia for bioprocessing. *Curr Opin Biotechnol* **23**, 798-802, doi:10.1016/j.copbio.2012.02.001 (2012).

88 Liu, F. *et al.* Bioconversion of distillers' grains hydrolysates to advanced biofuels by an Escherichia coli co-culture. *Microb Cell Fact* **16**, 192, doi:10.1186/s12934-017-0804-8 (2017).

89 Khankal, R., Chin, J. W. & Cirino, P. C. Role of xylose transporters in xylitol production from engineered Escherichia coli. *J Biotechnol* **134**, 246-252 (2008).

90 Hasona, A., Kim, Y., Healy, F. G., Ingram, L. O. & Shanmugam, K. T. Pyruvate formate lyase and acetate kinase are essential for anaerobic growth of Escherichia coli on xylose. *J Bacteriol* **186**, 7593-7600 (2004).

91 Wang, L., York, S. W., Ingram, L. O. & Shanmugam, K. T. Simultaneous fermentation of biomass-derived sugars to ethanol by a co-culture of an engineered Escherichia coli and Saccharomyces cerevisiae. *Bioresour Technol* **273**, 269-276, doi:10.1016/j.biortech.2018.11.016 (2018).

92 Datsenko, K. A. & Wanner, B. L. One-step inactivation of chromosomal genes in Escherichia coli K-12 using PCR products. *Proc Natl Acad Sci U S A* **97**, 6640-6645, doi:10.1073/pnas.120163297 (2000).

93 Jantama, K. *et al.* Eliminating side products and increasing succinate yields in engineered strains of Escherichia coli C. *Biotechnol Bioeng* **101**, 881-893, doi:10.1002/bit.22005 (2008).

94 Martinez, A. *et al.* Low salt medium for lactate and ethanol production by recombinant Escherichia coli B. *Biotechnol Lett* **29**, 397-404 (2007).

95 Abdel-Rahman, M. A., Tashiro, Y. & Sonomoto, K. Recent advances in lactic acid production by microbial fermentation processes. *Biotechnol Adv* **31**, 877-902, doi:10.1016/j.biotechadv.2013.04.002 (2013).

96 Es, I. *et al.* Recent advancements in lactic acid production - a review. *Food Res Int* **107**, 763-770, doi:10.1016/j.foodres.2018.01.001 (2018).

97 Ahn, J. H., Jang, Y. S. & Lee, S. Y. Production of succinic acid by metabolically engineered microorganisms. *Curr Opin Biotechnol* **42**, 54-66, doi:10.1016/j.copbio.2016.02.034 (2016).

98 Jansen, M. L. & van Gulik, W. M. Towards large scale fermentative production of succinic acid. *Curr Opin Biotechnol* **30**, 190-197, doi:10.1016/j.copbio.2014.07.003 (2014).

99 Okano, K., Tanaka, T., Ogino, C., Fukuda, H. & Kondo, A. Biotechnological production of enantiomeric pure lactic acid from renewable resources: recent achievements, perspectives, and limits. *Appl Microbiol Biotechnol* **85**, 413-423, doi:10.1007/s00253-009-2280-5 (2010).

100 Abdel-Rahman, M. A., Tashiro, Y. & Sonomoto, K. Lactic acid production from lignocellulose-derived sugars using lactic acid bacteria: overview and limits. *J Biotechnol* **156**, 286-301, doi:10.1016/j.jbiotec.2011.06.017 (2011).

101 Lynd, L. R. The grand challenge of cellulosic biofuels. *Nat Biotechnol* **35**, 912-915, doi:10.1038/nbt.3976 (2017).

102 Nieves, L. M., Panyon, L. A. & Wang, X. Engineering Sugar Utilization and Microbial Tolerance toward Lignocellulose Conversion. *Front Bioeng Biotechnol* **3**, 17, doi:10.3389/fbioe.2015.00017 (2015).

103 Song, S. & Park, C. Organization and regulation of the D-xylose operons in Escherichia coli K-12: XylR acts as a transcriptional activator. *J Bacteriol* **179**, 7025-7032 (1997).

104 Wang, Q., Ingram, L. O. & Shanmugam, K. T. Evolution of D-lactate dehydrogenase activity from glycerol dehydrogenase and its utility for D-lactate production from lignocellulose. *Proc Natl Acad Sci U S A* **108**, 18920-18925 (2011).

105 Ishida, N. *et al.* D-lactic acid production by metabolically engineered Saccharomyces cerevisiae. *J Biosci Bioeng* **101**, 172-177, doi:10.1263/jbb.101.172 (2006).

106 Grabar, T. B., Zhou, S., Shanmugam, K. T., Yomano, L. P. & Ingram, L. O. Methylglyoxal bypass identified as source of chiral contamination in l(+) and d(-)-lactate fermentations by recombinant Escherichia coli. *Biotechnol Lett* **28**, 1527-1535 (2006).

107 Awasthi, D. *et al.* Metabolic engineering of Bacillus subtilis for production of D-lactic acid. *Biotechnol Bioeng* **115**, 453-463, doi:10.1002/bit.26472 (2018).

108 Litsanov, B., Kabus, A., Brocker, M. & Bott, M. Efficient aerobic succinate production from glucose in minimal medium with Corynebacterium glutamicum. *Microb Biotechnol* **5**, 116-128, doi:10.1111/j.1751-7915.2011.00310.x (2012).

109 Utrilla, J., Vargas-Tah, A., Trujillo-Martinez, B., Gosset, G. & Martinez, A. Production of d-lactate from sugarcane bagasse and corn stover hydrolysates using metabolic engineered Escherichia coli strains. *Bioresour Technol* **220**, 208-214, doi:10.1016/j.biortech.2016.08.067 (2016).

110 Sawisit, A. *et al.* Mutation in galP improved fermentation of mixed sugars to succinate using engineered Escherichia coli AS1600a and AM1 mineral salts medium. *Bioresour Technol* **193**, 433-441, doi:10.1016/j.biortech.2015.06.108 (2015).

111 Zhou, K., Qiao, K. J., Edgar, S. & Stephanopoulos, G. Distributing a metabolic pathway among a microbial consortium enhances production of natural products. *Nature Biotechnology* **33**, 377-U157, doi:10.1038/nbt.3095 (2015).

112 Jones, J. A. *et al.* Complete Biosynthesis of Anthocyanins Using E. coli Polycultures. *MBio* **8**, doi:10.1128/mBio.00621-17 (2017).

113 Camacho-Zaragoza, J. M. *et al.* Engineering of a microbial coculture of Escherichia coli strains for the biosynthesis of resveratrol. *Microb Cell Fact* **15**, 163, doi:10.1186/s12934-016-0562-z (2016).

114 Roell, G. W. *et al.* Engineering microbial consortia by division of labor. *Microb Cell Fact* **18**, 35, doi:10.1186/s12934-019-1083-3 (2019).

115 Lu, H., Villada, J. C. & Lee, P. K. H. Modular Metabolic Engineering for Biobased Chemical Production. *Trends Biotechnol* **37**, 152-166, doi:10.1016/j.tibtech.2018.07.003 (2019).

116 Wang, L., York, S. W., Ingram, L. O. & Shanmugam, K. T. Simultaneous fermentation of biomass-derived sugars to ethanol by a co-culture of an engineered Escherichia coli and Saccharomyces cerevisiae. *Bioresour Technol* **273**, 269-276, doi:10.1016/j.biortech.2018.11.016 (2019).

117 Flores, A. D., Ayla, E. Z., Nielsen, D. R. & Wang, X. Engineering a Synthetic, Catabolically Orthogonal Coculture System for Enhanced Conversion of Lignocellulose-Derived Sugars to Ethanol. *ACS Synth Biol* **8**, 1089-1099, doi:10.1021/acssynbio.9b00007 (2019).

118 Khunnonkwao, P., Jantama, S. S., Kanchanatawee, S. & Jantama, K. Re-engineering Escherichia coli KJ122 to enhance the utilization of xylose and xylose/glucose mixture for efficient succinate production in mineral salt medium. *Appl Microbiol Biotechnol* **102**, 127-141, doi:10.1007/s00253-017-8580-2 (2018).

119 Herre, E. A., Knowlton, N., Mueller, U. G. & Rehner, S. A. The evolution of mutualisms: exploring the paths between conflict and cooperation. *Trends Ecol Evol* **14**, 49-53 (1999).

120 Ponomarova, O. & Patil, K. R. Metabolic interactions in microbial communities: untangling the Gordian knot. *Curr Opin Microbiol* **27**, 37-44, doi:10.1016/j.mib.2015.06.014 (2015).

121 Scott, S. R. & Hasty, J. Quorum Sensing Communication Modules for Microbial Consortia. *ACS Synth Biol* **5**, 969-977, doi:10.1021/acssynbio.5b00286 (2016).

122 Li, X. T., Thomason, L. C., Sawitzke, J. A., Costantino, N. & Court, D. L. Positive and negative selection using the tetA-sacB cassette: recombineering and P1 transduction in Escherichia coli. *Nucleic Acids Res* **41**, e204, doi:10.1093/nar/gkt1075 (2013).

123 Langholtz MH, S. B., & Eaton LM Vol. 1 (Oak Ridge National Laboratory, Oak Ridge, TN, (Energy USDo), 2016).

124 Lynd, L. R. Large-Scale Fuel Ethanol from Lignocellulose - Potential, Economics, and Research Priorities. *Appl Biochem Biotech* **24-5**, 695-719 (1990).

125 Blaschek, Z. L. L. a. H. P. *Biomass to biofuels: strategies for global industries.*, (2010).

126 Bogorad, I. W., Lin, T. S. & Liao, J. C. Synthetic non-oxidative glycolysis enables complete carbon conservation. *Nature* **502**, 693-697, doi:10.1038/nature12575 (2013).

127 Jarboe, L. R., Grabar, T. B., Yomano, L. P., Shanmugan, K. T. & Ingram, L. O. Development of ethanologenic bacteria. *Adv Biochem Eng Biotechnol* **108**, 237-261, doi:10.1007/10_2007_068 (2007).

128 Ingram, L. O., Conway, T., Clark, D. P., Sewell, G. W. & Preston, J. F. Genetic engineering of ethanol production in Escherichia coli. *Appl Environ Microbiol* **53**, 2420-2425 (1987).

129 Atsumi, S., Hanai, T. & Liao, J. C. Non-fermentative pathways for synthesis of branched-chain higher alcohols as biofuels. *Nature* **451**, 86-89, doi:10.1038/nature06450 (2008).

130 Shen, C. R. *et al.* Driving forces enable high-titer anaerobic 1-butanol synthesis in Escherichia coli. *Appl Environ Microbiol* **77**, 2905-2915, doi:10.1128/AEM.03034-10 (2011).

131 Bond-Watts, B. B., Bellerose, R. J. & Chang, M. C. Enzyme mechanism as a kinetic control element for designing synthetic biofuel pathways. *Nat Chem Biol* **7**, 222-227, doi:10.1038/nchembio.537 (2011).

132 Meadows, A. L. *et al.* Rewriting yeast central carbon metabolism for industrial isoprenoid production. *Nature* **537**, 694-697, doi:10.1038/nature19769 (2016).

133 Lennen, R. M. & Pfleger, B. F. Engineering Escherichia coli to synthesize free fatty acids. *Trends in biotechnology* **30**, 659-667, doi:10.1016/j.tibtech.2012.09.006 (2012).

134 Davis, S. C., Williams, S. E. & Boundy, R. G. Vol. 36th Ed. (Oak Ridge National Lab, 2017).

135 Xu, Y., Isom, L. & Hanna, M. A. Adding value to carbon dioxide from ethanol fermentations. *Bioresour Technol* **101**, 3311-3319, doi:10.1016/j.biortech.2010.01.006 (2010).

136 Kheshgi, H. S. & Prince, R. C. Sequestration of fermentation CO2 from ethanol production. *Energy* **30**, 1865-1871, doi:10.1016/j.energy.2004.11.004 (2005).

137 Francois, J. M., Lachaux, C. & Morin, N. Synthetic Biology Applied to Carbon Conservative and Carbon Dioxide Recycling Pathways. *Front Bioeng Biotechnol* **7**, 446, doi:10.3389/fbioe.2019.00446 (2019).

138 Mattozzi, M., Ziesack, M., Voges, M. J., Silver, P. A. & Way, J. C. Expression of the sub-pathways of the Chloroflexus aurantiacus 3-hydroxypropionate carbon fixation bicycle in E. coli: Toward horizontal transfer of autotrophic growth. *Metab Eng* **16**, 130-139, doi:10.1016/j.ymben.2013.01.005 (2013).

139 Guadalupe-Medina, V. *et al.* Carbon dioxide fixation by Calvin-Cycle enzymes improves ethanol yield in yeast. *Biotechnol Biofuels* **6**, 125, doi:10.1186/1754-6834-6-125 (2013).

140 Gong, F. *et al.* Quantitative analysis of an engineered CO2-fixing Escherichia coli reveals great potential of heterotrophic CO2 fixation. *Biotechnol Biofuels* **8**, 86, doi:10.1186/s13068-015-0268-1 (2015).

141 Li, Y. H., Ou-Yang, F. Y., Yang, C. H. & Li, S. Y. The coupling of glycolysis and the Rubisco-based pathway through the non-oxidative pentose phosphate pathway to achieve low carbon dioxide emission fermentation. *Bioresour Technol* **187**, 189-197, doi:10.1016/j.biortech.2015.03.090 (2015).

142 Papapetridis, I. *et al.* Optimizing anaerobic growth rate and fermentation kinetics in Saccharomyces cerevisiae strains expressing Calvin-cycle enzymes for improved ethanol yield. *Biotechnol Biofuels* **11**, 17, doi:10.1186/s13068-017-1001-z (2018).

143 Xia, P. F. *et al.* Recycling Carbon Dioxide during Xylose Fermentation by Engineered Saccharomyces cerevisiae. *ACS Synth Biol* **6**, 276-283, doi:10.1021/acssynbio.6b00167 (2017).

144 Fast, A. G., Schmidt, E. D., Jones, S. W. & Tracy, B. P. Acetogenic mixotrophy: novel options for yield improvement in biofuels and biochemicals production. *Curr Opin Biotechnol* **33**, 60-72, doi:10.1016/j.copbio.2014.11.014 (2015).

145 Jones, S. W. *et al.* CO2 fixation by anaerobic non-photosynthetic mixotrophy for improved carbon conversion. *Nat Commun* **7**, 12800, doi:10.1038/ncomms12800 (2016).

146 Gleizer, S. *et al.* Conversion of Escherichia coli to Generate All Biomass Carbon from CO2. *Cell* **179**, 1255-1263.e1212 (2019).

147 Charubin, K. & Papoutsakis, E. T. Direct cell-to-cell exchange of matter in a synthetic Clostridium syntrophy enables CO2 fixation, superior metabolite yields, and an expanded metabolic space. *Metab Eng* **52**, 9-19, doi:10.1016/j.ymben.2018.10.006 (2019).

148 Spona-Friedl, M. *et al.* Substrate-dependent CO2 fixation in heterotrophic bacteria revealed by stable isotope labelling. *FEMS Microbiol Ecol* **96**, doi:10.1093/femsec/fiaa080 (2020).

149 Erb, T. J. Carboxylases in natural and synthetic microbial pathways. *Appl Environ Microbiol* **77**, 8466-8477, doi:10.1128/AEM.05702-11 (2011).

150 Bar-Even, A., Noor, E., Lewis, N. E. & Milo, R. Design and analysis of synthetic carbon fixation pathways. *Proc Natl Acad Sci U S A* **107**, 8889-8894, doi:10.1073/pnas.0907176107 (2010).

151 Bar-Even, A., Noor, E. & Milo, R. A survey of carbon fixation pathways through a quantitative lens. *J Exp Bot* **63**, 2325-2342, doi:10.1093/jxb/err417 (2012).

152 Flores, A. D. *et al.* Catabolic Division of Labor Enhances Production of D-Lactate and Succinate From Glucose-Xylose Mixtures in Engineered Escherichia coli Co-culture Systems. *Front Bioeng Biotechnol* **8**, 329, doi:10.3389/fbioe.2020.00329 (2020).

153 Kurgan, G. *et al.* Parallel experimental evolution reveals a novel repressive control of GalP on xylose fermentation in Escherichia coli. *Biotechnol Bioeng* **116**, 2074-2086, doi:10.1002/bit.27004 (2019).

154 Zhang, X. *et al.* Metabolic evolution of energy-conserving pathways for succinate production in Escherichia coli. *Proc Natl Acad Sci U S A* **106**, 20180-20185, doi:10.1073/pnas.0905396106 (2009).

155 Vemuri, G. N., Eiteman, M. A. & Altman, E. Effects of growth mode and pyruvate carboxylase on succinic acid production by metabolically engineered strains of Escherichia coli. *Appl Environ Microb* **68**, 1715-1727 (2002).

156 Martinez, R., Flores, A. D., Dufault, M. E. & Wang, X. The XylR variant (R121C and P363S) releases arabinose-induced catabolite repression on xylose fermentation and enhances coutilization of lignocellulosic sugar mixtures. *Biotechnol Bioeng* **116**, 3476-3481, doi:10.1002/bit.27144 (2019).

157 Lindsay, R. T. *et al.* A model for determining cardiac mitochondrial substrate utilisation using stable 13C-labelled metabolites. *Metabolomics* **15**, 154, doi:10.1007/s11306-019-1618-y (2019).

158 Martinez, A. *et al.* Low salt medium for lactate and ethanol production by recombinant Escherichia coli B. *Biotechnol Lett* **29**, 397-404, doi:10.1007/s10529-006-9252-y (2007).

159 You, L. *et al.* Metabolic Pathway Confirmation and Discovery Through 13C-labeling of Proteinogenic Amino Acids. *J. Vis. Exp.*, e3583, doi:doi:10.3791/3583 (2012).

160 Varman, A. M., He, L., You, L., Hollinshead, W. & Tang, Y. J. Elucidation of intrinsic biosynthesis yields using ^{13}C-based metabolism analysis. *Microb Cell Fact* **13**, 42, doi:10.1186/1475-2859-13-42 (2014).

161 Varman, A. M., Xiao, Y., Pakrasi, H. B. & Tang, Y. J. Metabolic engineering of Synechocystis sp. Strain PCC 6803 for isobutanol production. *Appl Environ Microbiol* **79**, doi:10.1128/aem.02827-12 (2012).

162 Wahl, S. A., Dauner, M. & Wiechert, W. New tools for mass isotopomer data evaluation in (13)C flux analysis: mass isotope correction, data consistency

checking, and precursor relationships. *Biotechnol Bioeng* **85**, 259-268, doi:10.1002/bit.10909 (2004).

163 Butler, J. N. *Carbon dioxide equilibria and their applications*. (Addison-Wesley, 1982).

164 Goers, L., Freemont, P. & Polizzi, K. M. Co-culture systems and technologies: taking synthetic biology to the next level. *J R Soc Interface* **11**, doi:10.1098/rsif.2014.0065 (2014).

165 Johns, N. I., Blazejewski, T., Gomes, A. L. & Wang, H. H. Principles for designing synthetic microbial communities. *Curr Opin Microbiol* **31**, 146-153, doi:10.1016/j.mib.2016.03.010 (2016).

166 Kerner, A., Park, J., Williams, A. & Lin, X. N. A programmable Escherichia coli consortium via tunable symbiosis. *PLoS One* **7**, e34032, doi:10.1371/journal.pone.0034032 (2012).

167 Bolten, C. J., Kiefer, P., Letisse, F., Portais, J. C. & Wittmann, C. Sampling for metabolome analysis of microorganisms. *Anal Chem* **79**, 3843-3849, doi:10.1021/ac0623888 (2007).

168 Canelas, A. B. *et al.* Leakage-free rapid quenching technique for yeast metabolomics. *Metabolomics* **4**, 226-239, doi:10.1007/s11306-008-0116-4 (2008).

169 Taymaz-Nikerel, H. *et al.* Development and application of a differential method for reliable metabolome analysis in Escherichia coli. *Anal Biochem* **386**, 9-19, doi:10.1016/j.ab.2008.11.018 (2009).

170 Kosina, S. M. *et al.* Exometabolomics Assisted Design and Validation of Synthetic Obligate Mutualism. *Acs Synth Biol* **5**, 569-576, doi:10.1021/acssynbio.5b00236 (2016).

171 Paczia, N. *et al.* Extensive exometabolome analysis reveals extended overflow metabolism in various microorganisms. **11**, 122, doi:10.1186/1475-2859-11-122 (2012).

172 Kawaguchi, H., Vertès, A. A., Okino, S., Inui, M. & Yukawa, H. Engineering of a xylose metabolic pathway in Corynebacterium glutamicum. *Appl Environ Microbiol* **72**, 3418-3428, doi:10.1128/AEM.72.5.3418-3428.2006 (2006).

173 Ponomarova, O. & Patil, K. R. Metabolic interactions in microbial communities: untangling the Gordian knot. *Current Opinion in Microbiology* **27**, 37-44, doi:10.1016/j.mib.2015.06.014 (2015).

174 Zampieri, M. & Sauer, U. Model-based media selection to minimize the cost of metabolic cooperation in microbial ecosystems. *Bioinformatics* **32**, 1733-1739, doi:10.1093/bioinformatics/btw062 (2016).

175 Bull, J. J. & Harcombe, W. R. Population dynamics constrain the cooperative evolution of cross-feeding. *Plos One* **4**, e4115, doi:10.1371/journal.pone.0004115 (2009).

176 Callaway, R. M. *et al.* Positive interactions among alpine plants increase with stress. *Nature* **417**, 844-848, doi:DOI 10.1038/nature00812 (2002).

177 Hoek, T. A. *et al.* Resource Availability Modulates the Cooperative and Competitive Nature of a Microbial Cross-Feeding Mutualism. *Plos Biol* **14**, e1002540, doi:10.1371/journal.pbio.1002540 (2016).

178 Fredrickson, J. K. Ecological communities by design. *Science* **348**, 1425-1427, doi:10.1126/science.aab0946 (2015).

179 Minty, J. J. *et al.* Design and characterization of synthetic fungal-bacterial consortia for direct production of isobutanol from cellulosic biomass. *P Natl Acad Sci USA* **110**, 14592-14597, doi:10.1073/pnas.1218447110 (2013).

APPENDIX A

PERMISSION TO REPRODUCE PORTIONS OF CHAPTER 1 FROM SPRINGER NATURE

SPRINGER NATURE LICENSE
TERMS AND CONDITIONS

Mar 15, 2021

This Agreement between Arizona State University -- Andrew Flores ("You") and Springer Nature ("Springer Nature") consists of your license details and the terms and conditions provided by Springer Nature and Copyright Clearance Center.

License Number	5030521388644
License date	Mar 15, 2021
Licensed Content Publisher	Springer Nature
Licensed Content Publication	Springer eBook
Licensed Content Title	Engineering Bacterial Sugar Catabolism and Tolerance Toward Lignocellulose Conversion
Licensed Content Author	Andrew D. Flores, Gavin L. Kurgan, Xuan Wang
Licensed Content Date	Jan 1, 2017
Type of Use	Thesis/Dissertation
Requestor type	academic/university or research institute
Format	print and electronic

8. Limitations

8. 1. ***BOOKS ONLY:*** Where **'reuse in a dissertation/thesis'** has been selected the following terms apply: Print rights of the final author's accepted manuscript (for clarity, NOT the published version) for up to 100 copies, electronic rights for use only on a personal website or institutional repository as defined by the Sherpa guideline (www.sherpa.ac.uk/romeo/).

APPENDIX B

PERMISSION TO REPRODUCE PORTIONS OF CHAPTER 2 FROM ACS SYNTHETIC BIOLOGY

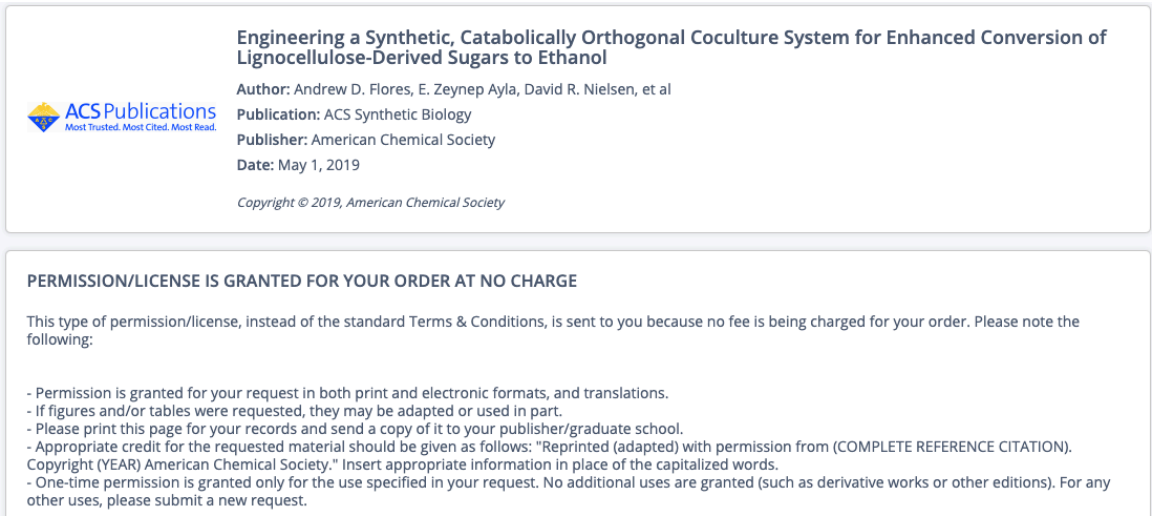

Engineering a Synthetic, Catabolically Orthogonal Coculture System for Enhanced Conversion of Lignocellulose-Derived Sugars to Ethanol

Author: Andrew D. Flores, E. Zeynep Ayla, David R. Nielsen, et al

Publication: ACS Synthetic Biology

Publisher: American Chemical Society

Date: May 1, 2019

Reprinted (adapted) with permission from: Flores, A. D., Ayla, E. Z., Nielsen, D. R., & Wang, X. (2019). Engineering a synthetic, catabolically-orthogonal coculture system for enhanced conversion of lignocellulose-derived sugars to ethanol. *ACS synthetic biology*, *8*(5), 1089-1099. Copyright (2019) American Chemical Society.

APPENDIX C

PERMISSION TO REPRODUCE PORTIONS OF CHAPTER 3 FROM FRONTIERS IN BIOENGINEERING AND BIOTECHNOLOGY

Reprinted with permission from: Flores, A. D., Choi, H. G., Martinez, R., Onyeabor, M., Ayla, E. Z., Godar, A., ... & Wang, X. (2020). Catabolic Division of Labor Enhances Production of D-Lactate and Succinate From Glucose-Xylose Mixtures in Engineered Escherichia coli Coculture Systems. *Frontiers in Bioengineering and Biotechnology*